PROTON/HYDROXYL TRANSMEMBRANE MOVEMENT ACROSS DIHEXADECYLPHOSPHATE VESICLE BILAYERS

Nianxin Jiao

M.S., Nankai University, China, 1990

B.S., Nankai University, China, 1987

A thesis submitted to the faculty of the

Oregon Graduate Institute of Science & Technology

in partial fulfillment of the

requirements for the degree

Master of Science

in

Chemistry

April, 1993

The thesis "Proton/hydroxyl Transmembrane Movement Across Dihexadecylphosphate Vesicle Bilayers" by Nianxin Jiao has been examined by the following Examination Committee:

_____

James K. Hurst
Professor
Thesis Advisor

_____

Joanne Sanders-Loehr
Professor

_____

David W. Grainger
Assistant Professor

DEDICATION

This thesis is dedicated to my mother, Zengshu Liu, and my father, Qiyin Jiao. Without their love and support, I cannot achieve anything. This thesis is also dedicated to my husband, Jinshu Ling, for his understanding and help.

ACKNOWLEDGEMENTS

TABLE OF CONTENTS

TABLE OF CONTENTS (CONTINUED)

LIST OF ABBREVIATIONS

bR .... Bacteriorhodopsin

CCCP .... Carbonyl cyanide 3-chlorophenylhydrazone

DHP .... Dihexadecylphosphate

DNP 2,4-dinitrophenol

MB^+ .... 1-methyl-4,4'-bipyridinium

MSV^+ .... 1-methyl-1'-sulfanato-n-propyl-4,4'-bipyridinium

MV^{2+} .... 1,1'-dimethyl-4,4'-bipyridinium

PM .... Purple membrane

Pyranine (pyr^{3-}) 8-hydroxyl-1,3,6-pyrenetrisulfonate

SUV .... Small unilamellar vesicle

TBAH .... Tetrabutylammonium hydroxide

TPP^+ .... Tetraphenylphosphonium

Tris .... Tris(hydroxymethyl)aminomethane

LIST OF TABLES

LIST OF FIGURES

LIST OF FIGURES (CONTINUED)

LIST OF FIGURES (CONTINUED)

ABSTRACT

Proton/hydroxyl Transmembrane Movement Across Dihexadecylphosphate Vesicle
. Bilayers

Nianxin Jiao

Oregon Graduate Institute of Science & Techonology

Supervising Professor: James K. Hurst

The proton/hydroxyl permeability across dihexadecylphosphate (DHP) vesicle
bilayers was measured by applying an external pH jump. A pH-sensitive fluorescence
dye, 8-hydroxy-1,3,6-pyrenetrisulfonate (pyranine) was used to determine the internal
pH of the DHP vesicles. The dye could be entrapped within the internal aqueous
compartment of the vesicle by ultrasonication and gel filtration. The pH was then
obtained from the fluorescence excitation profiles by comparison to standard curves.
Perturbation of the external pH in DHP vesicle suspensions caused an apparent
biphasic change of the internal pH, which was characterized by a fast large initial step
followed by a small slower change in the same direction. The proton/hydroxyl
movement across the vesicles is an electrogenic process which establishes a
transmembrane potential that blocks further ion movement. The lipophilic ion,
tetraphenylphosphonium (TPP$^+$), was used to dissipate this transmembrane potential;
its effect was to remove the slow pH change phase and to increase the total
proton/hydroxyl movement. The permeability coefficient of proton/hydroxyl across
the DHP vesicle bilayers was estimated from the slow phase to be in the range of 10^{-4}
to 10^{-5} cm/s, which is in agreement with reported values for the abnormally high

permeability of proton/hydroxyl across lipid membranes.

The incorporation of a membrane protein, bacteriorhodopsin (bR), into the DHP vesicle bilayers was also attempted. Bacteriorhodopsin is a light-driven proton pump, and a potential switch for transmembrane charge separation processes in bifunctional doped membranes. Mixtures of DHP vesicles and bR were either cosonicated or incubated, then put on a linear sucrose density gradient to separate unmodified vesicles, vesicles incorporating bR, and the unincorporated bR. Only partial incorporation was achieved using these two methods.

CHAPTER 1

INTRODUCTION

Two types of supramolecular structures are responsible for most membrane functions in the living cell. One is the lipid bilayer, which acts as both a structural matrix and barrier, and the other includes a variety of lipid-protein complexes which mediate important membrane functions such as passive and active ion translocation, light transduction, and coupling of electron transport to ATP synthesis. Many such functions require ion gradients to be maintained against leaks, and therefore the permeability of the barrier is a significant aspect of membrane-related activities.

The membrane presents a large energy barrier to the movement of ions. There are a number of factors that contribute to the work required to move a charge from a large distance away from the membrane to the membrane interface and then into the bilayer core[1]. These are:

1). Work associated with moving between media of different dielectric constants, e.g., from aqueous phase to the membrane interior. This is due to a difference in dipolar polarization of media and is the major factor destabilizing charges within the bilayer interior. This is primarily Born energy, i.e., differences in the energy required to charge a sphere in various dielectric media; the magnitude of this work decreases with increasing size of the ions. Membrane permeable ions are therefore large organic ions, e.g., tetraphenylphosphonium, tetraphenylborate, or complexes of small inorganic ions with lipid-soluble ligands, e.g., K^+-valinomycin. In addition to Born energy, there is a second component due to the polarization forces arising at the dielectric interface. The presence of a charge on one side of interface causes the dipoles in the medium on the other side to reorient. This results in "image charge" forces.

2). A dipole potential due mostly to the oriented ester carbonyls on the

phospholipid molecules and, possibly, oriented water.

3). A surface potential due to interactions of charged groups on the membrane surface.

4). A transmembrane potential due to charge imbalances caused by chemical gradients of membrane permeable ions or by electrogenic electron transfer processes, e.g., photosynthesis, respiration.

The sum of these four terms constitutes the net potential energy barrier to ion transport through the membrane. Transport rates are determined by the height of the potential energy barrier. All four terms in the potential energy barrier are important contributors in determing the magnitude of the membrane permeability rates. Figure 1-1 shows theoretical membrane free energy profiles for different ions across neutral phospholipid bilayers and Figure 1-2 gives the potential profiles across a membrane showing the effects of surface charge on the transmembrane potential.

As a result of the above energy barrier, the permeability of ions found in pure lipid bilayer systems is typically very low. The permeability coefficient of inorganic ions such as K^+ and Na^+ is in the range of 10^{-14} to 10^{-12} cm/s[2, 3, 4, 5]. Because the sodium and potassium permeabilities are so low, the first measurements of lipid bilayer permeability to proton/hydroxide (H^+/OH^-) were surprising and controversial when coefficients in the range of 10^{-5} to 10^{-4} cm/s were reported by Nichols and Deamer[6]. These are 7 to 10 orders of magnitude larger than those of other cations! Many laboratories have studied the H^+/OH^- transport properties in a variety of membrane systems, including phospholipid vesicles, phospholipid bilayers, and biological membranes[7]. In general, the original observations of Nichols and Deamer have been confirmed. However, the mechanisms of H^+/OH^- permeability remain unknown. Two models have been proposed, one called the weak-acid model, which was based primarily on the behavior of weakly acidic proton carriers[8], the other called the water-wire model[7(a), 9], in which it is proposed that protons or hydroxyls or both interact with clusters of hydrogen-bonded water molecules in the lipid bilayer such that they are transferred across the bilayer by rearrangement of hydrogen bonds
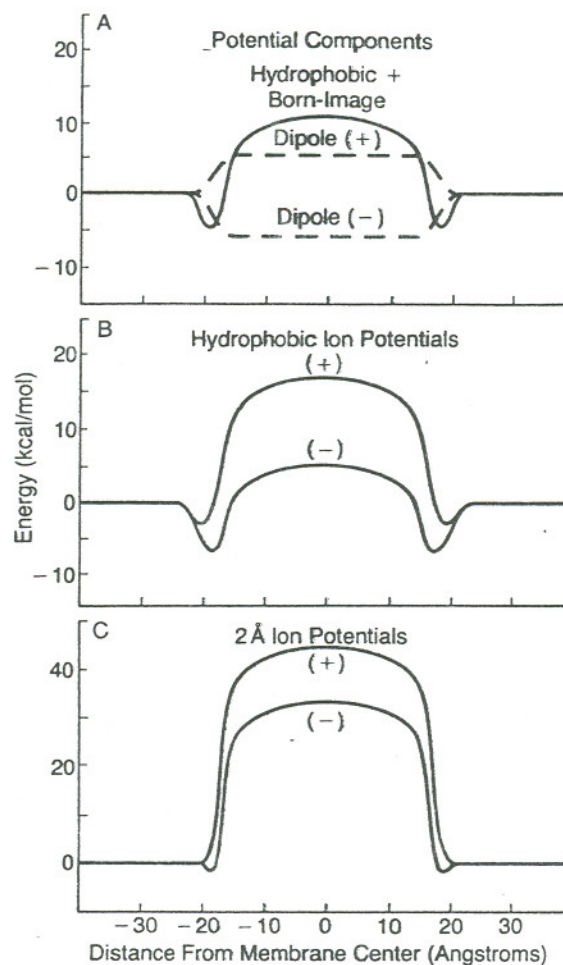
Figure 1-1. Theoretical membrane free energy profiles showing contributions from the Born, image, dipole, and hydrophobic (neutral) components. (A) *Hydrophobic ions*. The Born, image, and hydrophobic contributions (——) are the same for ions that are identical except for the sign of the charge. The dipole potentials (-----) are very different and this stabilizes anions within the bilayer for phospholipids, but may stabilize cations for DHP lipids because DHP is negatively charged. (B) *Hydrophobic ions*. Total free energy profiles for an anion and cation, assuming a 4 Å radius. Again, a hydrophobic cation may have a lower energy barrier for the negatively-charged DHP lipid bilayer, which is the opposite to that shown in this figure. (C) *Ions with 2 Å radii*. The total potential for ordinary inorganic ions presents a large barrier against translocation which is slightly less for anions due to the dipole potential in a phospholipid bilayer, and more for anions in a negatively charged DHP lipid bilayer. Adapted from reference 1.
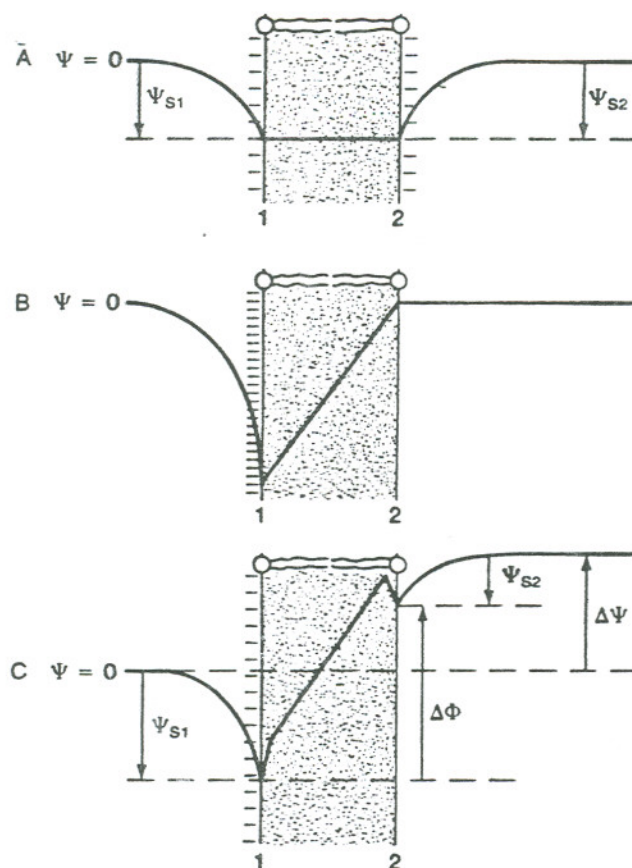
Figure 1-2. Potential profiles across a membrane showing the potential caused by surface charges and the effect of transmembrane potentials. (A) A membrane with the same negative charge density on both sides results in equal surface potentials at both interfaces but no transmembrane potential. (B) A membrane with a large surface charge density on one side which has a surface potential, but no charge on the other side which has no surface potential. There is no transmembrane potential in this case. (C) The transmembrane potential ($\Delta\Psi$), the two surface potentials (Ψ_{s1}, Ψ_{s2}), and the potential difference between the membrane surfaces ($\Delta\Phi$) are shown on a membrane with negative charge on one surface and none on the other side. The dipole potential within the membrane is also shown in this case. Adapted from reference 1.

in a manner similar to their transport in water and ice. Neither model can fully explain the abnormal permeability of H^+/OH^- across membranes.

The permeability of membranes to ions and molecules can be modified by various forces such as temperature and electric fields[10]. Many ions and polar molecules exhibit a maximum permeation at the gel-to-liquid crystal phase transition temperature of lipid vesicles. The effect of an applied transmembrane electric potential ($E_{appl.}$) on membrane permeability is described by the term "electroporation"[11, 12]. Electric pulses of intensity in kilovolts per centimeter and of duration in microseconds to milliseconds exceed the dielectric strength of a membrane, causing reversible or irreversible breakdown of the membrane. This action results in the formation of "pores" that are large enough to allow the transmembrane movement of ions and molecules. The breakdown potential for lipid planar bilayers is in the range of 150-500 mV when the field duration is in microseconds to milliseconds. This value translates into a dielectric strength of 300-1000 kV/cm when the thickness of the bilayer is 5 nm. For spherical cells and lipid vesicles, transmembrane potentials ($\Delta\Psi_{membr.}$) induced by a dc pulse have different values at different locations on the membranes that can be expressed by the Maxwell relationship

$$\Delta\Psi_{membr.} = 1.5 \, R \, E_{appl.} \cos\theta$$

where R is the cell's or vesicle's radius, and θ is the angle between the direction of $E_{appl.}$ and the location on the membrane. The maximum change occurs at the poles ($\cos\theta = \pm 1$), so that a widely used low-field estimate is

$$\Delta\Psi_{membr.} = 1.5 \, R \, E_{appl.}$$

Cell membranes, e.g., human erythrocytes can sustain as much as 1 V of $\Delta\Psi_{membr.}$, i.e., an electric field strength of 2.1 kV/cm, when microsecond to millisecond electric pulses are used[13, 14]. Pure lipid unilamellar vesicles of diameter around 95 ± 5 nm can sustain 210 mV of $\Delta\Psi_{membr.}$ which corresponds to an electric field strength of 30 kV/cm[10, 15]. Proposed structures of transient pores are shown in Figure 1-3[16, 17].

Understanding the mechanism(s) of H^+/OH^- movement across biological
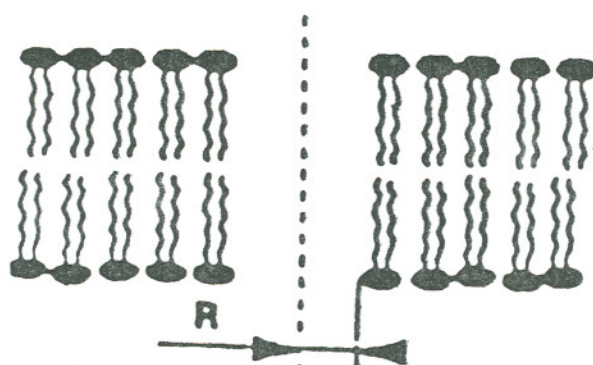
Hydrophobic transient pore
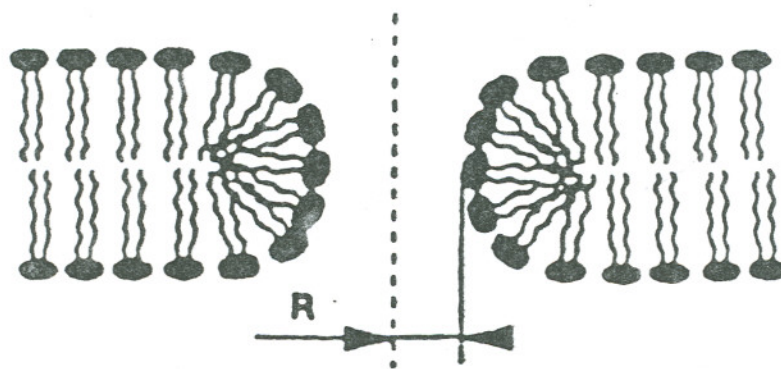
Hydrophilic transient pore

Figure 1-3. Hypothetical structures of transient pores in membrane bilayers during electroporation. Hydrophobic pores expose their hydrophobic part to aqueous phase, while hydrophilic pores only expose their hydrophilic headgroups to the aqueous phase. Adapted from references 16 and 17.

membranes is very important to cellular physiology, specifically various bioenergetic coupling processes that generate proton gradients, regulation of intracellular pH, and the creation of localized compartments of acidic (or basic) pH. Model membrane systems such as monolayers, planar bilayer membranes, and liposomes provide useful models to study the fundamental behavior of biological membranes. The advantage of such systems is that solute flux can be readily monitored by a variety of techniques including ion-selective electrodes, radioactive tracers, and fluorescent dyes in liposomes, and electrical conductance across planar lipid bilayers.

The lipids used in model membrane systems usually are phospholipids. In this work a synthetic lipid, dihexadecylphosphate (DHP), was used exclusively, because it has found widespread use in fundamental studies on interfacial structure and dynamics and transmembrane charge separation processes, and as organizing matrices for integrated chemical and photochemical systems[18, 19]. For example, mechanisms of oxidation-reduction reactions across DHP vesicle bilayers have been extensively studied in this lab. Electrogenic charge transfer across the vesicle membranes gives rise to a transmembrane electrical potential that opposes further reaction. Lipophilic ion movement is required to dissipate the electrical potential established; often the net reaction becomes rate-limited by the permeabilities of these charge-compensating ions.

Patterson and Hurst have described a microheterogeneous system wherein oxidation-reduction across DHP vesicle bilayers is controlled by addition of a lipophilic ion to the system[20]. DHP vesicles were prepared containing equal concentrations of entrapped 1,1'-dimethyl-4,4'-bipyridinium (MV^{2+}) and external 1-methyl-1'-sulfanato-n-propyl-4,4'-bipyridinium (MSV^+) ions. In the absence of lipophilic ions, addition of dithionite ions gave reduction of only 60% of the total viologen present. When a lipophilic cation, 1-methyl-4,4'-bipyridinium (MB^+), was added in slight molar excess to this system, the remainder of the viologen was reduced within a few minutes. Because reduced MSV^0 is uncharged, its transmembrane movement does not dissipate the electric gradient generated by inward transmembrane movement of electrons. Consequently, a transmembrane potential

quickly developed that blocked further reaction. Adding MB^+, which has no redox chemistry under these conditions but does have high intrinsic permeability towards bilayer membranes, provided a mechanism for collapsing the electrical gradient. The MB^+ ion was taken up in a 1:1 stoichiometric ratio with electrons transferred across the bilayer, thereby allowing transmembrane redox to proceed to completion. So, the lipophilic ion provided a switching mechanism controlling electron conduction across the bilayer. Because this kind of system is limited by lipophilic ion permeability, a gated ion channel is probably necessary both for microstructural stability and to provide acceptable ion transfer rates. These properties are found in the membrane protein, bacteriorhodopsin (bR), which is considered as a potential switching element.

Bacteriorhodopsin was discovered by W. Stoeckenius in the late 1960s. It is the only protein of purple membrane of *Halobacterium halobium*, and accounts for 75% of the dry mass of the purple membrane, while the remainder is lipids[22, 23]. Bacteriorhodopsin contains one mole of retinal per mole of protein. The retinal is covalently linked as a Schiff base to a lysine (Lys216) residue of the protein. In the native membrane, the retinal-protein complex has an absorption maximum at 560 nm ($\epsilon = 5.4 \times 10^4$ M^{-1} cm^{-1}). The protein consists of a single polypeptide chain of 248 amino acids and has a molecular weight of 2.6×10^4 daltons. The polypeptide chain arranges in the lipid bilayer as 7 α-helical rods about 40 Å in length with the C-terminus in the cytoplasmic side and the N-terminus in the extracellular side. This arrangement places the protein's charged residues near the surfaces of the membrane in contact with the aqueous solvent; the internal charged residues line in the center of the helix bundle so as to form a hydrophilic channel that permits the passage of protons. Properly oriented bR functions as a light-driven proton pump[24], i.e., adsorption of a photon by the retinal causes 13-trans to 13-cis isomerization which leads to configurational changes with simultaneous release of protons to the exterior, and the original chromophore is then regenerated by uptake of protons from the cytoplasmic side. The photochemical cycle of the purple membrane upon illumination
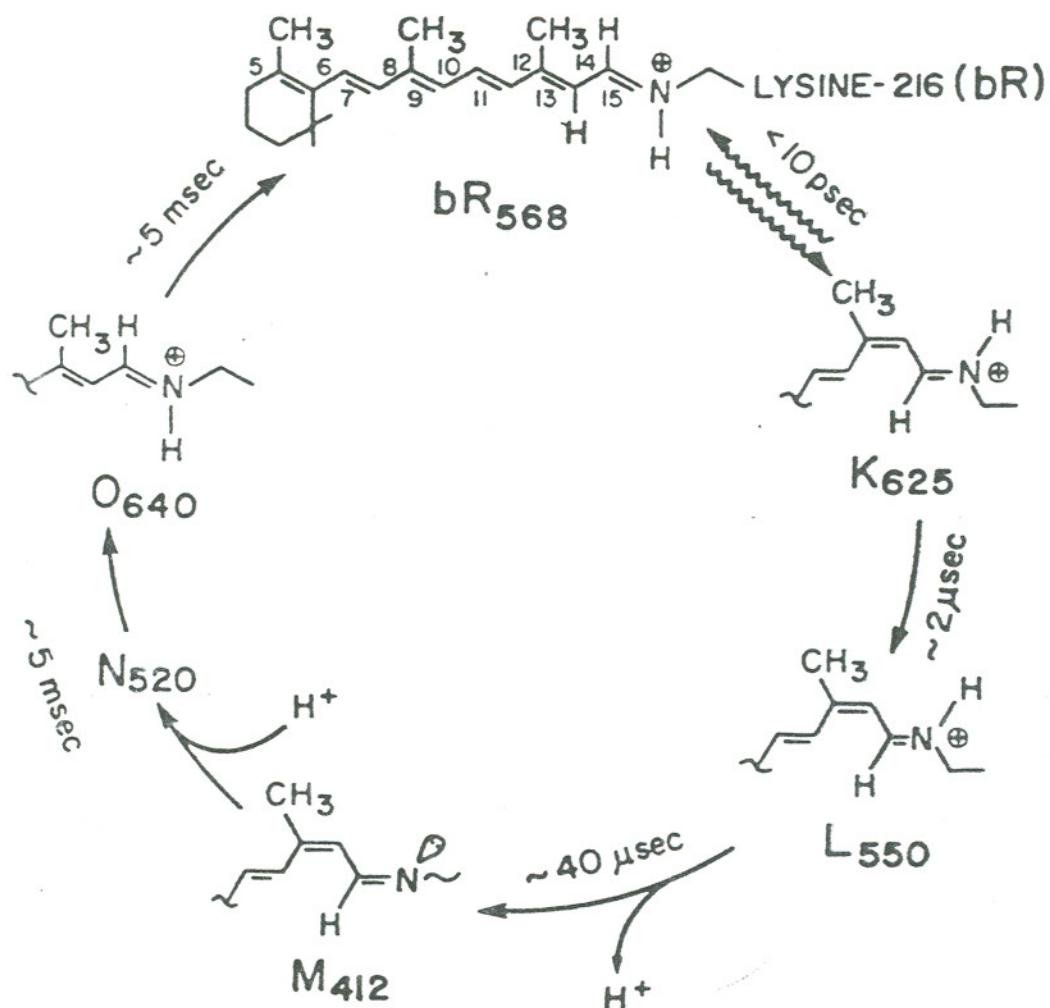
Figure 1-4. Photochemical cycle of the purple membrane. K, L, M, N, and O represent the intermediates in the cycle. The numbers in subscripts are the absorption maxima in the optical spectra. In L — early M, the protonated Schiff base gives its proton to the carboxyl group of Asp85. In late M —— N, the deprotonated Schiff base receives a proton from the carboxyl group of Asp96 , and possibly Asp85 releases a proton to the extracellular phase. The exact time of release of the proton from Asp85 to extracellular phase is not yet clear. In N, the carboxyl group of Asp96 takes a proton from cytoplasmic surface, thus a proton is transferred from intracellular space to the extracellular medium. Adapted from reference 25.

is shown in Figure 1-4[25]. Bacteriorhodopsin has been incorporated into various lipid vesicles[26]. Usually the orientation of bR in the reconstituted vesicles was opposite to that in native membrane, so that bR pumped protons from the vesicle exterior to the interior when illuminated with light. If bR could be incorporated into the DHP vesicle bilayers containing a vectorially oriented redox system that transfers electrons the same direction as protons, the transmembrane oxidation-reduction reaction might be regulated using protons as compensatory ions just by controlling light levels. Such an assembly is shown in Figure 1-5.

Small unilamellar vesicles (SUV) of DHP can be formed by ultrasonication[27]. The vesicles are highly hydrated spherical, or nearly spherical, particles with mean hydrodynamic radii of 10-13 nm. Each vesicle contains 4×10^3 DHP molecules. Figure 1-6 shows the structure of DHP vesicles. The passive H^+/OH^- permeability across DHP vesicle bilayers was studied by a pH jump experiment. The pH change inside DHP vesicles was monitored by a pH sensitive fluorescent dye, 8-hydroxy-1,3,6-pyrenetrisulfonate (pyranine)[28]. A pH jump outside DHP vesicles caused a fast large initial pH change followed by a slow continued change in the same direction. A typical curve of pH change with time is shown in Figure 1-7.

Incorporation of bacteriorhodopsin into DHP vesicle bilayers was performed by simply cosonicating or incubating the mixture of two in 20 mM, pH 8.0, Tris-HCl buffer. The ratio of protein to vesicle was 1:1 (mole/mole). The distribution of bR in the vesicles was characterized by centrifugation on a linear sucrose density gradient.
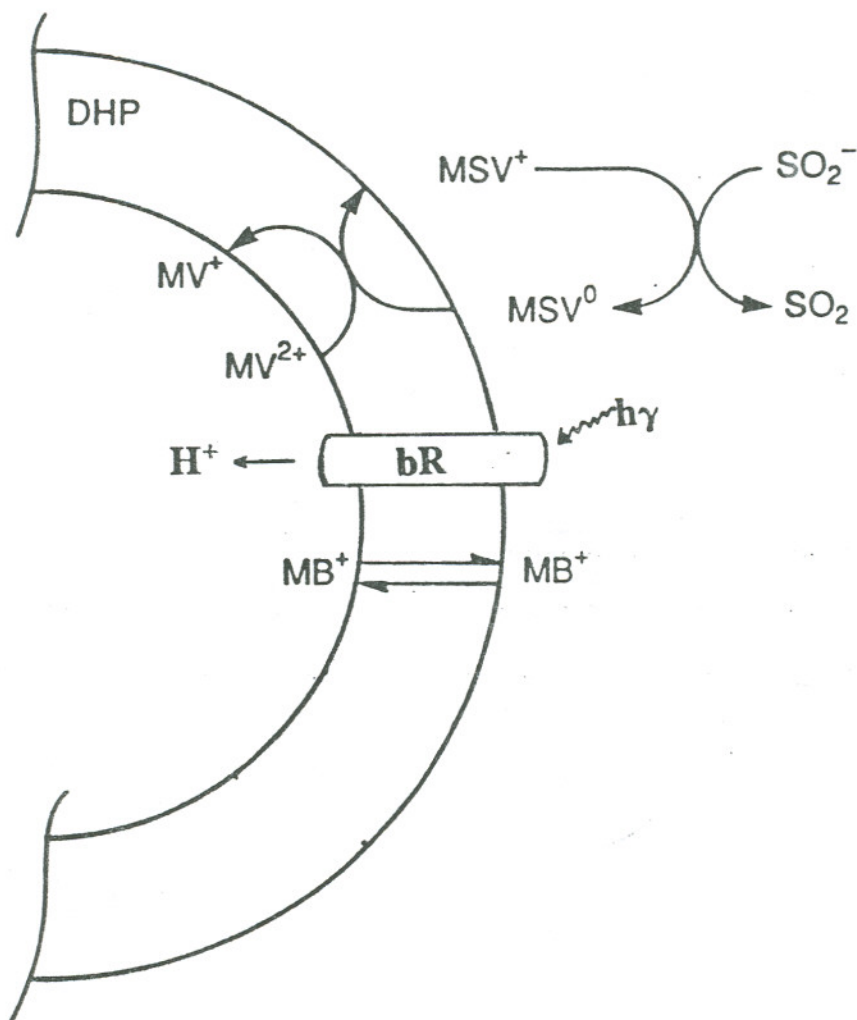
Figure 1-5. An assembly using bacteriorhodopsin as a switch to control electron movement across the DHP membrane. With the light on, bR pumps protons from the external medium to the internal medium collapsing the transmembrane potential, electrons move inwardly and the membrane is conducting; with the light off, protons, and hence electrons, do not move and the membrane is nonconducting. Adapted from reference 20.

a

Aqueous phase   Membrane   Aqueous phase

DHP

~40Å

b

|40| —180— |40|
 Å   Å   Å
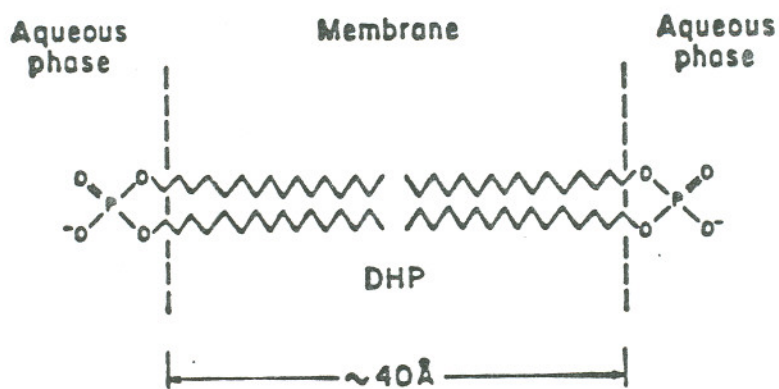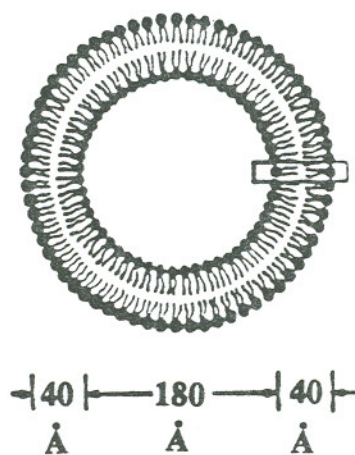
Figure 1-6. (a) The chemical structure of dihexadecylphosphate (DHP) and the relative orientation of DHP within the membrane. (b) Cross-section of DHP small unilamellar vesicles. Adapted from reference 19.
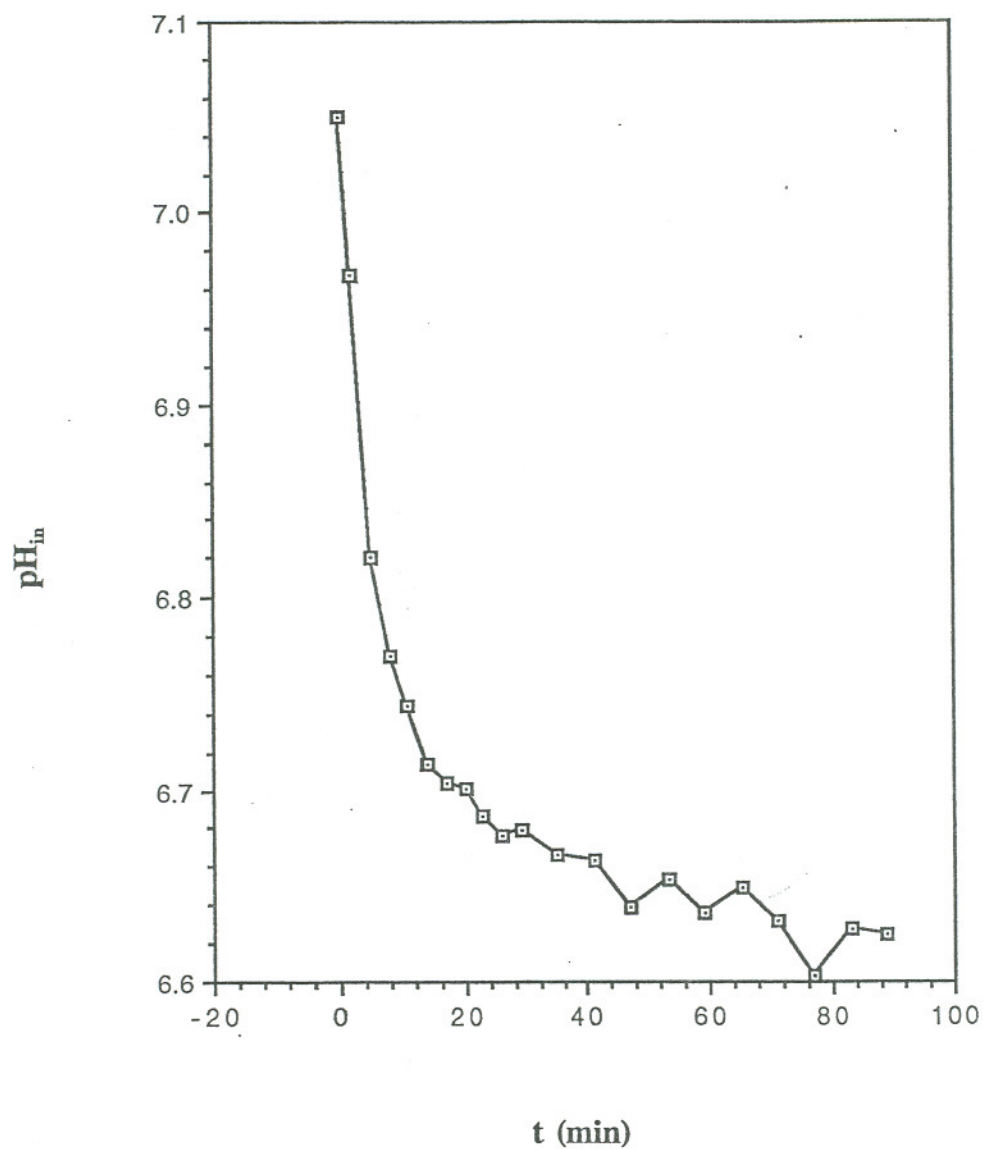
Figure 1-7. Changes in pH$_{in}$ in DHP vesicles with time after applying an external pH jump. 0.5 ml of 20 mM Tris-HCl, pH 2.02, was added to 0.5 ml of 8 mM DHP vesicles with entrapped pyranine in 20 mM Tris-HCl buffer, pH 7.96. pH$_{in}$ was determined from the excitation fluorescence profiles at 404 and 455 nm (λ_{em} = 510 nm) of entrapped pyranine according to the pyranine calibration curve.

CHAPTER 2
EXPERIMENTAL

Materials:

Dihexadecylphosphate (DHP), tris(hydroxymethyl)aminomethane, tetraphenylphosphonium chloride, and tetrabutylammonium hydroxide (40%) were purchased from Aldrich, pyranine was purchased from TCI, and thiamine from Sigma. DHP was recrystallized from methanol; other chemicals were used as received. Sephadex G-25-80 Fine gel was purchased from Sigma and Chelex 100 ion exchange resin from Bio-Rad. Deionized water was used throughout the experimental process.

Vesicle Preparation:

The DHP small unilamellar vesicles (SUV) were prepared using methods developed in this lab[21, 27]. Usually 8 mM DHP SUVs were formed by ultrasonic dispersal using either a Heat Systems Ultrasonics Model W-185F or W-225 instrument equipped with a 0.5 inch flat tip on a conventional horn operated at a power setting of 4.0 (30 W). Appropriate amounts of DHP powder in 20 mM Tris-HCl or Tris-HNO$_3$, pH 8.0, buffer or in H$_2$O whose pH was adjusted with NaOH or tetrabutylammonium hydroxide were sonicated for two 10-minute periods separated by 5-minute cooling time. The resulting opalescent solution was then filtered through a cellulose nitrate membrane filter with a pore size of 0.2 μm to remove titanium particles sloughed from the sonicator tip and larger DHP aggregates. The suspension was then centrifuged for 90 minutes at 20°C in TY 65 rotor at 36,000 rpm (approximately 100,000 g) using either a Beckman L5-65 or L8-M ultracentrifuge.

14

This procedure removed multilamellar vesicles, any remaining undispersed lipids, and titanium particles. By completion of the centrifugation, the sample had separated into three fractions consisting of a very small gelatinous pellet covered with a relatively viscous layer, which together represented less than 5% of the total liquid volume, and a slightly translucent bulk supernatant, which appeared homogeneous. The supernatant was carefully removed by aspiration with a Pasteur pipet for further use.

For pH jump experiments, it was necessary to entrap pyranine inside DHP vesicles. Therefore, 1 mM pyranine was added to the initial DHP dispersing solution. The mixture was cosonicated as described above. The unentrapped pyranine was then removed using Sephadex gel filtration columns.

Column Chromatography:

In this work two types of chromatography were employed: gel exclusion and ion exchange. Gel exclusion chromatography was used to remove pyranine from exterior of DHP vesicles. Cation exchange chromatography was used to remove tetraphenylphosphonium cations, methylviologen, or potassium ions from the outer surfaces of DHP vesicles.

The gel exclusion chromatography column was packed using Sephadex G-25-80 Fine packing material. The gel was first hydrated for 3 hours in water and then packed into a large column (1.5 × 17.5 cm) and a small one (1.5 × 6.5 cm). Column void volumes were then determined by measuring the volume of solvent needed to elute a concentrated solution of Blue Dextran. The columns were then pre-equilibrated to the desired pH by washing the column with ten times the void volumes of the buffer to be used. The cosonicated DHP and pyranine vesicle suspension was then loaded onto the large column and eluted with the same buffer in which the vesicles were prepared. After the void volume had eluted, effluent was collected to a total volume that was 1 ml greater than the volume loaded. This

chromatography procedure removed most of unentrapped pyranine. In order to determine whether the separation was complete, the effluent from the first column was applied to the small column. The total fluorescence before and after passing the vesicle suspensions down this column was compared by fluorescence spectroscopy. Complete removal of unentrapped pyranine was also checked by adding thiamine, which is a membrane-impermeable quencher of pyranine fluorescence and therefore presumably only quenched the unentrapped pyranine[29]. Sephadex resin was regenerated by unpacking the column and washing exhaustively with water to ensure it was clean for the next experiment.

Cation exchange chromatography was performed to remove external tetraphenylphosphonium, methylviologen, and potassium ions using Chelex 100 ion exchange resin. The resin itself consisted of diacetic acid amine groups attached to a styrene divinylbenzene copolymer matrix[30]. It was effective over the pH range of 2-14. Figure 2-1 shows changes in the degree of ionization of Chelex resin with increasing pH. The resin was packed into a column (0.8×10 cm) with a glass frit at the bottom. The void volume was determined using a concentrated solution of Blue Dextran. The column was at first pre-equilibrated with the buffer to be used to the exact pH of the sample. The mixture of DHP vesicles and cations was slowly added to the column while eluting with the buffer. After the void volume was eluted, a volume of effluent 1 ml greater than the sample volume was collected. The concentration of tetraphenylphosphonium ion inside the DHP vesicles was determined by spectrophotometry using the absorption maximum at 270 nm ($\epsilon = 3.5 \times 10^3$ M^{-1} cm^{-1})[31]. The concentration of potassium ion in the interior of DHP vesicles was determined by atomic absorption spectrophotometry at a wavelength of 766.5 nm (see below). The Chelex resin was regenerated by the following procedures:

First, 2 bed volumes of 1 N HCl or HNO_3 were run through, followed by 5 bed volumes of water, then 2 bed volumes of 1 N NaOH, followed by 5 bed volumes of water. Then one bed volume of 0.5 M Tris-HCl or Tris-HNO_3 was run through in order to quickly equilibrate the pH of column close to the pK_a of Tris buffer.
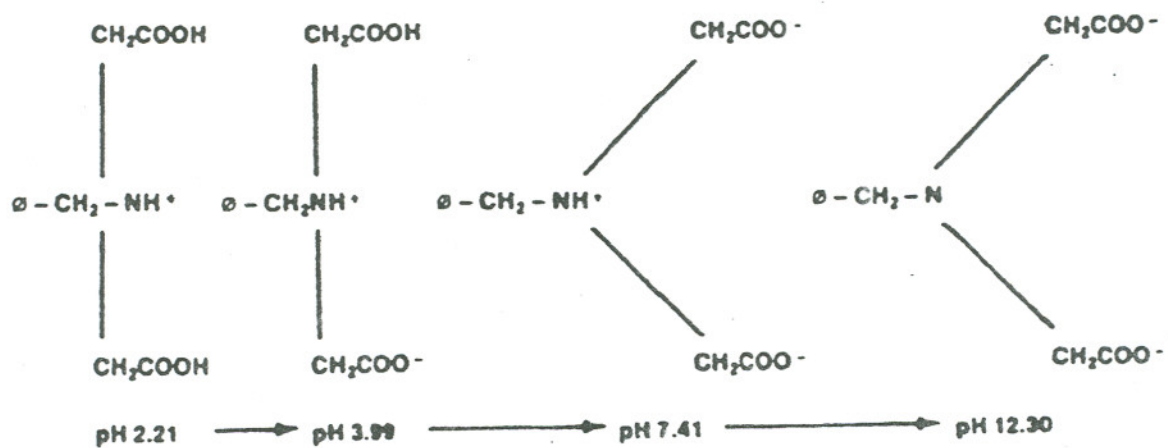
Figure 2-1. Change in the degree of ionization of Chelex resin with increasing pH. Adapted from reference 30.

Finally, 5 bed volumes or more of less concentrated buffer to be used was eluted to give the desired pH.

Equilibrium Dialysis:

Equilibrium dialysis techniques were employed to determine the strength of pyranine binding to the DHP vesicle surfaces. The dialysis cells were made of two 5 ml chambers separated by a Scienceware #40299 cellulose membrane (6×10^3 M.W. cutoff). The experiment was done by filling one chamber with 8 mM unloaded DHP vesicles in 20 mM Tris-HCl buffer solution and the other with 1 mM pyranine in the same buffer at the same pH. A comparable experiment was done by filling one chamber with 8 mM DHP vesicles plus 1 mM pyranine in 20 mM Tris-HCl buffer and the other with 20 mM Tris-HCl buffer at the same pH. The dialysis cells were then placed on a slow-moving shaker and the solutions were allowed to equilibrate overnight. The concentration of pyranine in each chamber was determined with a HP 8452A Diode Array spectrophotometer.

Phosphate Analysis:

The concentration of DHP was determined by analyzing the phosphate concentration as described by Ames[32]. Briefly, this analysis involved pyrolyzing the sample, then coordinating the phosphate ion as a phosphomolybdate complex that was subsequently reduced with ascorbic acid, resulting in a blue solution which had an absorption maximum at 820 nm. Analytical reagents used were:
(a) 10% $Mg(NO_3)_2 \cdot 6\ H_2O$ dissolved in 95% alcohol. (b) HCl, 0.5 N. (c) ascorbic acid, 10%. (d) 0.42% ammonium molybdate$\cdot 4\ H_2O$ in 1 N H_2SO_4 (28.6 ml conc. H_2SO_4 and 4.2 g ammonium molybdate$\cdot 4\ H_2O$ to 1000 ml H_2O). Reagent (c) was stored in the refrigerator, and was replaced monthly. One part reagent (c) was mixed with 6 parts reagent (d) for daily use. Explicit analytical procedures were as follows:

To 10-100 μl of phosphate sample (containing up to 0.07 micromole of phosphate) in a Pyrex 13×100 mm test tube was added 30 μl of the magnesium nitrate solution. The material was taken to dryness and ashed by shaking the tube over a strong flame until the brown fumes disappeared. The tube was then allowed to cool and 300 μl of 0.5 N HCl was added. The tube was capped and heated in a boiling water bath for 15 minutes to hydrolyze any pyrophosphate formed in the ashing to phosphate. Cooling the tops of the tubes with a stream of air helped to minimize evaporation. After the tube had cooled, 700 μl of the reagent (c) and (d) mix was added and the tubes were incubated 20 minutes at 45°C. The absorbance was then read at 820 nm and compared to a calibration curve prepared from standards (Figure 2-2) to determine the phosphate concentration.

Atomic Absorption Spectroscopy:

Atomic absorption spectroscopy was used to analyze the concentration of potassium ions in the sample[33]. The light source for potassium ion was a combined NaK Hollow Cathode Lamp (Perkin-Elmer Intensitron Lamp M-1915). The flame used was air-acetylene with a maximum temperature of 2200°C. Detection was at 766.5 nm wavelength using a 1.4 nm slit; the instrument sensitivity under these conditions was 0.043 mg / l. The working condition for potassium was that the absorbance fell below 0.30. For the oxidant (air), the pressure at the tank regulator was set to 50-80 psi, the burner regulator pressure to 30 psi, and the flow rate to about 21.5 l / min. For the fuel (acetylene), the pressure at the tank regulator was at 12 psi, burner regulator pressure at 8 psi, and the flow rate at about 3.5 l / min.

For each series of measurements a working curve was first made by measuring the absorbances of several standard solutions containing potassium chloride. A plot of absorbance versus potassium ion concentration was linear at concentrations ≤ 2 mg/l. Then the absorbances of samples were measured and the concentrations of potassium ions in samples were obtained from the working curve.

$$y = -1.2850e\text{-}2 + 2.3265e\text{-}2x \quad R^2 = 0.942$$
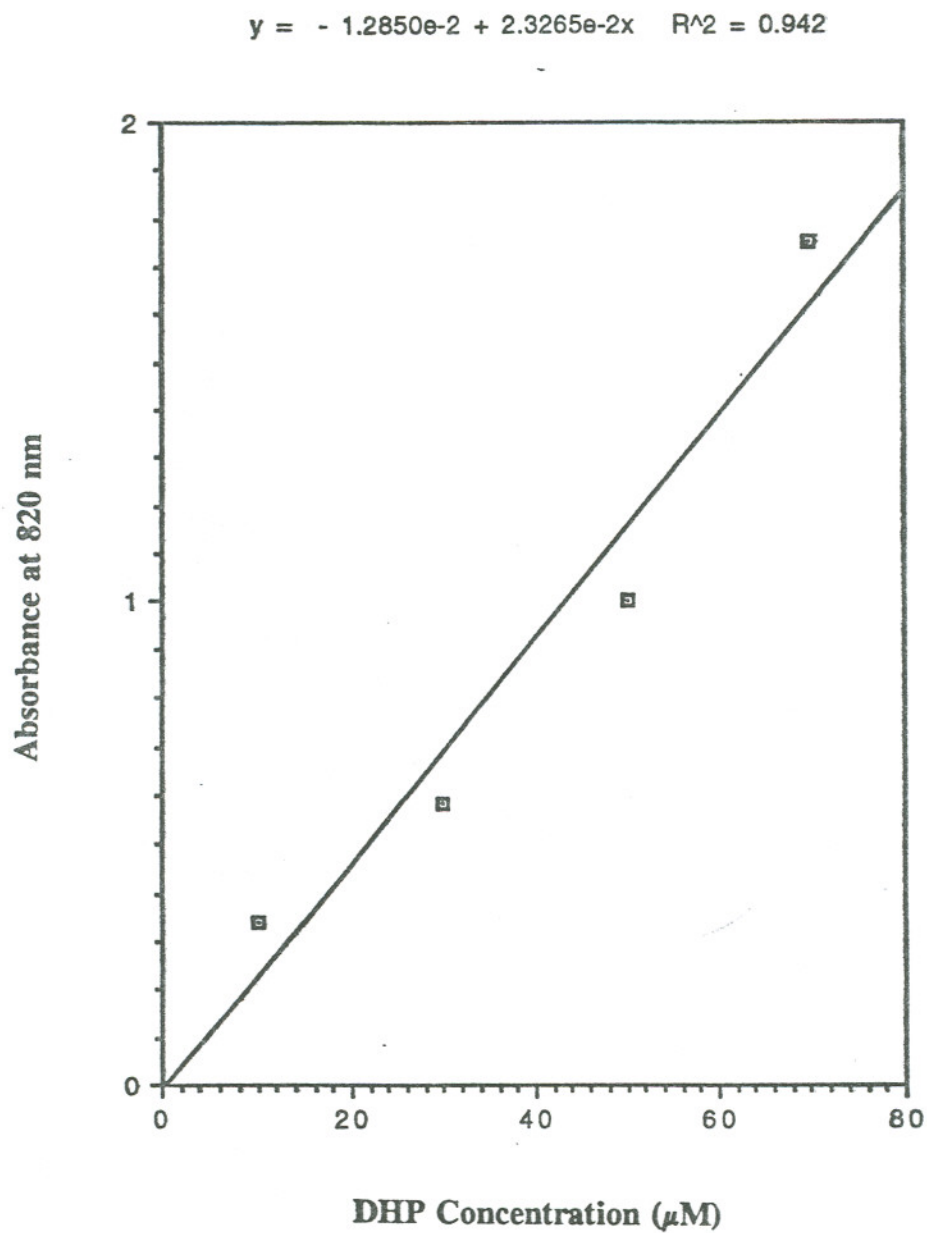
Figure 2-2. Phosphate calibration curve. Known concentrations of DHP vesicles were used in the phosphate analysis as described in Experimental Methods. The absorption intensity of phosphomolybdate complex at 820 nm was plotted versus phosphate concentration.

Growth of *Halobacterium halobium*:

Bacteriorhodopsin (bR) was isolated from *Halobacterium halobium*[34] in the laboratory of Professor George Rayfield at the University of Oregon. The absorption spectrum is shown in Figure 2-3.

Sucrose Density Gradient:

A linear sucrose density gradient was prepared using a small acrylic plastic Hoefer gradient maker[35]. It was constructed of two chambers, a mixing chamber and a reservoir chamber connected by a Teflon stopcock valve. A side outlet port from the mixing chamber was connected to a peristaltic pump for delivery of the gradient to an appropriate receptacle. Equal volumes of two starting sucrose solutions in 20 mM Tris-HCl buffer, pH 7.80, 5% and 35% (wt%), which defined the limits of the gradient, were placed in the two chambers with the valve between them closed. When the stopcock was opened, solution from the reservoir chamber entered the mixing chamber and equilibrated with the constantly changing mixing solution, which was simultaneously withdrawn as the gradient was poured into a centrifuge tube which had a 1-ml 45% sucrose solution as a cushion. The level of the liquid in both chambers fell at the same rate. The concentration of solute in the mixing chamber at any time was a linear fraction of volume poured. Thus, a linear sucrose density gradient from 5% to 35% was made.

The cosonicated mixture of bacteriorhodopsin and DHP vesicles was then placed on top of the sucrose density gradient and centrifuged at 17,500 rpm for 17 hr at 20°C in a Beckman SW 27.1 swinging bucket rotor[36]. Vesicles containing no bR remained at the top of the gradient, vesicles incorporating protein formed a band in the middle, and the unincorporated protein sedimented to the bottom of the gradient.
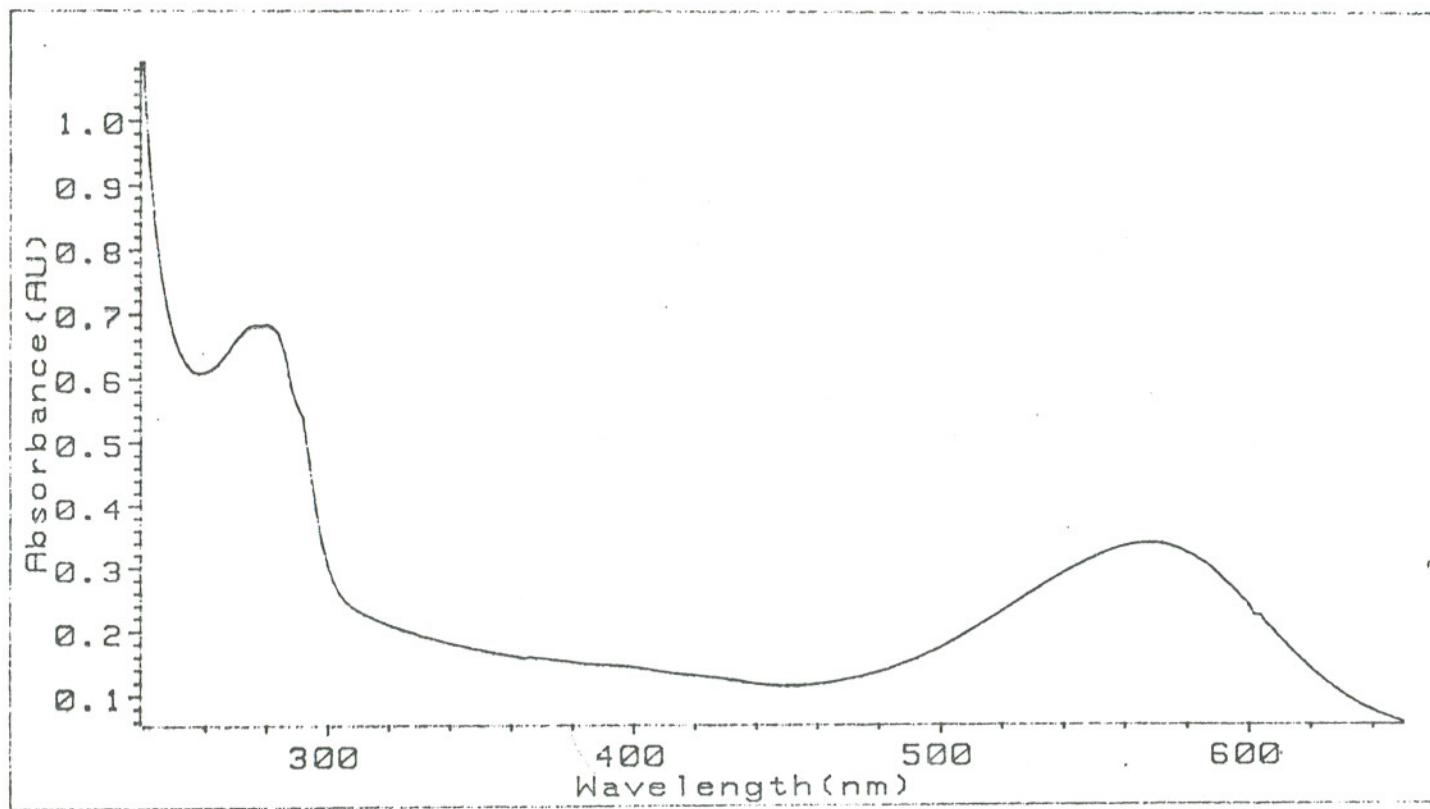
Figure 2-3. Absorption spectrum of *Halobaterium halobium* purple membrane.

Instruments:

Fluorescence spectra were obtained using a Perkin-Elmer MPF 66 Fluorescence Spectrophotometer, which has an excitation and emission range of 200-900 nm. Its light source is a xenon lamp, and the detector is a standard photomultiplier tube. It was operated using a 7700 Professional Computer. The absorption spectra from phosphate analysis were taken on a Perkin-Elmer Lambda 9 UV/Vis/NIR Spectrophotometer with a wavelength range of 185-3200 nm. It is a continuous scanning, double beam, double monochromator instrument. All other absorption spectra were taken on a HP 8452A Diode Array Spectrophotometer which scans the spectrum over the entire range of 190-820 nm at a maximal rate of 0.6 seconds. Analysis of potassium ions was done using a Perkin-Elmer 703 Atomic Absorption Spectrophotometer which measures the concentration of metallic elements in a variety of matrices. It provides integrated readings in absorbance, concentration or emission intensity over a period of 0.2 to 60 seconds. It is a double-beam, time-shared system and the detector is a single photomultiplier. DHP vesicle suspension was prepared using Model W-225 or W-185F Sonicator, and Beckman L8-M or Beckman L5-65 Ultracentrifuge. The stopped-flow apparatus used was a Hi-Tech Scientific SFA-II Rapid Kinetics Accessory.

CHAPTER 3

RESULTS AND DISCUSSION

I.   Pyranine Calibration Curve

The fluorescence intensity (at 510 nm) of the hydrophilic pyrene analogue 8-hydroxy-1,3,6-pyrenetrisulfonate (pyranine) was strongly dependent upon the degree of ionization of the 8-hydroxyl group, and hence upon the medium pH, over the range of pH 5-9[28]. The structure of pyranine is

$\lambda_{max} = 404$ nm $\lambda_{max} = 455$ nm
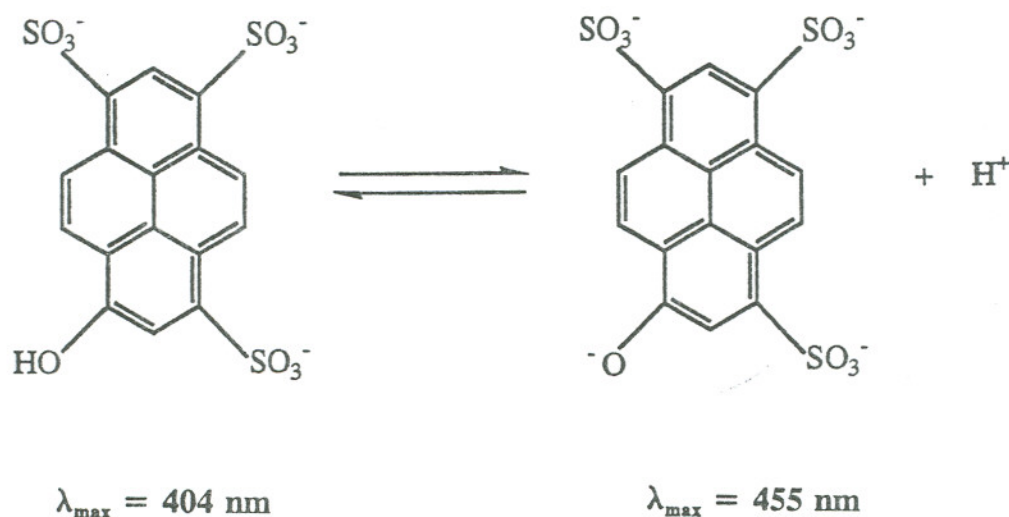
The excitation spectra of pyranine at the emission wavelength of 510 nm had two maxima. The one at 404 nm corresponds to the protonated form of the dye, the other at 455 nm is due to the deprotonated form. There is only one emission maximum of pyranine at 510 nm over the entire pH range. This is due to the deprotonated form of pyranine. The excitation and emission spectra of pyranine at different pH values are shown in Figure 3-1.

The quantitative relationship between fluorescence intensity $(I_f)_\lambda$ and

a

b
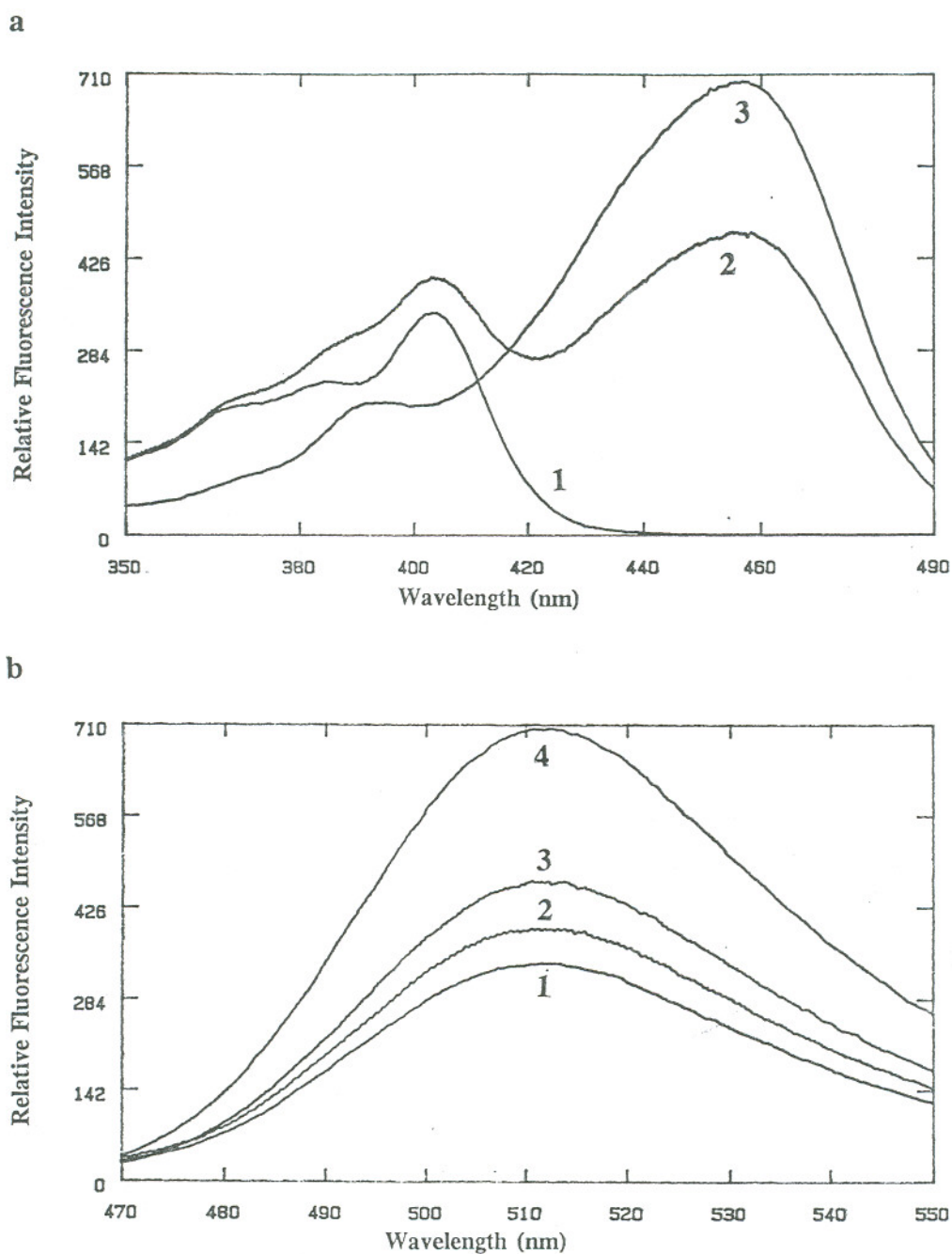
Figure 3-1. (a) Excitation spectra (λ_{em} = 510 nm) of 0.1 μM pyranine in 25 mM phthalate buffer at pH 4.05 (trace 1), phosphate buffer at pH 7.57 (trace 2), and borate buffer at pH 10.00 (trace 3) at room temperature. (b) Emission spectra (λ_{ex} = 404 nm) of 0.1 μM pyranine at pH 4.05 (trace 1), and pH 7.57 (trace 2); emission spectra (λ_{ex} = 455 nm) of 0.1 μM pyranine at pH 7.57 (trace 3), and pH 10.00 (trace 4).

concentration has been described as follows[37]:

$$(I_f)_\lambda = f(\theta)\, g(\lambda)\, I_o\, \phi_f\, \epsilon\, b\, c\, \exp(-\epsilon\, b\, c) \tag{1}$$

where:

$(I_f)_\lambda$ is the sample fluorescence intensity at a given wavelength

$f(\theta)$ is the geometric factor depending on the effective solid angle viewed by the detector

$g(\lambda)$ is the response characteristic of the detector (varies with wavelength)

I_o is the intensity of the excitation radiation

ϕ_f is the quantum efficiency of the molecule

ϵ is the extinction coefficient for the sample at the exciting wavelength

b is the sample path length along the axis of irradiation

c is the concentration of the fluorescing material in moles/liter

When the concentration of fluorescing material is very small ($\epsilon.b.c$ for the sample is less than 0.05), Equation (1) reduces to:

$$(I_f)_\lambda = f(\theta)\, g(\lambda)\, I_o\, \phi_f\, \epsilon\, b\, c = J_\lambda\, \phi_f\, \epsilon\, b\, c \tag{2}$$

where J_λ, equal to $f(\theta)\, g(\lambda)\, I_o$, varies only with wavelength.

The fluorescence intensity at the excitation wavelength of 455 nm ($\lambda_{em} = 510$ nm), I_{455}, and the intensity at the excitation wavelength of 404 nm ($\lambda_{em} = 510$ nm), I_{404}, were related to the bulk pH as follows:

In very basic solution, the intensity at 455 nm is very strong and the intensity at 404 nm is relatively weak, while in very acidic solution, the intensity at 404 nm is strong and emission at 455 nm is negligible. It follows according to equation (2) that:

$$I_{455} = J_{455}\, \phi_{py}\, \epsilon_{py}^{455}\, x \tag{3}$$

$$I_{404} = J_{404}\, [\, \phi_{pyH}\, \epsilon_{pyH}^{404}\, (c - x) + \phi_{py}\, \epsilon_{py}^{404}\, x\,] \tag{4}$$

where ϕ_{pyH} and ϕ_{py} are the quantum efficiencies of the protonated and deprotonated forms of pyranine, respectively; ϵ_{py}^{455} and ϵ_{py}^{404} are the extinction coefficients of the deprotonated form of pyranine at excitation wavelength of 455 and 404 nm, respectively; ϵ_{pyH}^{404} is the extinction coefficient of the protonated form of pyranine at excitation wavelength of 404 nm; c is the total analytical concentration of pyranine;

and x is concentration of the deprotonated form of pyranine.

The ratio of equations (3) and (4) is:

$$\frac{I_{455}}{I_{404}} = \frac{J_{455}}{J_{404}} \frac{\phi_{py} \, \epsilon_{py}^{455} \, x}{[\phi_{pyH} \, \epsilon_{pyH}^{404} \, (c-x) + \phi_{py} \, \epsilon_{py}^{404} \, x]}$$

Given that $\phi_{pyH} = \alpha \, \phi_{py}$; $\epsilon_{pyH}^{404} = \beta \, \epsilon_{py}^{404}$; $J_{455} \, \epsilon_{py}^{455} / J_{404} \, \epsilon_{py}^{404} = \gamma$, where α, β and γ are constants, we obtain upon substitution into the above equation:

$$\frac{I_{455}}{I_{404}} = \frac{J_{455}}{J_{404}} \frac{\epsilon_{py}^{455} \, x}{[\alpha \epsilon_{pyH}^{404} \, (c-x) + \epsilon_{py}^{404} \, x]}$$

$$\frac{I_{455}}{I_{404}} = \frac{J_{455} \, \epsilon_{py}^{455}}{J_{404} \, \epsilon_{py}^{404}} \frac{1}{\{\alpha \, \beta \, [(c-x)/x] + 1\}}$$

$$\frac{I_{455}}{I_{404}} = \frac{\gamma}{\alpha \, \beta \, [(c-x)/x] + 1}$$

$$\frac{c-x}{x} = \frac{\gamma \, I_{404} - I_{455}}{I_{455}} \frac{1}{\alpha \, \beta}$$

Since $pH = pK_a - \log [(c-x)/x]$,

$$\log [(c-x)/x] = -\log(\alpha \, \beta) + \log [(\gamma \, I_{404} - I_{455})/I_{455}]$$

it follows:

$$\log [(\gamma \, I_{404} - I_{455})/I_{455}] = pK_a + \log(\alpha \, \beta) - pH \tag{5}$$

There were two limiting conditions:

(a). At very high acidity, $x \cong 0$, $(c-x) \cong c$, and equations (3) and (4) become

$$(I_{455})_a = 0$$

$$(I_{404})_a = J_{404} \, \phi_{pyH} \, \epsilon_{pyH}^{404} \, c$$

From the optical absorption spectrum of a known concentration of pyranine, the extinction coefficient of the protonated form of pyranine at 404 nm, ϵ_{pyH}^{404}, was determined to be 1.8×10^4 M^{-1} cm^{-1}.

(b). Under very basic condition, $x \cong c$, $(c-x) \cong 0$, and equations (3) and

(4) become

$$(I_{455})_b = J_{455}\ \phi_{py}\ \epsilon_{py}^{455}\ c$$

$$(I_{404})_b = J_{404}\ \phi_{py}\ \epsilon_{py}^{404}\ c$$

From the optical absorption spectrum of known concentrations of pyranine, the extinction coefficients of protonated pyranine at 455 nm and 404 nm, ϵ_{py}^{455} and ϵ_{py}^{404}, were determined to be 2.0×10^4 and 6.8×10^3 M^{-1} cm^{-1}, respectively.

From these limiting equations the proportionality constants γ and $\alpha\ \beta$ could be evaluated, i.e.:

$$\frac{(I_{455})_b}{(I_{404})_b} = \frac{J_{455}\ \epsilon_{py}^{455}}{J_{404}\ \epsilon_{py}^{404}} = \gamma \tag{6}$$

$$\frac{(I_{404})_a}{(I_{404})_b} = \frac{\phi_{pyH}\ \epsilon_{pyH}^{404}}{\phi_{py}\ \epsilon_{py}^{404}} = \alpha\ \beta \tag{7}$$

From equations (6) and (7) γ and $\alpha\ \beta$ were both determined to be 3.2. Knowing β from the ratio of ϵ_{pyH}^{404} to ϵ_{py}^{404} which was 2.6, then α, the ratio of ϕ_{pyH} to ϕ_{py}, was determined to be 1.2. From ϵ_{py}^{455}, ϵ_{py}^{404}, and γ the ratio of J_{455} to J_{404} was calculated to be 1.1. These values make sense under our experimental conditions. The plot of $\log\ [(\gamma\ I_{404} - I_{455}) / I_{455}]$ versus pH gave a line with the slope of -1 and intercept of $pK_a + \log\ (\alpha\ \beta)$. At $pH = \log\ (\alpha\ \beta)$, $pK_a = \log\ [(\gamma\ I_{404} - I_{455}) / I_{455}]$. Figure 3-2 shows the pyranine calibration curve, from which pK_a of pyranine was found to be 7.52 in the bulk solution. The pH over the range of 5-9 could be determined by this method.

Kano and Fendler[28] reported a pK_a value for pyranine of 7.2. They related the ratio of the emission intensities at 510 nm upon exciting pyranine at 450 nm and 400 nm, $I_{450} : I_{400}$, to the hydrogen ion concentration. However, as the above derivation shows, no linear relationship exits between $\log\ (I_{450} / I_{400})$ and pH. Specifically, from

$$\frac{I_{455}}{I_{404}} = \frac{\gamma}{\alpha\ \beta\ [(c - x) / x] + 1}$$
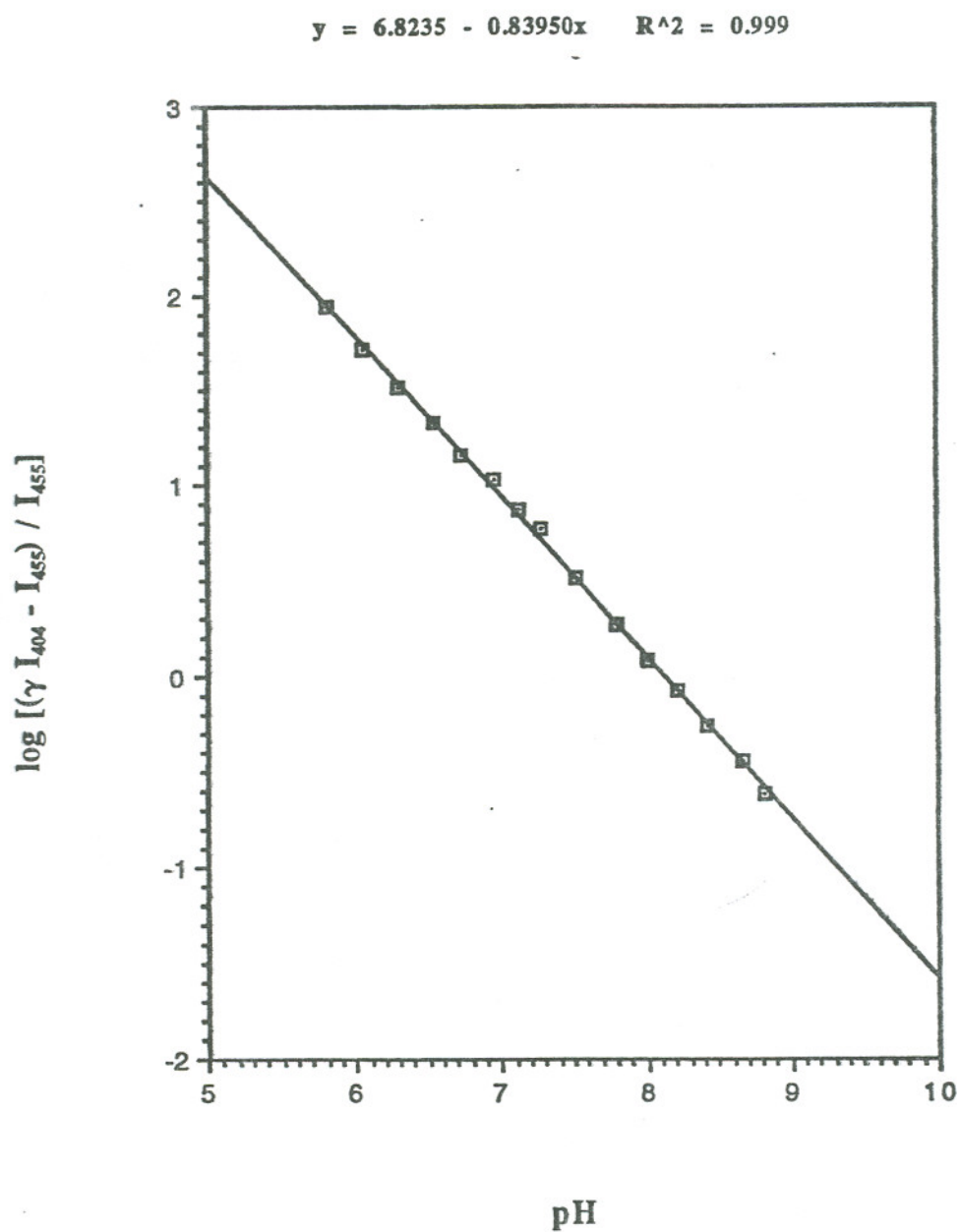
Figure 3-2. Pyranine calibration curve obtained from relative fluorescence intensities at excitation wavelengths of 404 nm and 455 nm (λ_{em} = 510 nm) at room temperature. (0.01 μM pyranine, 20 mM buffers: imidazole, pH 5.80-7.28, Tris-HCl, pH 7.12-8.82).

we obtain

$$\log (I_{455} / I_{404}) = \log \gamma - \log [1 + \alpha\beta 10^{(pKa - pH)}]$$

When $\alpha\beta 10^{(pKa - pH)} \geq 10$, the above equation could be reduced to

$$\log (I_{455} / I_{404}) \cong \log \gamma - \log [\alpha\beta 10^{(pKa - pH)}]$$

$$\log (I_{455} / I_{404}) \cong \log \gamma - \log (\alpha\beta) - pK_a + pH$$

Given the cited values of the constants, i.e., $\alpha\beta = 3.2$ and $pK_a = 7.52$ this approximation holds when $pH \leq 7.03$. Therefore, when $pH \rangle 7.03$, $\log (I_{455} / I_{404})$ is nonlinear with respect to pH. This is apparent from their calibration curve, which is reproduced in Figure 3-3.
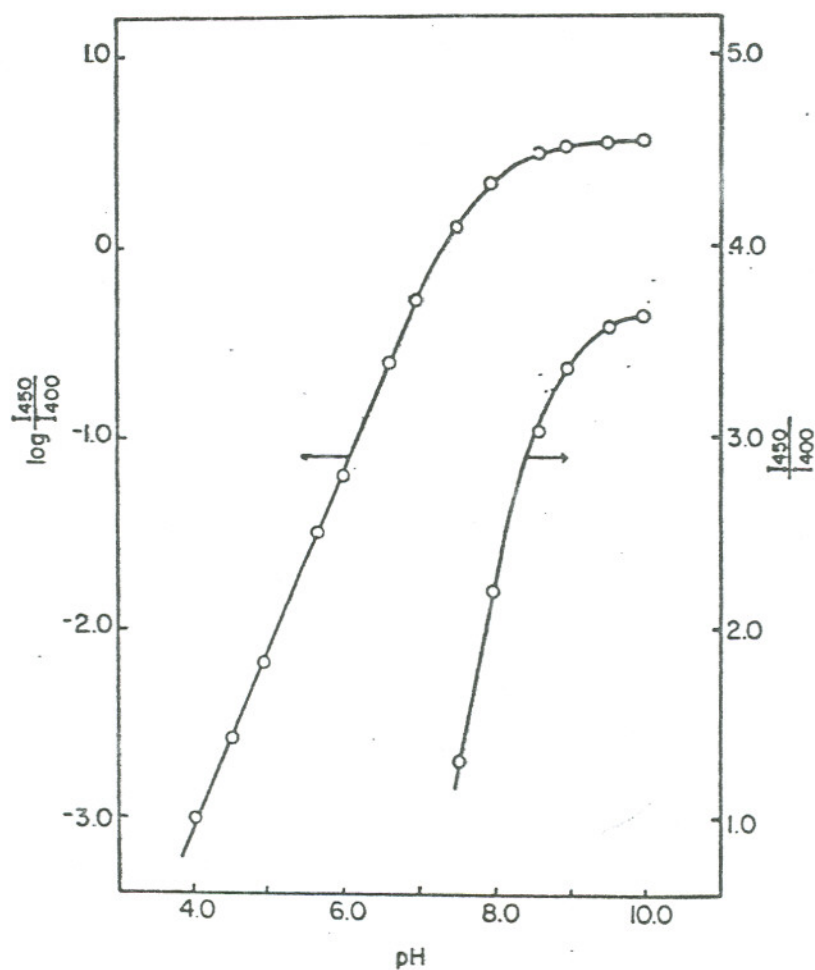
Figure 3-3. Ratios of relative intensities in the excitation spectra at 450 and 400 nm, observed at an emission wavelength of 510 nm, for 3.3×10^{-7} M aqueous air-saturated pyranine as a function of pH at 25.0°C. 5.0×10^{-3} M buffers (sodium acetate in pH 4.0-5.7, sodium phosphate in pH 6.0-8.0, and sodium borate in pH 8.6-10.0) were at a constant ionic strength of 0.10 M NaCl. Adapted from reference 6.

II. Equilibrium Dialysis

Pyranine is an extremely sensitive probe for monitoring pH in the interiors of negatively charged and at the outer surface of positively charged liposomes[28, 38]. Since the three sulfonate groups in pyranine were completely ionized over the measurable pH range, the probe should be repelled from the surface of the negatively charged liposomes. Therefore, the acidity of the bulk interior vesicle solution should be probed rather than the lipid/aqueous interfaces since DHP vesicles have highly negatively charged interfaces.

Equilibrium dialysis experiments were made to see if the pyranine anions would bind to the surfaces of DHP vesicles in 20 mM Tris-HCl, the experimental reaction medium. The principle of equilibrium dialysis is that the small molecules or ions, e.g., pyranine (M.W. 524) freely diffuse through a semipermeable membrane (6×10^3 M.W. cutoff) that separates two chambers. Large aggregates, e.g., a DHP vesicle (M.W. 2×10^6 Daltons), containing 4×10^3 DHP surfactant monomers per vesicle cannot diffuse through the membrane. If there were no binding of pyranine to the DHP vesicles, the pyranine would eventually distribute to give equal concentrations on both sides of the membrane. If there were binding, then the concentration of pyranine on the DHP vesicle side would be higher than that on the side without DHP vesicles. The above statements are true only if the Donnan effect of the vesicles is negligible. The Donnan effect refers to the influence of the charged, impermeable macromolecules on the distribution of small ions across the membrane[39].

Free diffusion and equilibration of pyranine through the semipermeable membrane was checked by filling one chamber with about 1 mM pyranine in 20 mM Tris-HCl buffer, and the other with the same buffer containing no pyranine. The solutions were agitated by gently shaking the cell. The concentrations of pyranine on both sides of membrane were measured by optical absorption spectroscopy at different

shaking times. The data are shown in Table 3-1. After three days the concentration of pyranine in each chamber was about the same.

Next, two similar equilibrium dialysis experiments were done with 8 mM DHP vesicles present in one chamber. For one set of experiments the buffer contained initially about 1 mM pyranine, while for the other set the DHP vesicle suspension contained initially about 1 mM pyranine. The results are shown in Table 3-2.

Consider the system with the negatively-charged DHP vesicles of a net charge n and concentration [M] on one side of a semipermeable membrane, and with freely equilibrated ionizable salts Na$_3$pyr and TrisCl shown below:

Semipermeable Membrane

Side 1   Side 2
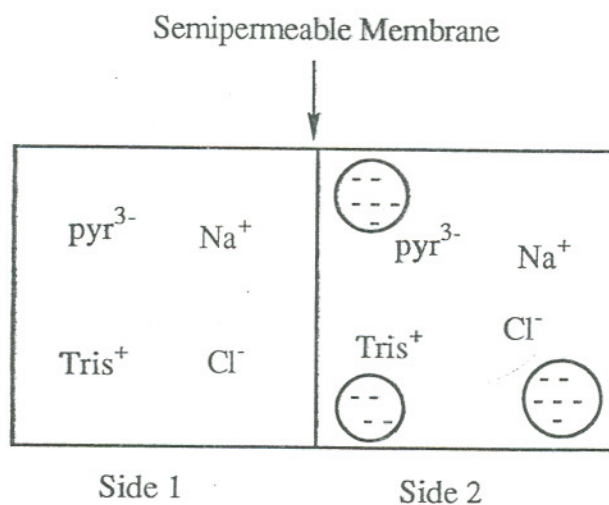
The salts ionize according to the equations:

Na$_3$pyr $\rightleftarrows$ 3Na$^+$ + pyr^{3-}
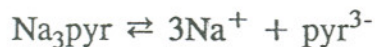
TrisCl $\rightleftarrows$ Tris$^+$ + Cl$^-$

The chemical potentials for Na$_3$pyr and TrisCl can be expressed as follows:

μ (Na$_3$pyr) $= 3\mu$ (Na$^+$) $+ \mu$ (pyr^{3-})

μ (Na$_3$pyr) $= \mu°$ (Na$_3$pyr) $+ RT\ln$ [Na$_3$pyr]

μ (Na$_3$pyr) $= 3\mu°$ (Na$^+$) $+ 3RT\ln$ [Na$^+$] $+ \mu°$ (pyr^{3-})$+ RT\ln$ [pyr^{3-}]

μ (Na$_3$pyr) $= 3\mu°$ (Na$^+$)$+ \mu°$ (pyr^{3-}) $+ RT\ln$ ([Na$^+$]^3[pyr^{3-}])

Table 3-1.   Equilibrium Dialysis of Pyranine in 20 mM Tris-HCl in the Absence of
DHP Vesicles

	Before Dialysis	After Dialysis		
		24 hours	48 hours	72 hours
Cell A[a]	1.31 mM	0.889 mM	0.683 mM	0.652 mM
Cell B[b]	0	0.448 mM	0.560 mM	0.634 mM
Total	1.31 mM	1.377 mM	1.243 mM	1.286 mM

[a] Pyranine in 20 mM Tris-HCl, pH 8.3.

[b] 20 mM Tris-HCl, pH 8.3.

Table 3-2   Equilibrium Dialysis of Pyranine in 20 mM Tris-HCl in the Presence of
8 mM DHP Vesicles

	Before Dialysis	After Dialysis		
		24 hours	48 hours	72 hours
Vesicle-containing cell[a]	0	0.510 mM	0.601 mM	0.618 mM
Vesicle-absent cell[b]	1.320 mM	0.897 mM	0.642 mM	0.566 mM
Total	1.320 mM	1.407 mM	1.243 mM	1.184 mM
Vesicle-containing cell[c]	1.433 mM	0.905 mM	0.607 mM	0.599 mM
Vesicle-absent cell[d]	0	0.490 mM	0.593 mM	0.580 mM
Total	1.443 mM	1.395 mM	1.200 mM	1.179 mM

[a] 8 mM DHP in 20 mM Tris-HCl, pH 8.3.

[b] Pyranine in 20 mM Tris-HCl, pH 8.3.

[c] 8 mM DHP and pyranine in 20 mM Tris-HCl, pH 8.3.

[d] 20 mM Tris-HCl, pH 8.3.

At equilibrium, $\mu^{(1)}$ (Na$_3$pyr) = $\mu^{(2)}$ (Na$_3$pyr). Assuming $\mu^{o(1)}$ (Na$^+$) = $\mu^{o(2)}$ (Na$^+$) and $\mu^{o(1)}$ (pyr^{3-}) = $\mu^{o(2)}$ (pyr^{3-}), we obtain:

$$RT\ln\left([Na^+]^{3(1)}\,[pyr^{3-}]^{(1)}\right) = RT\ln\left([Na^+]^{3(2)}\,[pyr^{3-}]^{(2)}\right)$$

$$[Na^+]^{(1)} / [Na^+]^{(2)} = \left([pyr^{3-}]^{(2)} / [pyr^{3-}]^{(1)}\right)^{1/3} = r_D \qquad (8)$$

where r_D is the Donnan ratio. Similarly, for TrisCl we obtain:

$$[Tris^+]^{(1)} / [Tris^+]^{(2)} = [Cl^-]^{(2)} / [Cl^-]^{(1)} = r_D \qquad (9)$$

When a charged macromolecule, e.g., a DHP vesicle is present, r_D may deviate significantly from unity. This deviation is a consequence of the condition for electrical neutrality, which requires that:

$$[Tris^+]^{(1)} + [Na^+]^{(1)} = [Cl^-]^{(1)} + 3[pyr^{3-}]^{(1)} \qquad (10)$$

$$[Tris^+]^{(2)} + [Na^+]^{(2)} = [Cl^-]^{(2)} + 3[pyr^{3-}]^{(2)} + n[M] \qquad (11)$$

Substituting Equations (8), (9) and (10) into Equation (11), we obtain:

$$[Tris^+]^{(1)} / r_D + [Na^+]^{(1)} / r_D = [Cl^-]^{(1)}r_D + 3[pyr^{3-}]^{(1)}r_D^3 + n[M]$$

$$3[pyr^{3-}]^{(1)}r_D^4 + [Cl^-]^{(1)}r_D^2 + n[M]r_D - \left([Cl^-]^{(1)} + 3[pyr^{3-}]^{(1)}\right) = 0 \qquad (12)$$

From dialysis experiments, we know the equilibrium concentration of protonated form of pyranine ($[pyr^{3-}]^{(1)} = 0.24$ mM), but we don't know the equilibrium concentration of chloride ($[Cl^-]^{(1)}$). 8 mM DHP monomers is converted to 2 μM DHP vesicles containing 4×10^3 DHP monomers per vesicle. The contribution of 2 mM DHP monomers (0.5 μM DHP vesicles) to the ionic strength (μ) has been estimated as 9 mM by comparing ZnTPPS^{4-} triplet-triplet annihilation rates in the presence and absence of vesicles[40]. From the partial dissociation of neutral DHP vesicles, i.e.:

$$Na_nDHP \rightleftarrows n\,Na^+ + DHP^{n-}$$

the value of n is estimated from the definition of ionic strength

$$\mu = \tfrac{1}{2} \sum m_i z_i^2$$

$$\mu = \tfrac{1}{2}\,(5\times10^{-7}\,n + 5\times10^{-7}\,n^2) = 9\times10^{-3}$$

to be about 190.

Equation (12) cannot be solved[41] because there is an unknown parameter in this equation. Therefore the magnitude of Donnan effect cannot be evaluated from the present experimental results. To minimize the Donnan effect in this system, we

need to perform the dialysis experiments at high ionic strengths. Then equations (10) and (11) can be simplified to

$$[Tris^+]^{(1)} = [Cl^-]^{(1)}$$
$$[Tris^+]^{(2)} = [Cl^-]^{(2)}$$

which give a r_D value of 1.

The fact that the pyranine concentration on the side with DHP vesicles is slightly greater than that on the side without DHP vesicles in the dialysis experiments implies that there is some weak binding of pyranine to the external surfaces of the DHP vesicles. Note that the Donnan effect is in the opposite direction so that, at equilibrium in the absence of binding, there should be less pyranine in the compartment containing the anionic vesicles, contrary to what was observed. If pyranine is entrapped inside the DHP vesicles, there should also be a small fraction on the internal surfaces and the remaining confined to the internal aqueous phase of DHP vesicles.

III. Titration of DHP Phosphate Headgroups

The DHP vesicles were usually formed in buffered solutions. The phosphate headgroups of DHP molecules themselves also contributed to the total buffer capacity of the suspensions. The pK_a of DHP vesicles was estimated to be approximately 6 by Tricot et al[42]. They prepared the DHP vesicles in water and various amounts of NaOH. After DHP vesicles formed, the pH was measured using a glass electrode. They found that the measurement of the pH of DHP dispersions, particularly above 7, was not very reproducible. A drift of measured values was observed when the pH-measuring electrode was left for extended periods in the vesicle suspension. Agitation also modified the apparent pH. So they measured the pH after immersing the electrode for about 30 seconds, when the measured pH was relatively stable, and without stirring. The same problem was encountered in our studies and overcome by using the pyranine as pH indicator in the external medium.

10 mM DHP vesicles were prepared in water and small volumes of 40% (8 mM) tetrabutylammonium hydroxide were added to adjust the solution to the desired pH value. Then 0.01 μM of pyranine was added to the bulk medium. The pH was determined from the pyranine calibration curve by measuring the fluorescence intensities at 455 and 404 nm ($\lambda_{em} = 510$ nm). Figure 3-4 gives the titration curve obtained by plotting the pH versus the volume of base added. From the curve the pK_a of DHP vesicles was estimated as 7.45, which was higher than that reported by Tricot et al[42]. One difference in these studies was the way in which the titration was done. We added base after DHP vesicles had been formed, therefore, only exterior phosphate groups were titrated, while they added base before sonicating the DHP suspensions, so the internal phosphate groups of DHP vesicles were also titrated.
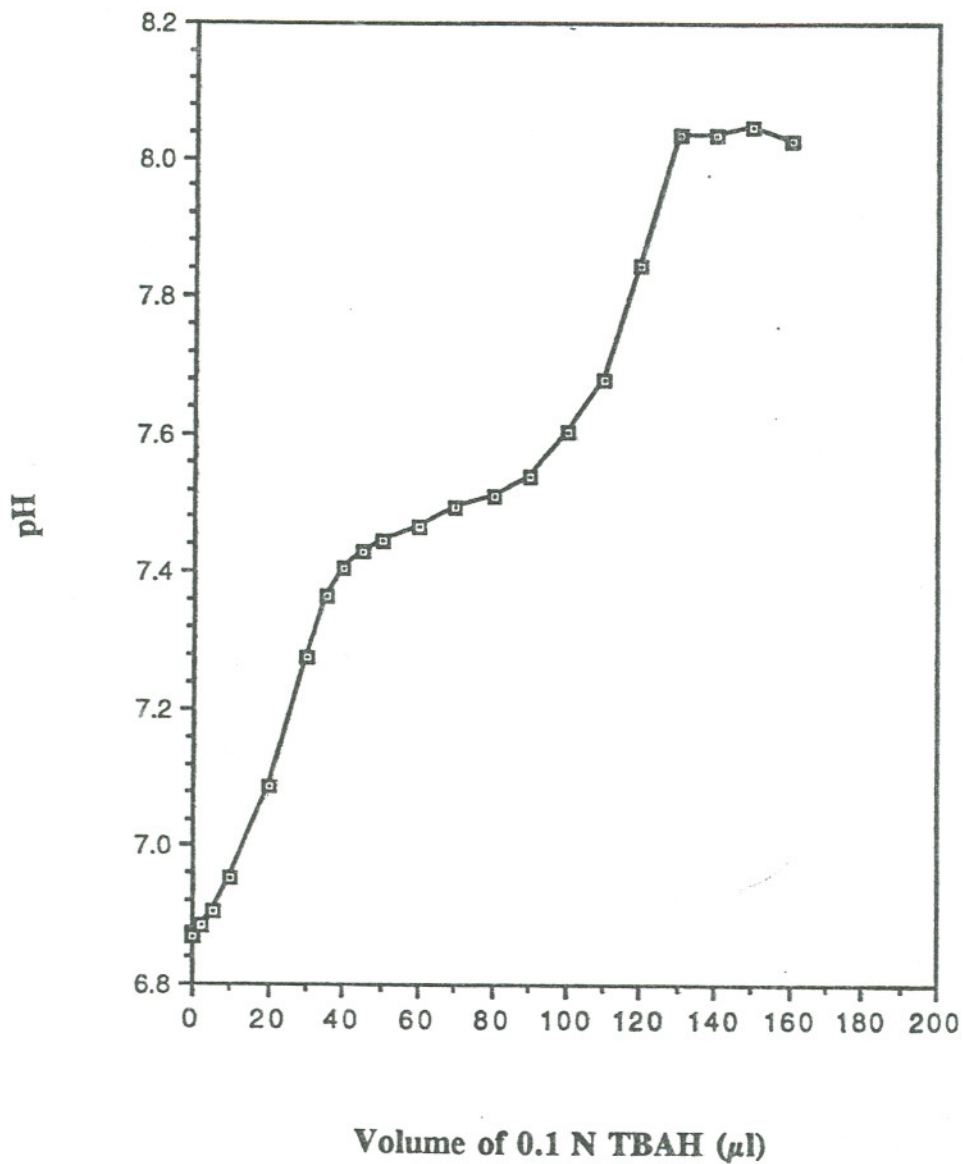
Figure 3-4. Titration curve of 1 ml of a 10 mM DHP vesicle suspension by 0.1 N tetrabutylammonium hydroxide (TBAH). The DHP vesicle suspension was prepared in water and neutralized with 8 mM TBAH. 0.01 μM pyranine was added to the external medium of DHP vesicles. The pH values were obtained from the pyranine calibration curve.

IV. The pH Jump Experiment

A. Entrapment of Pyranine Inside DHP Vesicles

The pH jump experiment was done by monitoring the internal pH change upon changing the external pH of DHP SUVs. The internal pH was obtained from the ratio of the fluorescence intensity of entrapped pyranine measured at 455 nm and 404 nm (λ_{em} = 510 nm). To ensure that the observed fluorescence signal came only from the internal solution of vesicles, separation of unentrapped pyranine from exterior of DHP vesicles must be complete. This was checked in two ways:

1. Fractionation Method——A suspension of DHP vesicles containing entrapped methyl viologen (MV^{2+}) and external pyranine was passed through Sephadex columns, one milliliter effluent fractions were collected, and the amount of DHP and pyranine in each fraction was determined by measuring the absorption maximum of MV^{2+} at 260 nm and the fluorescence spectrum of pyranine, respectively.

A mixture of 8 mM of DHP powder and 320 μM methyl viologen in 10 ml 20 mM Tris-HCl buffer was cosonicated for two 10-minute periods. After centrifugation, the supernatant was passed through a Chelex 100 cation exchange column (0.8 × 10 cm) to remove the unentrapped MV^{2+} cations[21]. About 1 mM pyranine was then added to the above DHP vesicle suspension. Two milliliters of the above mixture was passed through the large Sephadex column (void volume 11 ml) and fractions 10 to 19 were collected. The amount of DHP and pyranine in each fraction was determined by measuring the optical spectra of MV^{2+} at its absorption maximum (260 nm, ϵ_{260} = 2.19 × 10^4 M^{-1} cm^{-1}) and fluorescence spectra at excitation wavelength 455 nm (λ_{em} = 510 nm) of pyranine, respectively. The percentage of DHP vesicles and the relative fluorescence in each fraction were plotted versus the fraction number, which is shown in Figure 3-5. Then fractions 12,

Figure 3-5. Percentage of DHP vesicles (open square) and relative fluorescence intensities at excitation wavelength of 455 nm (λ_{em} = 510 nm) (solid diamond) versus fraction number after the mixture of 8 mM DHP vesicle suspension with entrapped methylviologen (MV^{2+}) and 1 mM external pyranine was passed through the large Sephadex column. The percentage of DHP vesicles was calculated from the optical absorbance intensity of MV^{2+} in each fraction divided by the sum of the absorbance intensities of MV^{2+} in all fractions. The DHP vesicle suspension was prepared in 20 mM Tris-HCl buffer.

13, and 14 were mixed and the mixture was passed through the small Sephadex column (void volume 3ml). Fractions 3 to 10 were collected. The amount of DHP and pyranine in each fraction was again determined by optical and fluorescence spectrophotometry, respectively. The percentage of DHP and relative fluorescence were plotted versus the fraction number (Figure 3-6). It can be seen that after passing through two Sephadex columns, there is still some overlap between the elution profiles for DHP vesicles and pyranine. Therefore pyranine was either not completely removed from the exterior of the DHP vesicles or the smaller column could not effectively resolve the two species.

2. The Fluorescence Quencher Method——In this method, the pyranine fluorescence quencher, thiamine, was added to DHP vesicle suspensions[29]. Expectations were that entrapped pyranine would not be quenched while the unentrapped pyranine would be quenched.

Fluorescence quenching refers to any process which decreases the fluorescence intensity of a given fluorophore[43]. Two kinds of fluorescence quenching mechanisms will be considered - dynamic or collisional and static quenching. Dynamic quenching arises from collisional encounters between fluorophore and quencher during the lifetime of the excited state, resulting in fluorophore returning to the ground state without emission of a photon. Static quenching is due to nonfluorescent ground state complex formation between the fluorophore and the quencher. In either mechanism, the fluorophore and quencher must be in contact. Dynamic quenching is usually treated mathematically by applying the Stern-Volmer equation

$$I_0/I = 1 + K_{sv} [Q] \qquad (13)$$

where I_0 and I, respectively are the fluorescence intensities of the fluorophore in the absence and presence of a quencher (Q); K_{sv} is the overall quenching constant. A Stern-Volmer plot of I_0/I versus the quencher concentration [Q] is expected to be linear when quenching is strictly dynamic.

Since pyranine has net negative charges, its fluorescence is best quenched by cationic quenchers by forming complexes with the quencher. The structure of
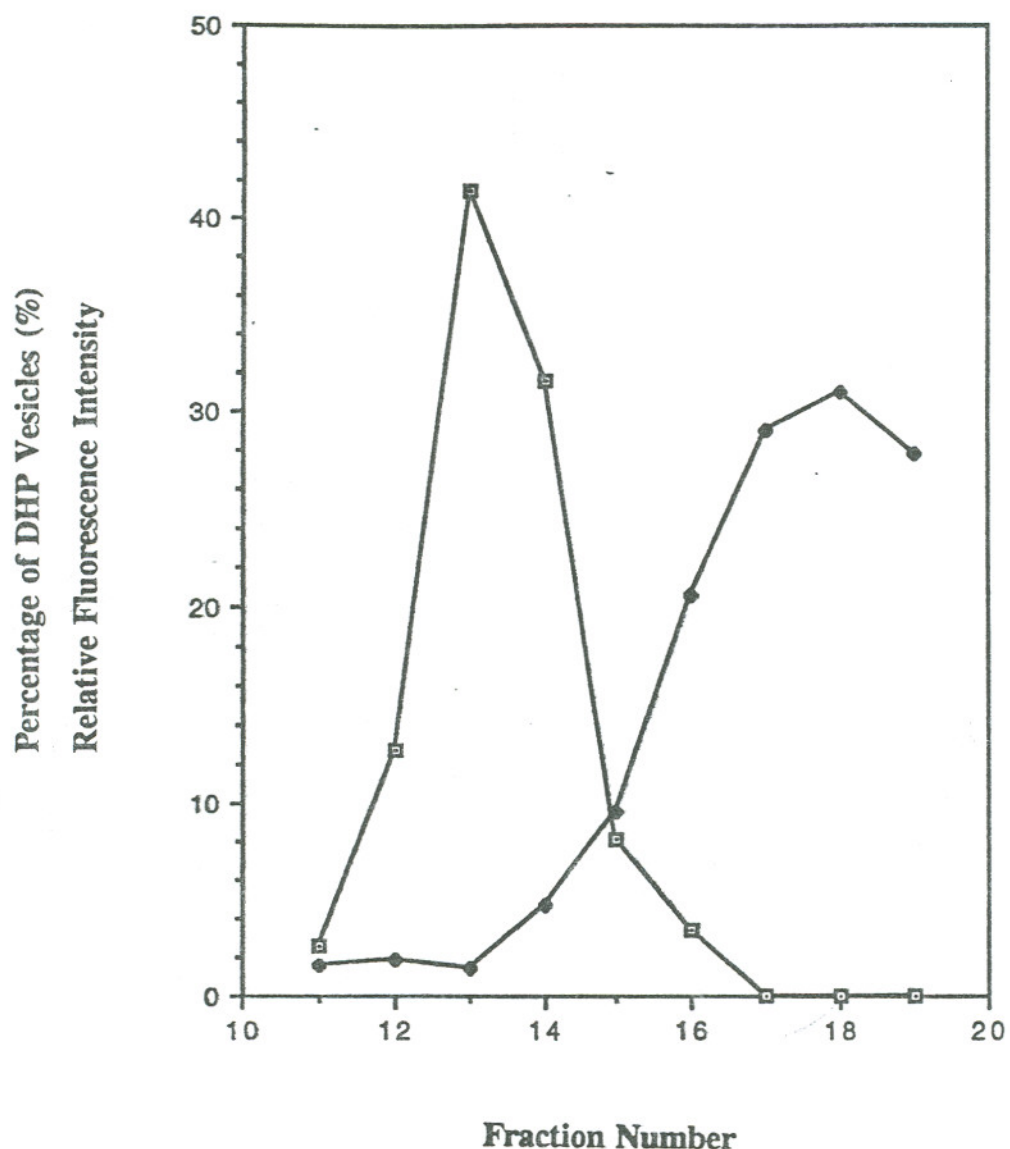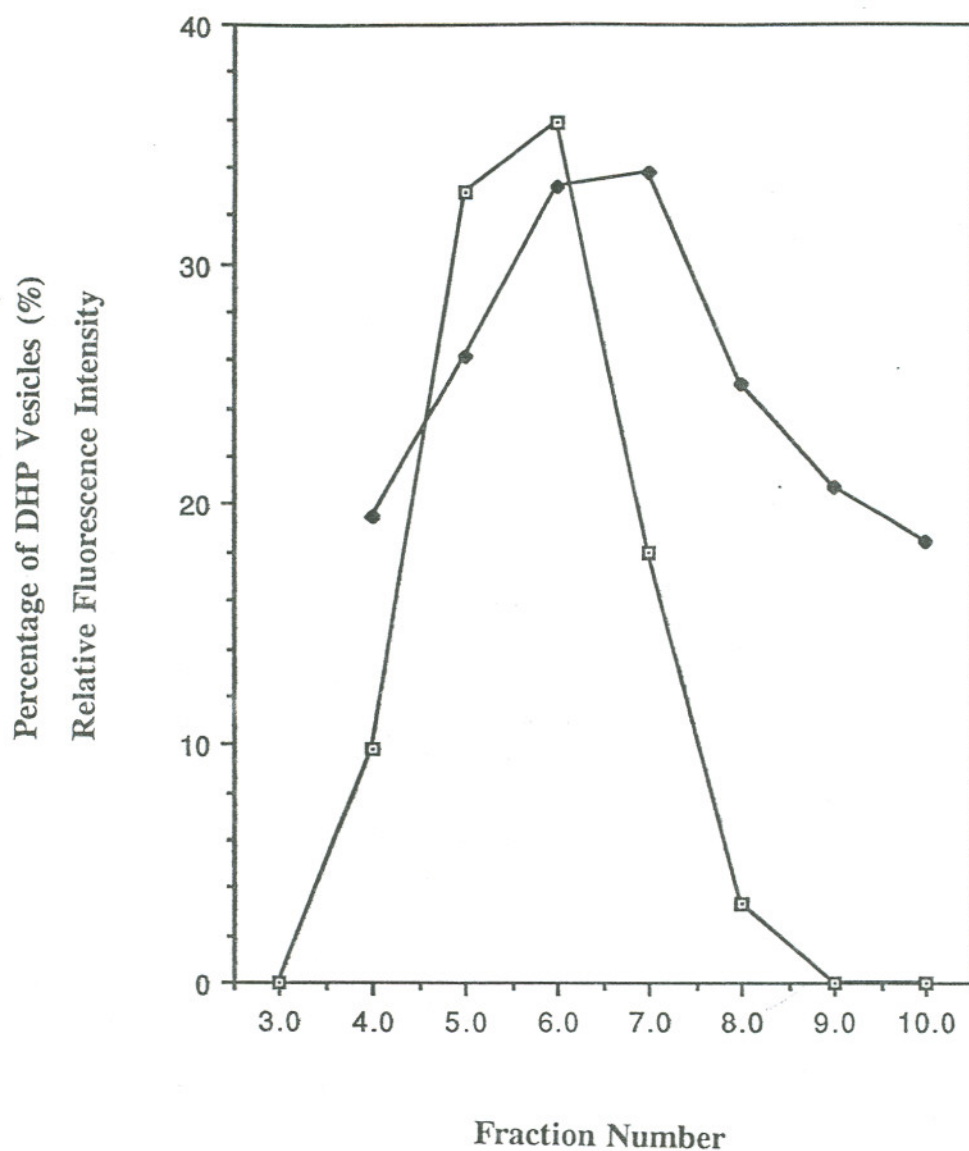
Figure 3-6. Percentage of DHP vesicles (open square) and relative fluorescence intensities at excitation wavelength at 455 nm (λ_{em} = 510 nm) (solid diamond) versus fraction number after the mixture of fraction 12, 13, and 14 from the large Sephadex column was passed through the small Sephadex column. The percentage of DHP vesicles was obtained from the optical absorbance intensity of MV^{2+} in each fraction divided by the sum of the absorbance intensities of MV^{2+} in all fractions. The DHP vesicle suspension was prepared in 20 mM Tris-HCl buffer.

thiamine is:
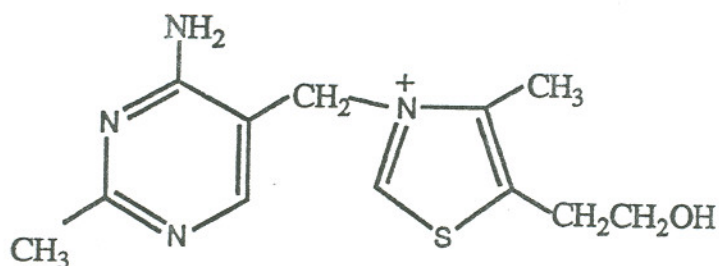
Because the thiazolium part is positively charged, it might be an efficient static quencher of pyranine fluorescence. The results of quenching experiments are summarized in the Stern-Volmer plot shown in Figure 3-7 and reflect a complex quenching mechanism. Thiamine shows a maximum quenching effect at concentration of 10 mM. I_0/I increases with thiamine concentrations $\leq$ 10 mM and decreases with thiamine concentrations $>$ 10 mM.

An 8 mM DHP vesicle suspension with entrapped pyranine was prepared as described in the experimental section. The excitation spectra (λ_{em} = 510 nm) of the DHP vesicle suspension alone, and with 2 mM and 4 mM added thiamine are shown in Figure 3-8. For comparison, the excitation spectra (λ_{em} = 510 nm) of 0.01 μM pyranine in 20 mM Tris-HCl, pH 7.19, and with 2 mM and 4 mM added thiamine are shown in Figure 3-9. Pyranine at 0.1 μM was added to a suspension of DHP vesicles and the excitation spectra (λ_{em} = 510 nm) with and without 2 mM thiamine are shown in Figure 3-10. From these data, it appears that thiamine cannot quench entrapped pyranine, but is capable of extensively quenching external pyranine in the presence of DHP. Because quenching of vesicles containing entrapped pyranine was negligible (Figure 3-8), most or all of the pyranine originally located external to the vesicles must have been removed by the chromatographic procedures.
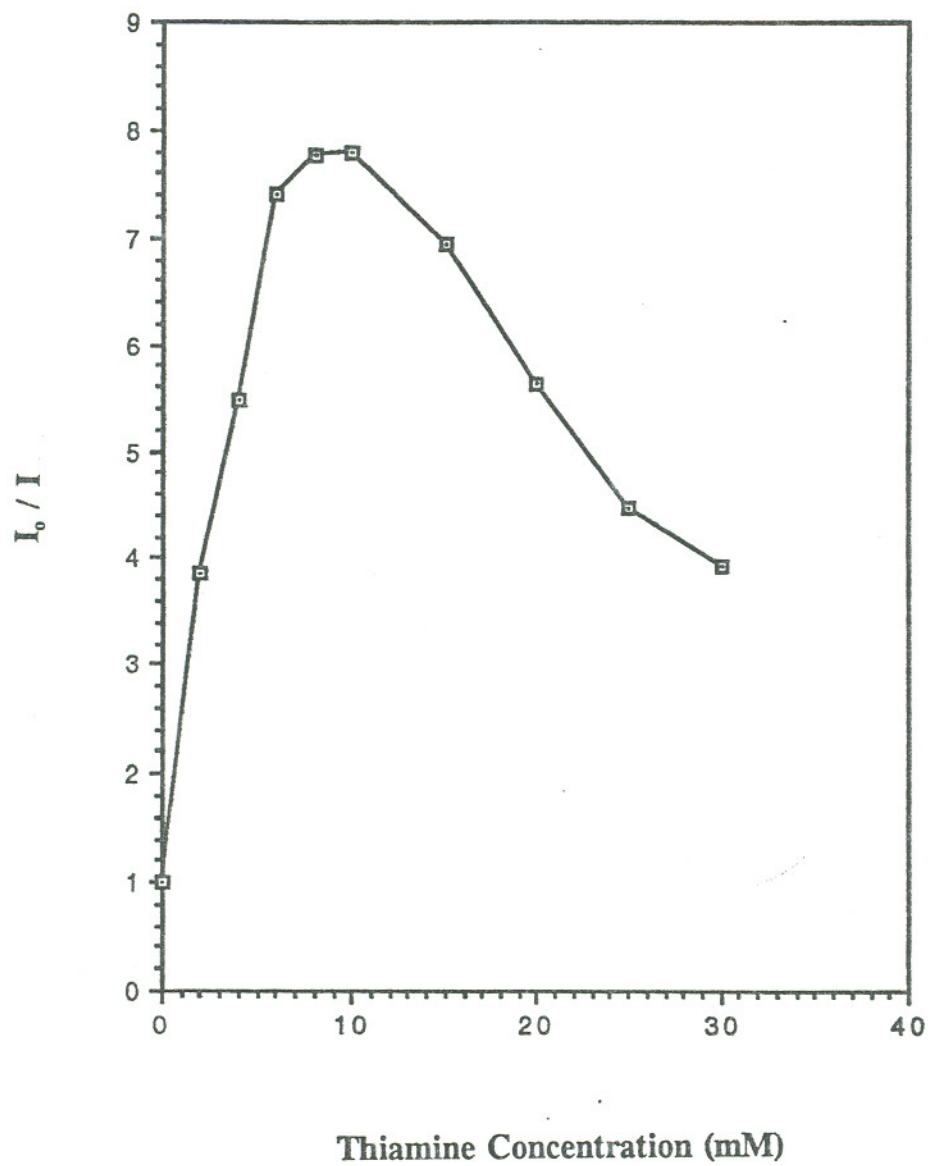
Figure 3-7. Stern-Volmer plot of pyranine fluorescence quenched by thiamine in 20 mM Tris-HCl buffer.
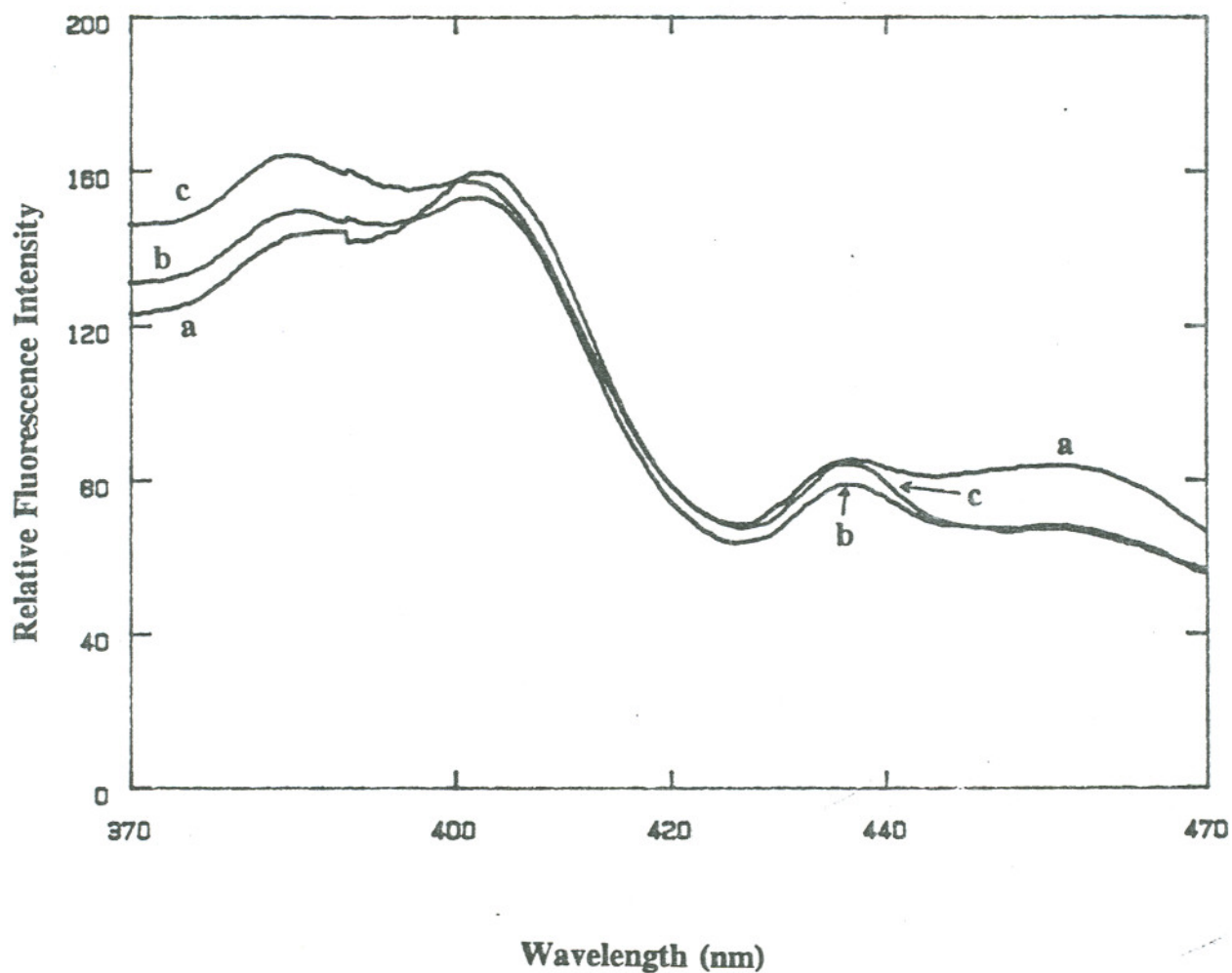
Figure 3-8. Excitation spectra (λ_{em} = 510 nm) of an 8 mM DHP vesicle suspension with entrapped pyranine (about 0.01 μM) in 20 mM Tris-HCl buffer, pH 7.8 (trace a), and with 2 mM (trace b) and 4 mM (trace c) added thiamine.
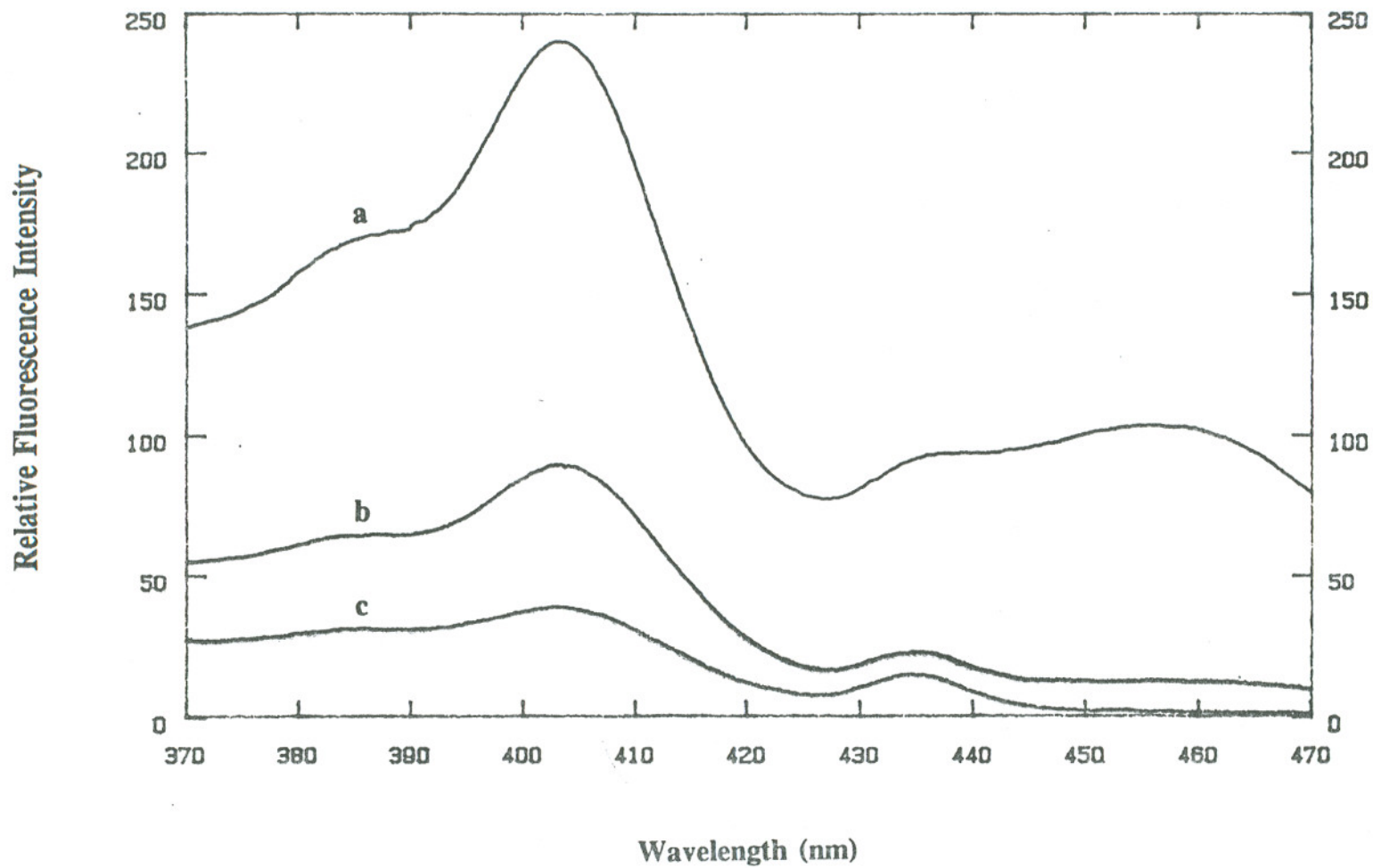
Figure 3-9. Excitation spectra (λ_{em} = 510 nm) of 0.01 μM pyranine in 20 mM Tris-HCl buffer, pH 7.2 (trace a), and with 2 mM (trace b) and 4 mM (trace c) added thiamine.
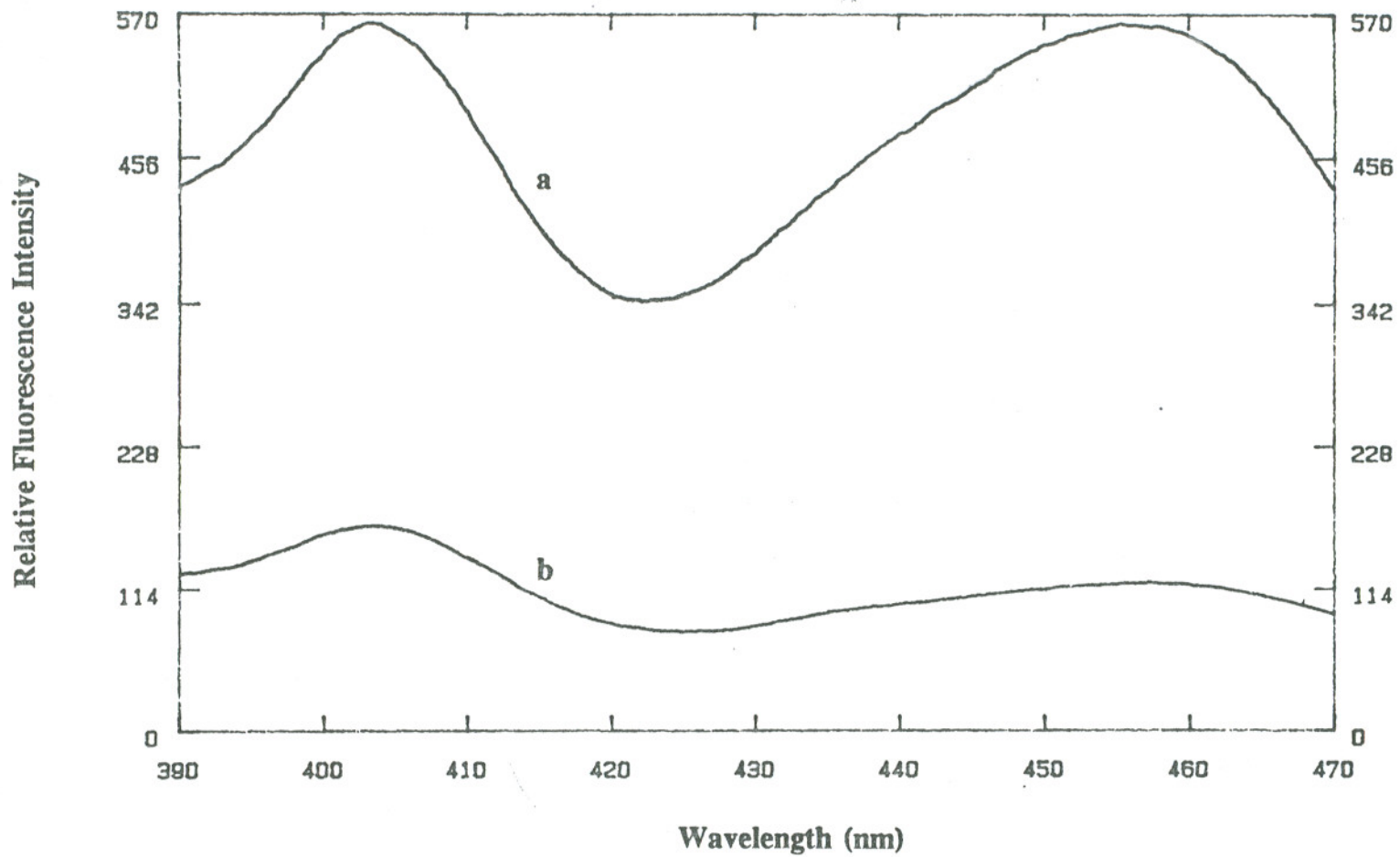
Figure 3-10. Excitation spectra (λ_{em} = 510 nm) of an 8 mM DHP vesicle suspension with 0.1 μM external pyranine in 20 mM Tris-HCl buffer, pH 7.88 (trace a), and with 2 mM (trace b) added thiamine.

B. pH Perturbations

1. Typical Response of Pyranine-containing DHP Vesicles

8 mM DHP vesicles with entrapped pyranine in 20 mM Tris-HCl buffer or in
water were used to execute the pH jump experiments. Usually the external pH of
DHP vesicle suspension was changed by rapidly mixing an equal volume of the DHP
vesicle suspension with buffer that was at a different pH. The internal pH change of
DHP vesicles with time following mixing was obtained from the pyranine
fluorescence intensity changes at 404 nm and 455 nm (λ_{em} = 510 nm) according to
the pyranine calibration curve. A typical plot of pH_{in} versus time is shown in Figure
3-11. The curve was biphasic, and composed of an initial fast pH change followed by
a slow continued increase in basicity. Table 3-3 and 3-4 contain a summary of
different sets of experimental results.

The final external pH could be measured using a pH meter. In order to
measure the external and internal pH of DHP vesicles by the same standard, the
external pH was also obtained from the pyranine fluorescence by adding to the
external medium 10 times more concentrated pyranine than the entrapped
concentration. This concentration of added pyranine did not alter perceptibly the pH
value determined from the calibration curve, as shown in Table 3-5 .

It was found that pH_{in} was usually lower than pH_{out} for DHP vesicles prepared
in 20 mM Tris-HCl buffer, and pH_{in} was higher than pH_{out} for DHP vesicles in
water. This might be explained by the high buffer capacity of the phosphate
headgroups of DHP vesicles. Because the phosphate headgroups of the DHP
surfactant used were in their acidic form, they were neutralized to a higher extent by
strong bases (hydroxyl) than by 20 mM Tris-HCl buffer during the sonication
procedure. Kano and Fendler also observed that pH_{in} was smaller than pH_{out} for
anionic liposomes[28]. They explained this in terms of the weak buffer capacity of the
buffer used and poor proton permeability across the negatively-charged phosphate
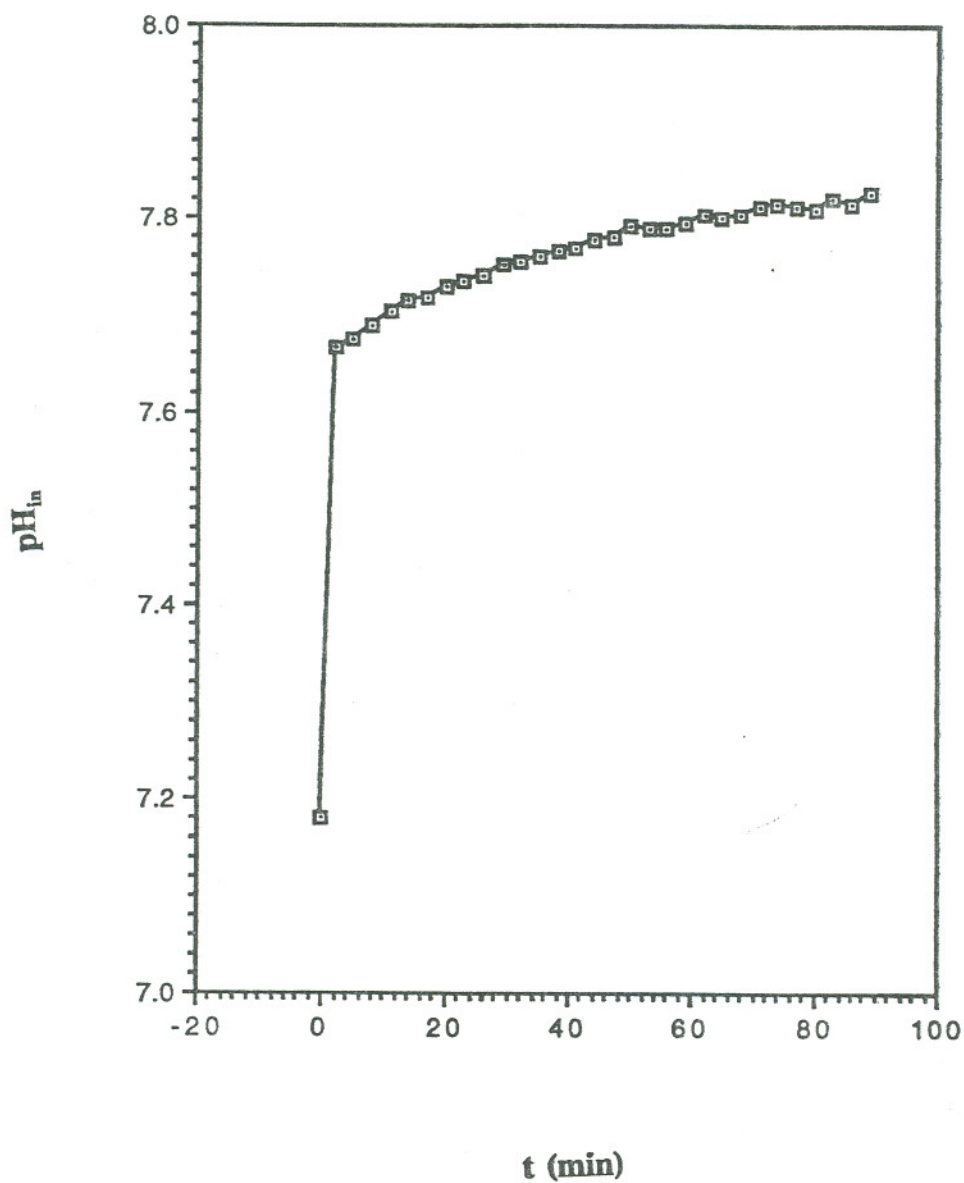
Figure 3-11. Changes in pH_{in} versus time for pyranine-containing DHP vesicles upon jumping the pH of the external solution. 0.5 ml of 20 mM Tris-HCl, pH 9.70 was added to 0.5 ml of 8 mM DHP vesicle suspension with entrapped pyranine in 20 mM Tris-HCl buffer, pH 8.07. pH_{in} was determined from the pyranine calibration curve.

Table 3-3.   pH Jump Experiments Made in DHP Vesicles in 20 mM Tris-HCl Buffer[a]

pH_e^i	pH_e^f	ΔpH_e	pH_{in}^0	pH_{in}^i	pH_{in}^f	ΔpH_{in}^{fast} (%)	n^{fast}	ΔpH_{in}^{slow} (%)	n^{slow}	ΔpH_{in}^{total}	n^{total}
7.91	8.48	0.57	7.15	7.19	7.52	0.04 (11.5)	49	0.33 (88.5)	400	0.37	449
7.91[b]	8.50	0.59	7.15		7.90					0.75	902
7.66	8.33	0.67	6.80	6.93	7.32	0.13 (24.2)	105	0.39 (75.8)	314	0.52	419
7.66[b]	8.35	0.69	6.80		7.81					1.01	821
7.66[c]	7.68	0.02	6.80	7.32	7.42					0.62	501
7.95[d]	8.74	0.79	7.10	7.28	7.57	0.18 (38.8)	206	0.29 (61.2)	331	0.47	537
7.95	5.94	-2.01	7.10	6.31	6.03	-0.79 (73.8)	830	-0.28 (26.2)	294	-1.07	1124
8.07	8.55	0.48	7.18	7.67	7.82	0.49 (76.6)	602	0.15 (23.4)	184	0.64	786
7.96	8.38	0.42	7.05	7.72	7.82	0.67 (86.9)	732	0.10 (13.1)	110	0.77	842
7.96[b]	8.42	0.46	7.05		8.02					0.97	1055
7.96	6.28	-1.68	7.05	6.97	6.62	-0.08 (19.2)	87	-0.35 (80.8)	382	-0.43	469
8.05	8.51	0.46	7.13	7.43	7.53	0.30 (75.7)	352	0.10 (24.3)	117	0.40	469
8.05[e]	—	—	7.13	7.26	7.37	0.13 (54.6)	153	0.11 (45.4)	129	0.24	282
7.85	8.26	0.41	7.38	7.45	7.53	0.07 (47.6)	91	0.08 (52.4)	104	0.15	195
7.86	8.55	0.69	7.10	7.20	7.58	0.10 (20.8)	115	0.38 (79.2)	439	0.48	554
7.88	8.33	0.45	7.32	7.38	7.72	0.06 (14.2)	78	0.34 (85.8)	442	0.40	520
7.88[e]	8.47	0.59	7.22	7.27	7.62	0.05 (12.3)	53	0.35 (87.7)	423	0.40	483
7.88[b]	8.47	0.59	7.36		8.15					0.79	1060
7.88	6.83	-1.05	7.41	7.37	7.21	-0.04 (20.0)	71	-0.16 (80.0)	210	-0.20	263

a) DHP vesicles with entrapped pyranine were prepared in 20 mM Tris-HCl buffer as described in Experimental Methods. The pH jump experiment was done by mixing 0.5 ml DHP vesicles and 0.5 ml of the same buffer at a different pH. pH_e^i was the initial external pH of the DHP vesicle suspension measured with a pH meter before a pH jump. pH_e^f was the final external pH of DHP vesicle suspension measured with a pH meter after a pH jump. ΔpH_e was the difference between pH_e^f and pH_e^i. pH_{in}^0 was the initial internal pH of DHP vesicles obtained from pyranine fluorescence excitation profiles before a pH jump. pH_{in}^i was the initial internal pH of DHP vesicles obtained from pyranine fluorescence excitation profiles after a pH jump. pH_{in}^f was the final internal pH of DHP vesicles from pyranine calibration curve after a pH jump. ΔpH_{in}^{fast} (%) was the difference between pH_{in}^i and pH_{in}^0 (its percentage in ΔpH_{in}^{total}). n^{fast} was the apparent number of protons moving across DHP vesicle bilayers contributed by the fast component. ΔpH_{in}^{slow} (%) was the difference between pH_{in}^f and pH_{in}^i (its percentage in ΔpH_{in}^{total}). n^{slow} was the apparent number of protons moving across DHP vesicle bilayers contributed by the slow component. ΔpH_{in}^{total} (%) was the difference between pH_{in}^f and pH_{in}^0. n^{total} was the apparent total number of protons moving across DHP vesicle bilayers.

b) The pH jump experiment was done in the presence of 1 mM TPP^+.

c) 1 mM of TPP^+ was added to 1ml DHP vesicles without imposing a pH jump.

d) The pH jump experiment was done by adding a small amount of NaOH or HCl to 1ml of DHP vesicles.

e) The pH jump experiment was done in the presence of 2 mM thiamine.

Table 3-4.   pH Jump Experiments Made in DHP Vesicles in Water[a]

pH_e^i	pH_e^f	ΔpH_e	pH_{in}^0	pH_{in}^i	pH_{in}^f	ΔpH_{in}^{fast} (%)	n^{fast}	ΔpH_{in}^{slow} (%)	n^{slow}	ΔpH_{in}^{tot}	n^{total}
7.62	9.06	1.44	7.97	8.15	8.36	0.18 (45.6)	174	0.21 (54.4)	202	0.39	376
7.62	6.38	-1.24	7.97	7.97	7.20	0 (0)	0	-0.77 (100)	742	-0.77	742
8.21	——	——	8.40	8.08	7.87	-0.32 (60.2)	157	-0.21 (39.8)	103	-0.53	260
8.18	——	——	8.60	8.46	8.12	-0.14 (28.5)	47	-0.34 (71.5)	114	-0.48	161
7.72	——	——	7.68	7.58	7.52	-0.10 (62.5)	127	-0.06 (37.5)	76	-0.16	203
7.72	——	——	7.68	7.75	7.94	0.07 (27.0)	89	0.19 (73.0)	243	0.26	332
7.21[b]	7.99	0.78	6.99	7.20	7.35	0.21 (58.6)	214	0.15 (41.4)	152	0.36	366
7.56[b]	8.17	0.61	7.17	7.38	7.46	0.21 (72.6)	257	0.08 (27.4)	98	0.29	355

a)   DHP vesicles with entrapped pyranine were prepared in H_2O and neutralized with NaOH or tetrabutylammonium hydroxide as described in Experimental Methods. The pH jump experiment was done by adding a small amount of NaOH or HCl to 1ml DHP vesicles. Other symbols were the same as in Table 3-3.

b)   The pH jump experiment was done by mixing 0.5 ml DHP vesicles with 0.5 ml diluted NaOH or HCl.

Table 3-5   Effect of Different Concentrations of Pyranine in 20 mM Tris-HCl, pH
8.06, on the Apparent pH of DHP Vesicle Suspensions

Pyranine Concentration (uM)	$pH_{pyr.}$
0.01	7.965
0.05	7.946
0.10	7.943

bilayer. These pH differences correspond to transmembrane potentials that are less than 50 mV, according to the equation:

$$\Delta G = F\Delta\Psi + 2.3RT\log([H^+]_{in} / [H^+]_o)$$

where ΔG is the electrochemical potential difference; F is the Faraday constant; $\Delta\Psi$ is the transmembrane potential; R is the gas constant; T is the temperature; $[H^+]_{in}$ is the proton concentration of the internal aqueous phase of the vesicles; $[H^+]_o$ is the proton concentration of the external medium of the vesicles.

The external pH change of DHP vesicles upon jumping the pH was also obtained from pyranine fluorescence profiles. A plot of pH_{out} versus time is shown in Figure 3-12. As can be seen, there was no slow pH change process in the pH_{out} versus time curve.

2. Effect of the Lipophilic Tetraphenylphosphonium Cation on Proton Dynamics in DHP Vesicle Suspensions

If there were no compensating ion movement when H^+/OH^- moved across DHP vesicle bilayers upon applying a pH jump, a transmembrane potential would develop to oppose further H^+/OH^- movement. Lipophilic ions and ionophores have been used to dissipate the transmembrane potential formed by charge separation. Several potential charge-dissipating ionophores were previously investigated in DHP vesicle suspensions[21]. Carbonyl cyanide 3-chlorophenylhydrazone (CCCP) and 2,4-dinitrophenol (DNP), which were effective protonophores in biological systems, did not work in the DHP system, although they could be incorporated properly into DHP vesicles. Valinomycin could not be incorporated into the DHP vesicle bilayers. As described below, the positively charged tetraphenylphosphonium ion (TPP$^+$) could apparently move freely across the DHP vesicle bilayers because its charge was surrounded by three large hydrophobic phenyl groups. The work required to move the large hydrophobic ions was reduced to a large extent, as illustrated in Figure 1-1.

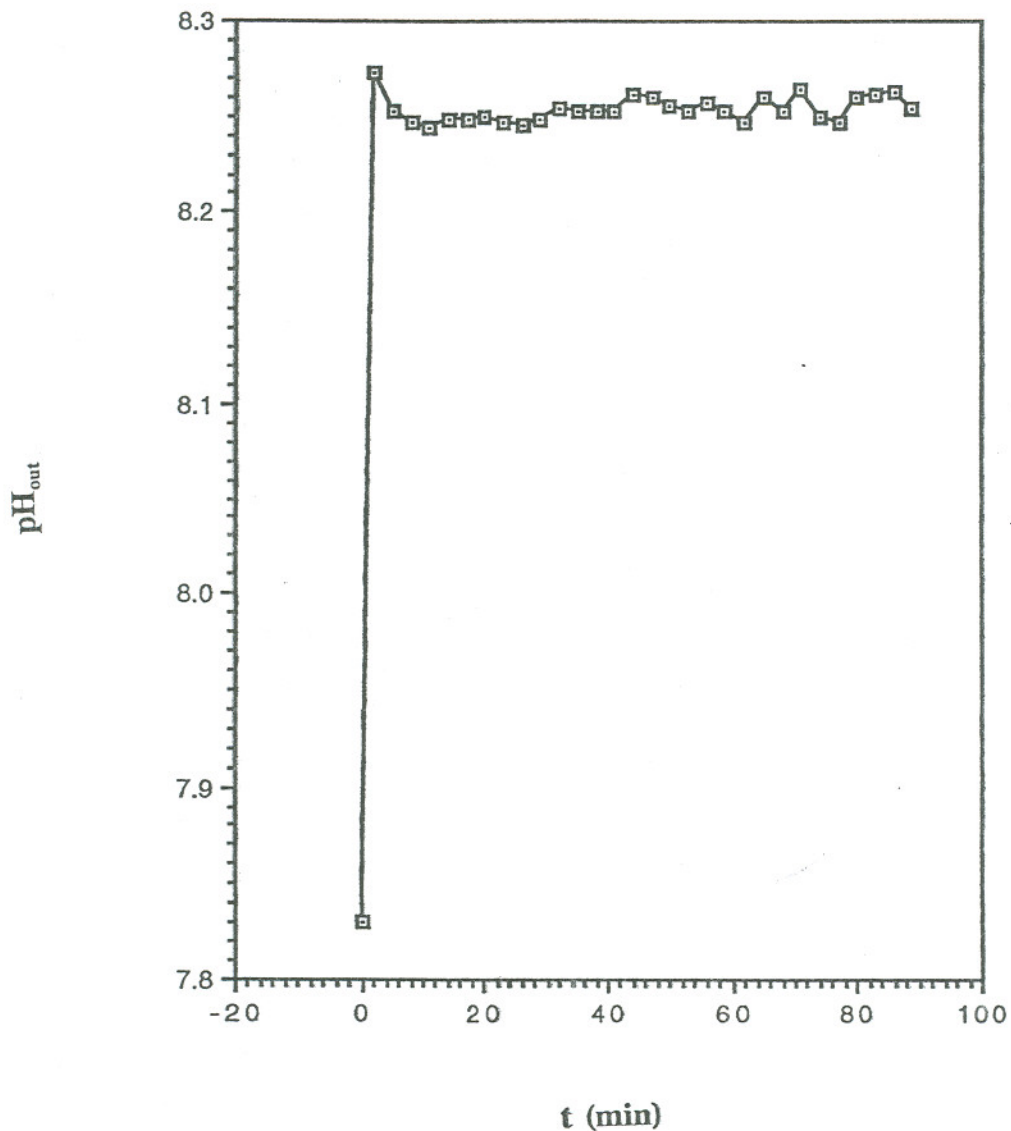1 mM TPP$^+$ was added to the external suspension of DHP vesicles several

Figure 3-12. Changes in pH_{out} versus time of DHP vesicles upon applying an external pH jump. 0.5 ml of 20 mM Tris-HCl, pH 9.70 was added to 0.5 ml of 8 mM DHP vesicle suspension with 0.1 μM external pyranine in 20 mM Tris-HCl buffer, pH 8.07. pH_{out} was determined from the pyranine calibration curve.

minutes before a pH jump experiment. In these experiments, the external medium was made more basic than the interior, so that protons must move outward from the vesicles to achieve equilibrium. The effect of TPP^+ is shown in Figure 3-13. As can be seen, not only did the slow phase disappear, but the total change in pH was about twice that obtained under identical conditions when TPP^+ was absent. However, TPP^+ uptake by the DHP vesicles in amounts required to compensate for the proton efflux could not be observed spectrophotometrically after passing the vesicles down a Chelex 100 cation exchange column to remove external ions. The optical spectra of TPP^+ before and after passing through the Chelex column are shown in Figure 3-14. The concentration of TPP^+ was determined from its absorbance maximum at 270 nm ($\epsilon_{270} = 3.5 \times 10^3$ M^{-1} cm^{-1})[31]. The concentration of TPP^+ that should have moved internally was calculated to be around 173 μM, considering dilution of the column chromatographic step, and, consequently should have been within the limits of optical detection.

C. Explanation of the Experimental Results

1. Calculation of the Number of Protons Moving Across the DHP Vesicle Bilayer for a Typical pH Jump Experiment

We can calculate approximately the number of protons moving across the vesicle bilayers for a given pH jump experiment. The total number of protons (m) transferred in a suspension containing a total number of N DHP vesicles is

$$m = n\,N$$

where n is the number of protons transferred per vesicle. The total internal volume (V_{in}) of N vesicles is

$$V_{in} = N\,v_{in}$$

where v_{in} is the internal volume per vesicle. This is equivalent to adding into the vesicle interior a strong acid of concentration C_a,
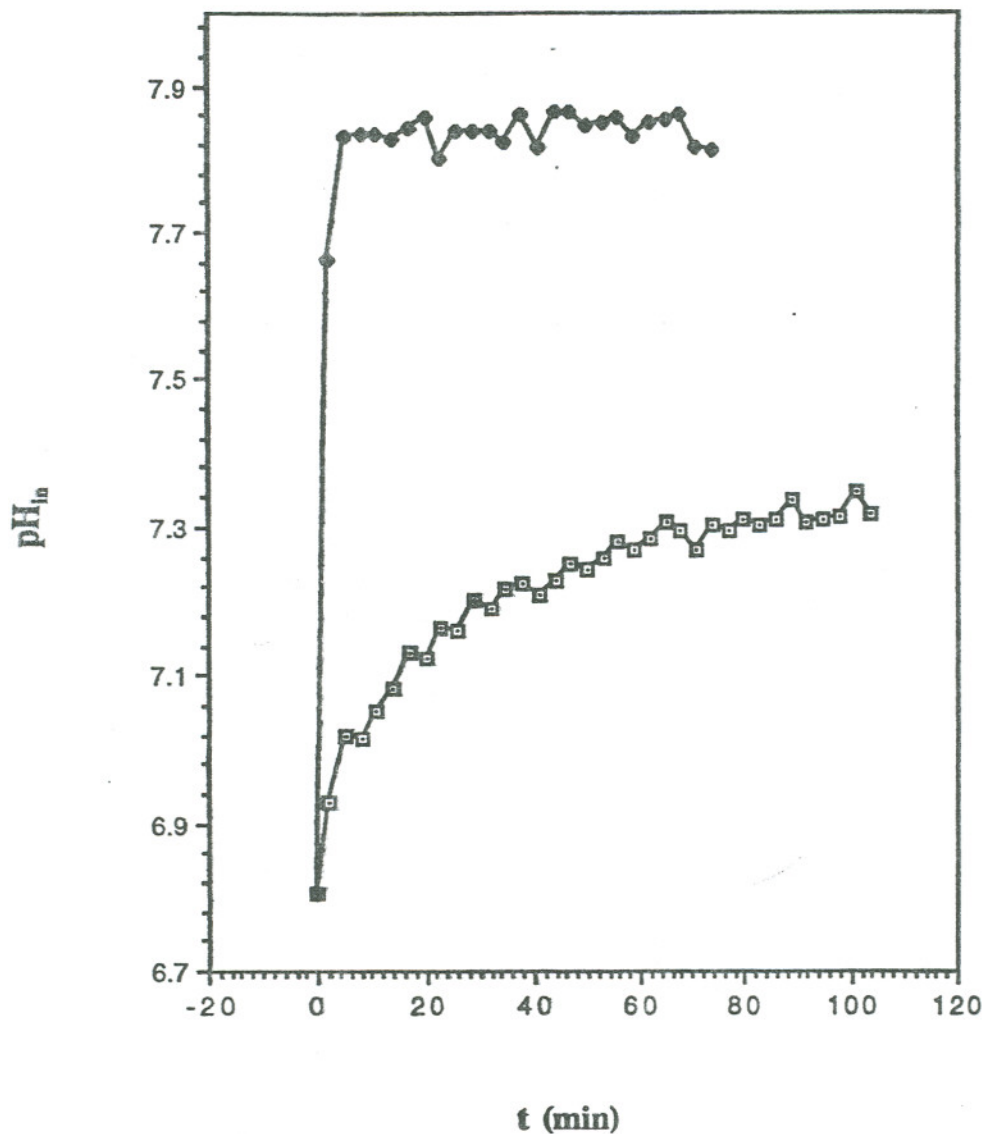
Figure 3-13. Changes in pH$_{in}$ versus time in a pH jump experiment in the absence (open square) and presence (solid diamond) of 1 mM TPP$^+$ in the external medium of a DHP vesicle suspension. 0.5 ml of 20 mM Tris-HCl, pH 9.29 was added to 0.5 ml of 8 mM DHP vesicle suspension with entrapped pyranine in 20 mM Tris-HCl buffer, pH 7.66 in the absence and presence of 1 mM TPP$^+$ in the external medium of DHP vesicles. pH$_{in}$ was determined from the pyranine calibration curve.
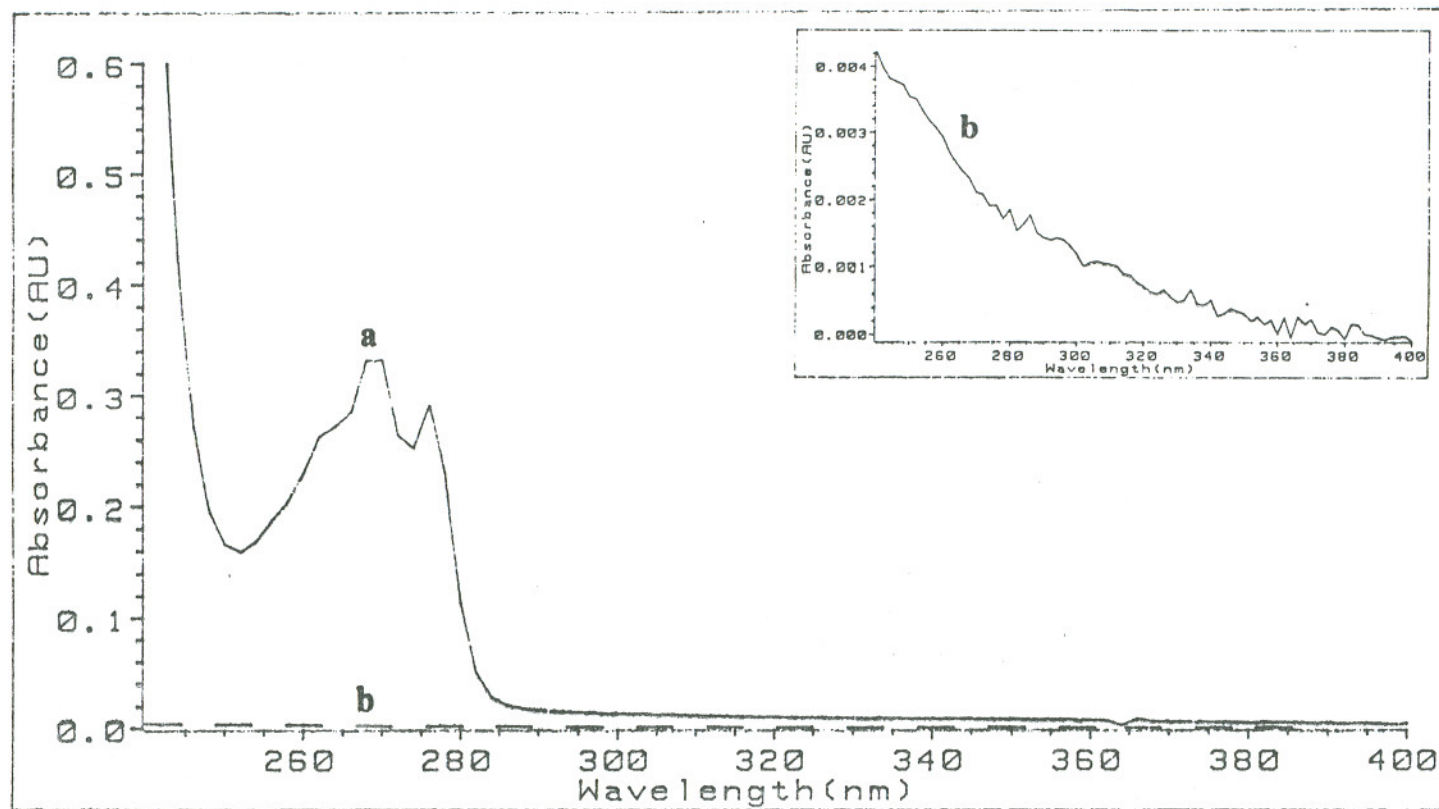
Figure 3-14. The absorption spectra of TPP$^+$ after applying a pH jump in the alkaline direction, before (trace a, 11 fold dilution) and after (trace b, 4 fold dilution) the final reaction solution was passed through a Chelex column. 0.5 ml of 20 mM Tris-HCl, pH 9.56, was added to 0.5 ml of 8 mM DHP vesicle suspension containing entrapped pyranine in 20 mM Tris-HCl buffer, pH 7.88, with 1 mM TPP$^+$ in the external medium.

$$C_a = m / N_a V_{in} = n / N_a v_{in} \ (\text{mol} / \text{l})$$

where N_a is Avogadro's constant (6.02×10^{23}). The buffer capacity of the vesicle interior (β_{in}) is defined as :

$$\beta_{in} = - d \ C_a / d \ (pH_{in})$$

where $d \ (pH_{in})$ is negative upon adding acid. From the Van Slyke equation

$$\beta_{in} = 2.303 \ \{K_w / [H^+] + [H^+] + C_b K_a [H^+] / (K_a + [H^+])^2 \} \qquad (14)$$

where $K_w = [H^+][OH^-] = 10^{-14} \ M^2$, K_a is the dissociation constant of the buffer, and C_b is the total concentration of the buffer. Therefore, the internal pH change upon transferring protons of concentration C_a is:

$$- \Delta pH_{in} = \Delta C_a / \beta_{in} = n / N_a v_{in} \beta_{in}$$

and the number of protons transferred is

$$n = N_a v_{in} \beta_{in} (- \Delta pH_{in}) \qquad (15)$$

Two components contribute to the buffer capacity of the DHP vesicle interior, one being the phosphate headgroups forming the internal aqueous/hydrocarbon interface, the other being the encapsulated buffer solution. The buffer capacity of internal phosphate headgroups of DHP vesicles was much larger than that of the Tris-HCl contained within the inner aqueous phase. This was concluded indirectly from titrating the external phosphate headgroups of DHP vesicles and Tris-HCl buffer with their concentrations at the same ratio as that of interior. For DHP vesicles with an outer radius (R) of 130 Å and inner radius (r) of 90 Å, the fraction of DHP molecules facing the interior (δ) is 0.3[27], and the ratio of entrapped volume to bulk volume is 0.001. The concentration of the internal phosphate headgroups of DHP vesicles was estimated to be 1.3 M (see below), and the effective concentration of external phosphate groups was 3 mM. The concentrations of internal and external Tris-HCl buffers were both 20 mM. Therefore, the ratio of internal concentrations of Tris-HCl to phosphate headgroups was 0.015, while the ratio of external concentrations of Tris-HCl to phosphate headgroups was 6.6. Titration of Tris-HCl and external phosphate headgroups of DHP vesicles was performed with their concentrations at ratios equivalent to that of vesicle interior, respectively. Figure 3-15 shows the titration
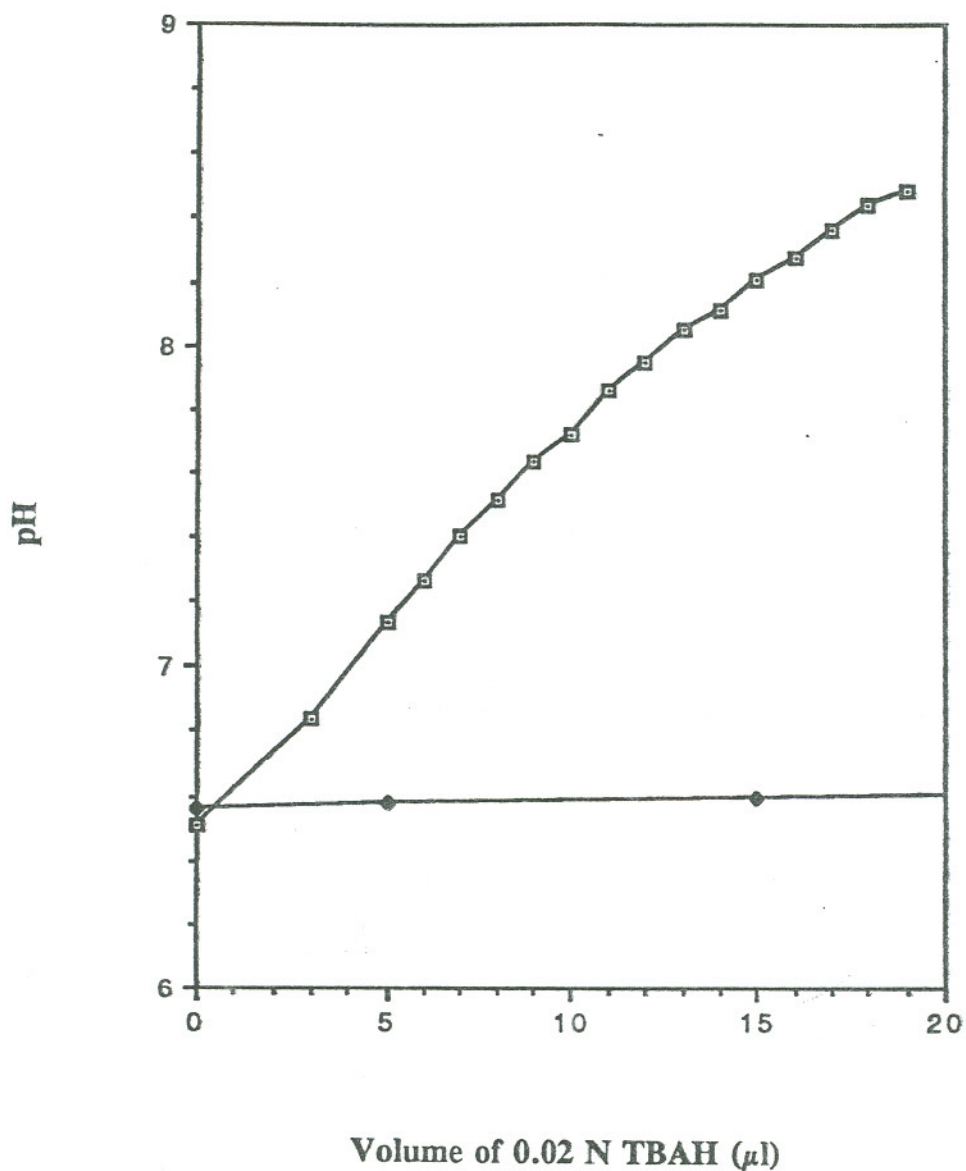
Figure 3-15. Titration curves of 1 ml of 0.15 mM Tris-HCl buffer (open square) and 1ml of 10 mM DHP vesicle suspension (solid diamond) by 0.02 N tetrabutylammonium hydroxide (TBAH) solution. The DHP vesicle suspension was prepared in water and neutralized with 8 mM TBAH. Pyranine (0.01 μM) was added to the above solutions. The pH values were determined from the pyranine calibration curve. 8 mM TBAH was added to Tris-HCl buffer to get the same ionic strength as that of DHP vesicle suspension.

curves. The buffer capacity of phosphate headgroups is much larger than that of the Tris-HCl buffer. The buffer capacity of external phosphate groups of DHP vesicles was obtained from the slope of the titration curve in Figure 3-4 to be about 33 mM $(pH)^{-1}$ around pH 7.40. The buffer capacity of internal phosphate headgroups of DHP vesicles should be approximately 400 fold larger than that of external phosphate considering the difference in concentration between the internal and external phosphate headgroups of DHP vesicles, i.e., 13 M $(pH)^{-1}$.

The buffer capacity of internal phosphate headgroups of the DHP vesicles can be calculated as follows:

From the dimension of DHP vesicles, the effective concentration of internal phosphate groups within the vesicles is given by:

$$C_b^{in} = \delta DHP \ (mol) \ / \ v_{in}N \ (mol \ / \ l)$$

N could be expressed as follows:

$$N = 3(FW)DHP \ (mol) \ / \ 4\rho\pi(R^3 - r^3)$$

where (FW) is the formula weight of DHP molecule (547), ρ is lipid density (1160 g / l), DHP (mol) is the total moles of DHP. Therefore

$$C_b^{in} = \delta\rho(R^3 - r^3) \ / \ (FW)^3 = 1.3 \ (mol/l)$$

depends only upon intensive parameters associated with DHP vesicles and is independent of the DHP concentration. The internal volume per DHP vesicle (v_{in}) was calculated to be 3×10^{-21} l. The internal buffer capacity of phosphate headgroups of DHP vesicles could then be calculated from equation (14) taking the pK_a of the DHP phosphate headgroups as 7.45, which had a maximum of 0.75 M $(pH)^{-1}$ at a pH value equal to pK_a, as shown in Figure 3-16. The calculated value for the buffer capacity of internal phosphate headgroups of DHP vesicles was about 20 times smaller than that determined from the titration experiment. One possible factor contributing to this difference might be that not only the external phosphate headgroups but also some internal phosphate headgroups were titrated during the titration experiment. The number of protons transferring per vesicle was obtained from equation (15) from the measured apparent pH change inside the DHP vesicles
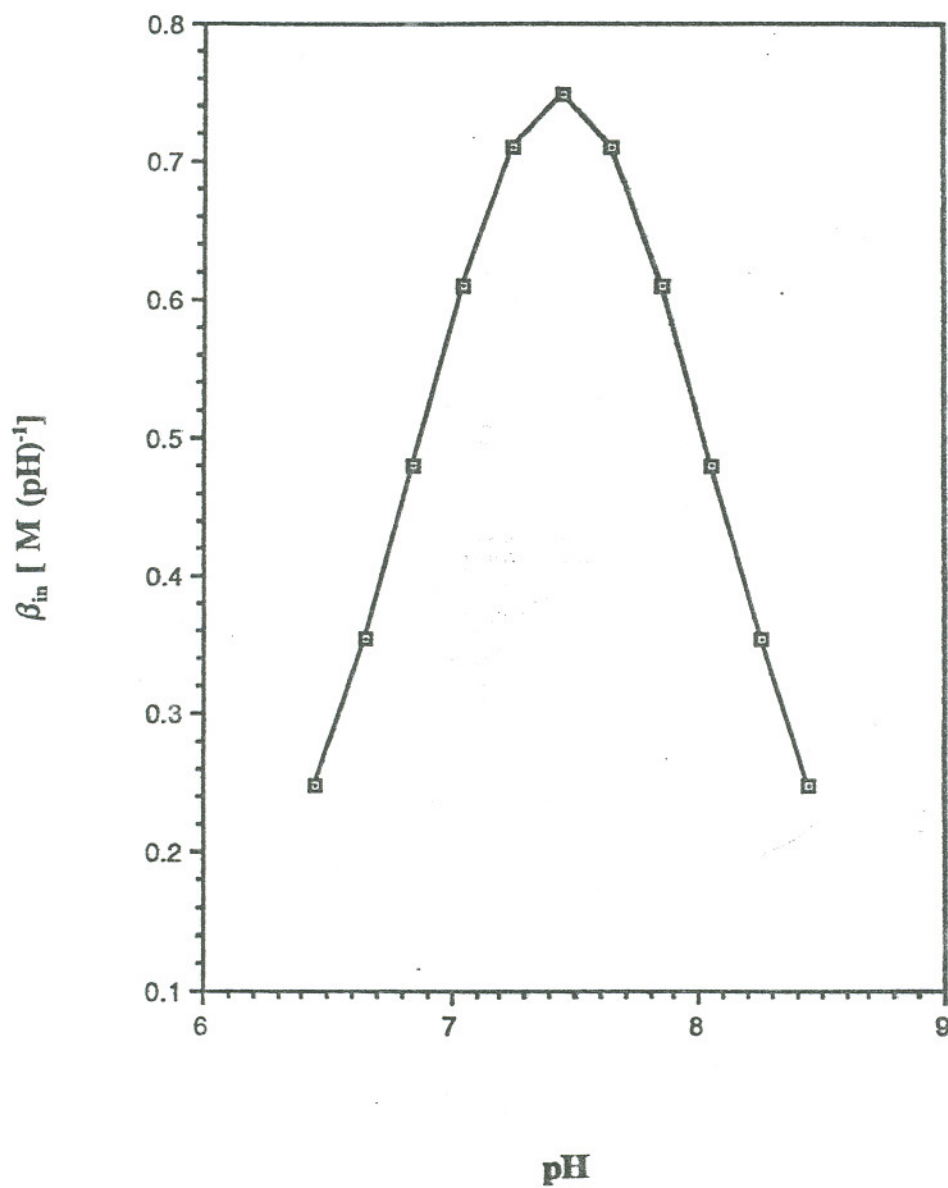
Figure 3-16. The calculated buffer capacity of internal phosphate headgroups of DHP vesicles versus pH_{in}. β_{in} was calculated according to Equation (14), assuming that the pK_a of DHP vesicles was 7.45 and that the effective concentration of internal phosphate headgroups was 1.3 M.

and the internal buffer capacity calculated from equation (14) (Figure 3-16). Table 3-3 and 3-4 show the calculated number of protons moving across DHP vesicle bilayers for each individual pH jump experiment.

2. "Electroporation" Experiments

The calculations suggest that several hundred protons move across DHP vesicle bilayers in these pH jump experiments. This corresponds to development of a transmembrane potential estimated to be greater than 1 volt (Figure 3-17) if this charge translocation is uncompensated, which is physically "impossible". One possible explanation is that the vesicles transferred electrolytes by "electroporation", i.e., formation of transient pores in the membrane caused by the developing transmembrane potential[11, 12]. The pores would allow transmembrane movement of other ions besides H^+/OH^-, hence, rapid dissipation of the potential.

8 mM DHP vesicle suspensions with entrapped pyranine were prepared in water and neutralized with NaOH to the desired pH. A pH jump perturbation was applied to make the external solution more alkaline, requiring that protons move out of the vesicles. The pH_{in} versus time curves for vesicle suspensions containing 10 mM KCl in the medium are compared in Figure 3-18 to the curves for suspensions where KCl was absent. The change of pH_{in} was larger for the pH jump experiment with 10 mM external K^+ ions present. If the pH jump was equivalent to applying an electric field to the DHP vesicles, transient pore formation could allow influx of K^+ ions, which would partially dissipate the potential, allowing more protons to move out. After the pH jump experiment was finished, the suspension was passed through a Chelex 100 cation exchange column to remove the external potassium ions. Detection of internal potassium ions was attempted using atomic absorption spectroscopy. The standard curve for potassium ions is shown in Figure 3-19. The concentration of K^+ ions in the medium before chromatography was 10.5 mM, but no K^+ ions were detected in the sample after passage through the Chelex column, within
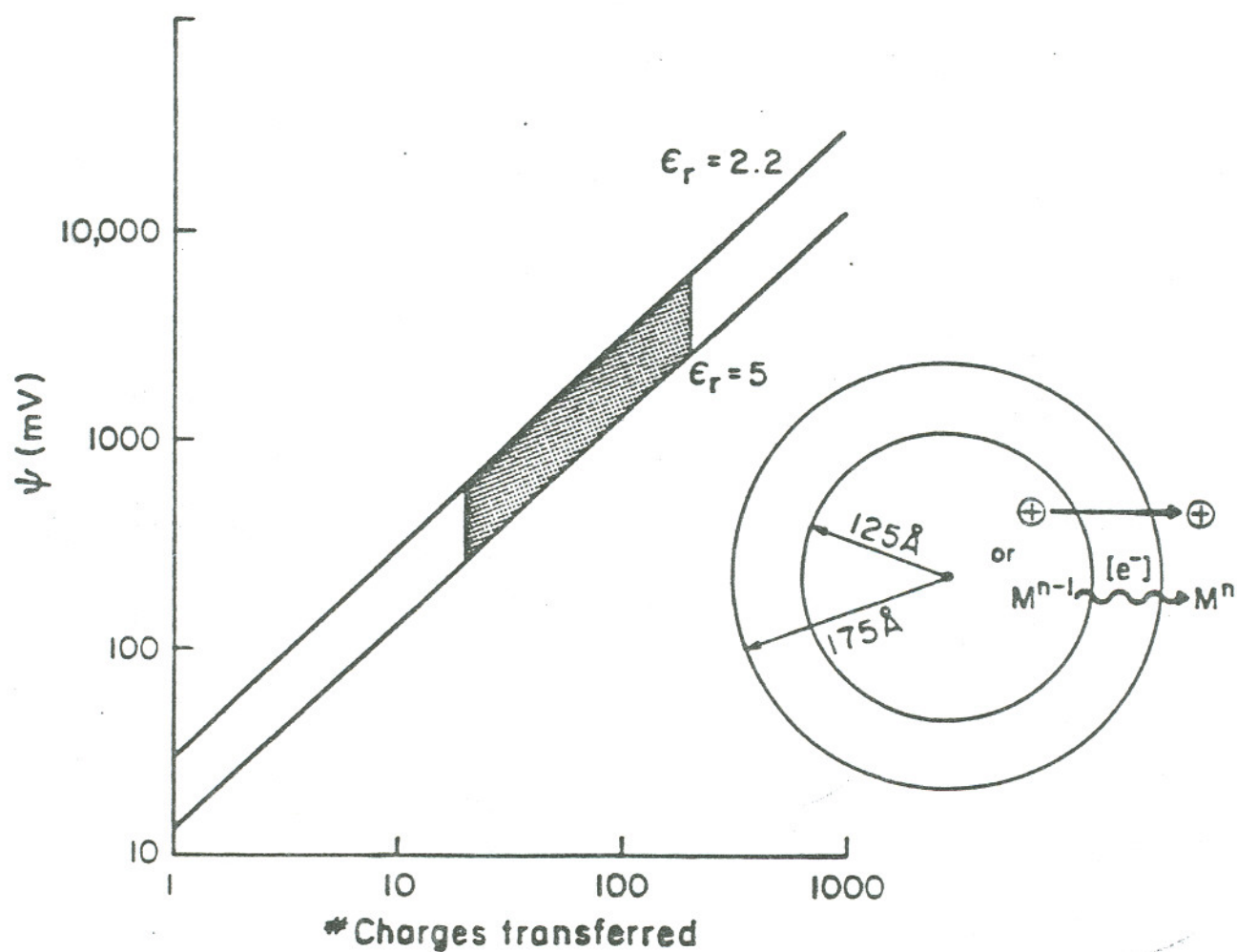
Figure 3-17. Electric polarization of a concentric plate capacitor with dimensions of a small unilamellar vesicle. Solid lines are electrical potentials (ψ) for an internal dielectric with relative permittivities (ε_r) of 2.2 and 5.0. For bilayer membranes, this graph is hypothetical since catastrophic breakdown of their electrical insulating properties occurs at transmembrane potentials larger than about 200 mV (corresponding to an electric field of 4×10^5 V/cm). Adapted from reference 19.
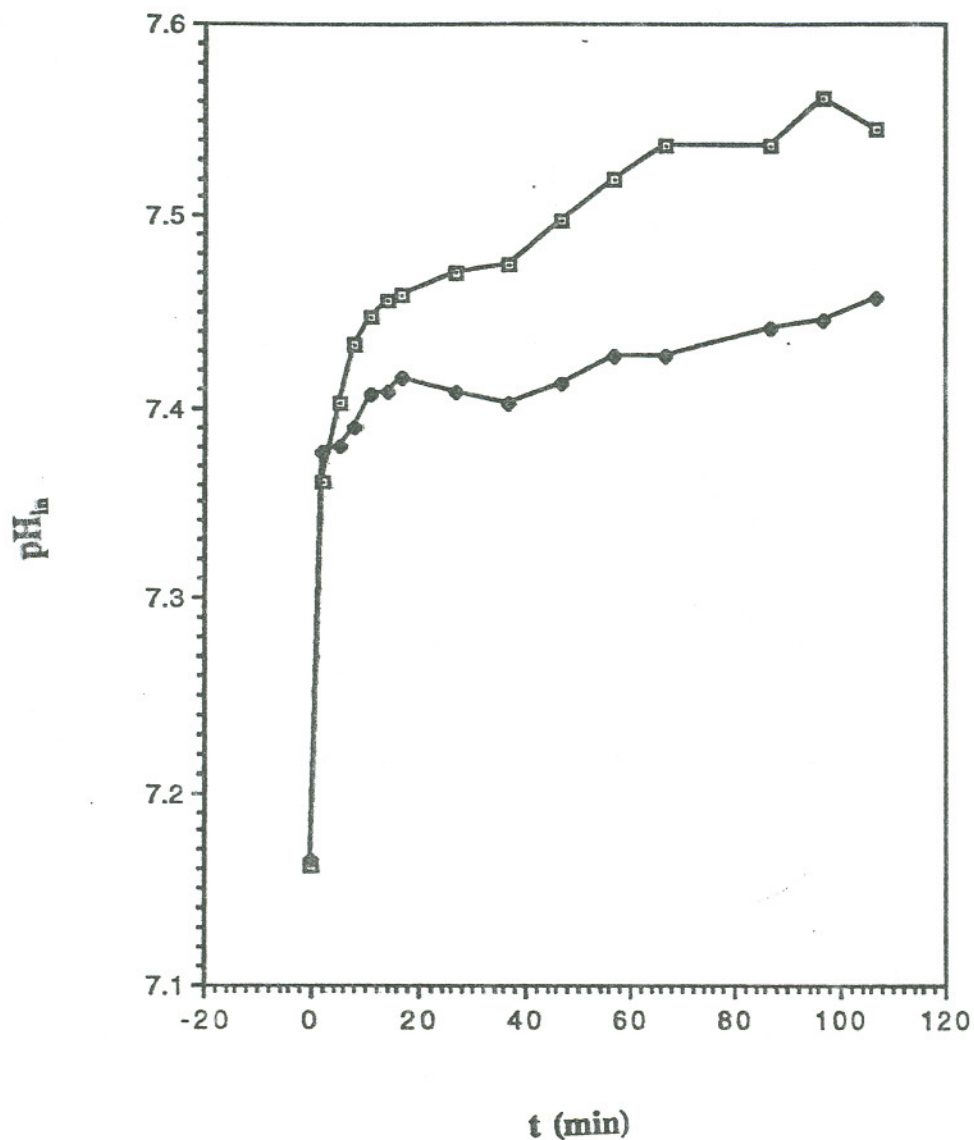
Figure 3-18. Changes in pH_{in} versus time of DHP vesicles upon applying an external pH jump in the absence (solid diamond) and presence (open square) of 10 mM K$^+$ ions in the external medium. 0.5 ml of 5 mM Tris-HCl, pH 8.80, was added to 0.5 ml of 8 mM DHP vesicle suspension with entrapped pyranine in 5 mM Tris-HCl buffer, pH 7.56. pH_{in} was determined from the pyranine calibration curve. The DHP vesicle suspension was prepared in water and neutralized with NaOH.
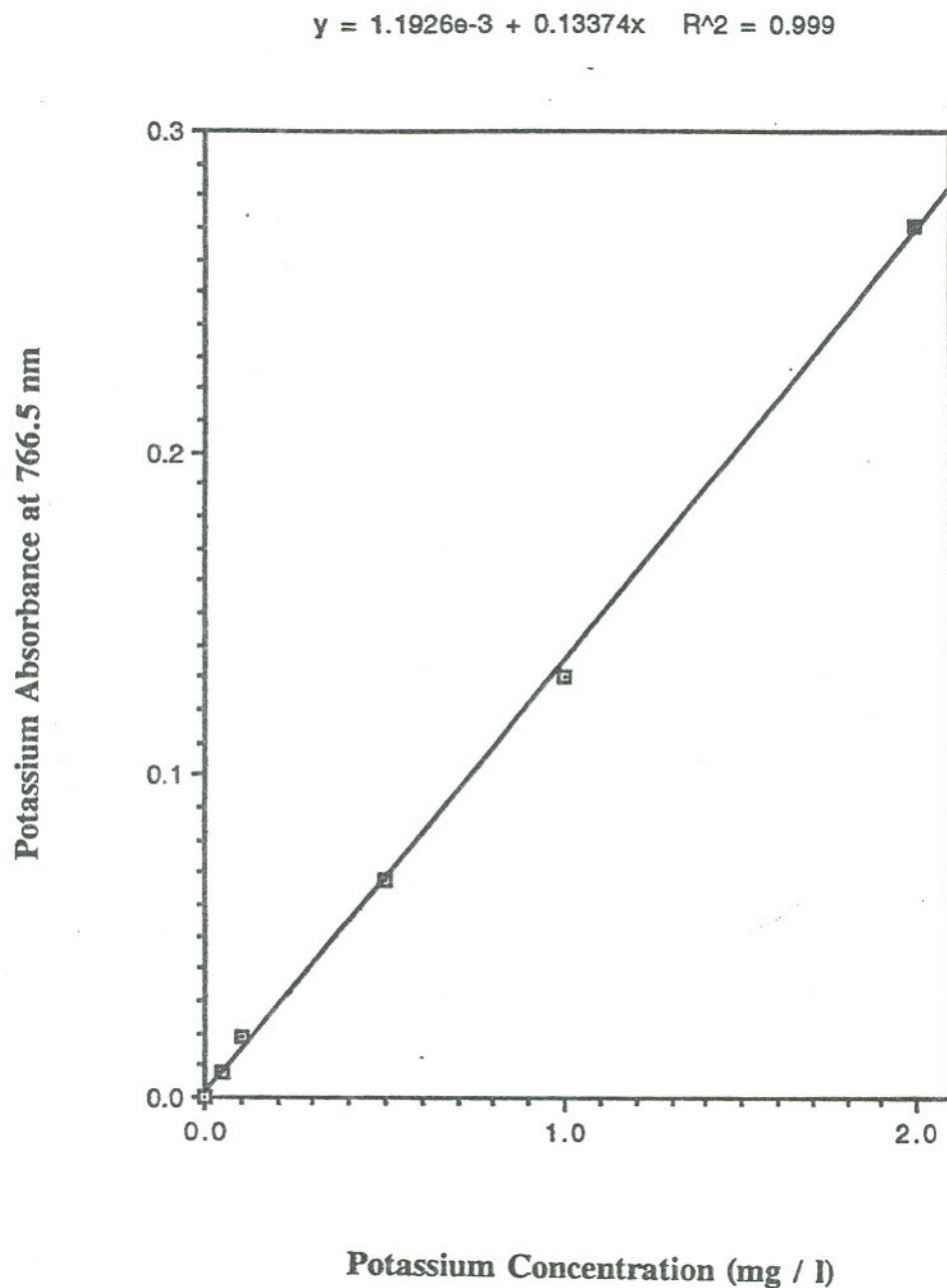
Figure 3-19. The standard curve for K⁺ ion determined by atomic absorption spectroscopy. The absorbance at 766.5 nm of several different concentrations of standard aqueous KCl solutions was measured.

an instrumental detection limit of 1.3 μM. The analytical concentration of K^+ taken up, assuming 1:1 stoichiometric counter-transport for H^+ ions, could be estimated from the measured difference in pH_{in} change between pH jump experiments made in the presence and absence of 10 mM external K^+ ions. The expected value was 9.1 μM. The reason why K^+ ions were apparently not taken up is unclear.

These experiments provide no direct evidence that electroporation occurs. There are more sensitive methods than atomic absorption spectroscopy to detect molecules or ions moving across membranes during electroporation. Radioactive metal ions such as $^{22}Na^+$, $^{86}Rb^+$ or ^{14}C-labeled glucose or sucrose molecules could be entrapped inside DHP vesicles. Their leakage out of vesicles induced by a pH jump during electroporation might be considered as future experiments[10, 14, 15]. The pH jump induced uptake of fluorescence probes of different molecular weights, or the efflux of soluble fluorescence-tagged molecules out of the vesicles could also be considered[44].

3. Other Possible Explanations for the Experimental Results

a. Dilution Effects

The pH jump experiments were usually initiated by mixing equal volumes of DHP vesicle suspensions and the same buffer at a higher or lower pH. To ensure that the pH jump was exclusively from the pH difference rather than an artifact arising from dilution of the vesicles, several control experiments were done.

8 mM DHP vesicles with entrapped pyranine were prepared in water and neutralized with NaOH to the desired pH. Either DHP vesicles with entrapped pyranine or with external pyranine were mixed with the same volume of 5 mM Tris-HNO_3. The pH values for the two solution were identical, as determined with a pH meter or by fluorescence spectrophotometry. The results are summarized in Table 3-6. Measured changes in pH were less than 0.06 pH units, indicating that dilution

Table 3-6. Dilution Effects on pH Jump Experiments[a]

0.5 ml 8 mM DHP vesicles			0.5 ml 5 mM Tris-HNO$_3$		Mixture	
$pH_{pyr.}^{in}$	$pH_{pyr.}^{out}$	$pH_{elec.}^{out}$	$pH_{pyr.}$	$pH_{elec.}$	$pH_{pyr.}^{in}$	$pH_{pyr.}^{out}$
7.22		7.66		7.66	7.25	
7.47		7.74		7.74	7.47	
	7.28	7.68		7.68		7.32
	7.52		7.51			7.49
	7.52		7.55			7.52

[a] 8 mM DHP vesicles with entrapped pyranine were prepared in water and neutralized with NaOH. 0.5 ml of the DHP vesicle suspension was mixed with 0.5 ml 5 mM Tris-HNO$_3$ for dilution experiments. $pH_{pyr.}^{in}$ was the internal pH of the DHP vesicles determined from the entrapped pyranine according to the pyranine calibration curve. $pH_{pyr.}^{out}$ was the external pH of DHP vesicles determined by adding excess pyranine to the external medium. $pH_{elec.}^{out}$ was the external pH of DHP vesicles measured using the pH meter. $pH_{pyr.}$ was the pH of bulk Tris-HNO$_3$ buffer determined by adding 0.01 μM pyranine. $pH_{elec.}$ was the pH of bulk Tris-HNO$_3$ measured using the pH meter.

effects in the pH jump experiments were negligible.

b. Existence of External Pyranine in DHP Vesicle
Suspensions After Chromatography

From Table 3-3 and 3-4, the percentage of ΔpH_{in}^{fast} contributing to ΔpH_{in}^{total} was from 12% to 87%. If ΔpH_{in}^{fast} arose from pyranine remaining in the external aqueous phase of DHP vesicles, its percentage contribution to ΔpH_{in}^{total} should be proportional to the magnitude of the external pH jump. This seemed not to be the case from Table 3-3 and 3-4.

Because the mixing was done manually and fluorescence intensities at two wavelengths (404 nm and 455 nm) were read, the first pH_{in} obtained after mixing took about 2 minutes. The fast phase of the pH jump experiment was analyzed using a stopped-flow rapid-mixing apparatus and monitoring the fluorescence intensity at a single wavelength.

An 8 mM DHP vesicle suspension with entrapped pyranine was prepared in 20 mM Tris-HCl buffer. Then equal volumes of DHP vesicles, pH 8.32 and 20 mM Tris-HCl, pH 2.02 were mixed using a Hi-Tech Scientific SFA-II Rapid Kinetics Accessory stopped-flow mixing apparatus. The rate of change of fluorescence intensity of the deprotonated form of pyranine was monitored at λ_{ex} = 455 nm, λ_{em} = 510 nm. Results are given in Figure 3-20. There was an initial fast decrease of intensity which was complete within 2 seconds, followed by a slower change in the same direction. The permeability coefficient of H^+/OH^- across the membrane for the fast phase is calculated to be around 0.1-1 cm/s; this corresponds to a first-order rate constant of $\sim 10^6$ s^{-1} (see following discussion), which is too large to be transmembrane movement of H^+/OH^-. Therefore, this fast phase must be caused by some external pyranine. This kind of phenomenon was also observed by Gould et al in asolectin vesicles[38]. They suggested that the fast component of the fluorescence decrease represented an initial rapid, and at least partially electrically uncompensated, diffusion
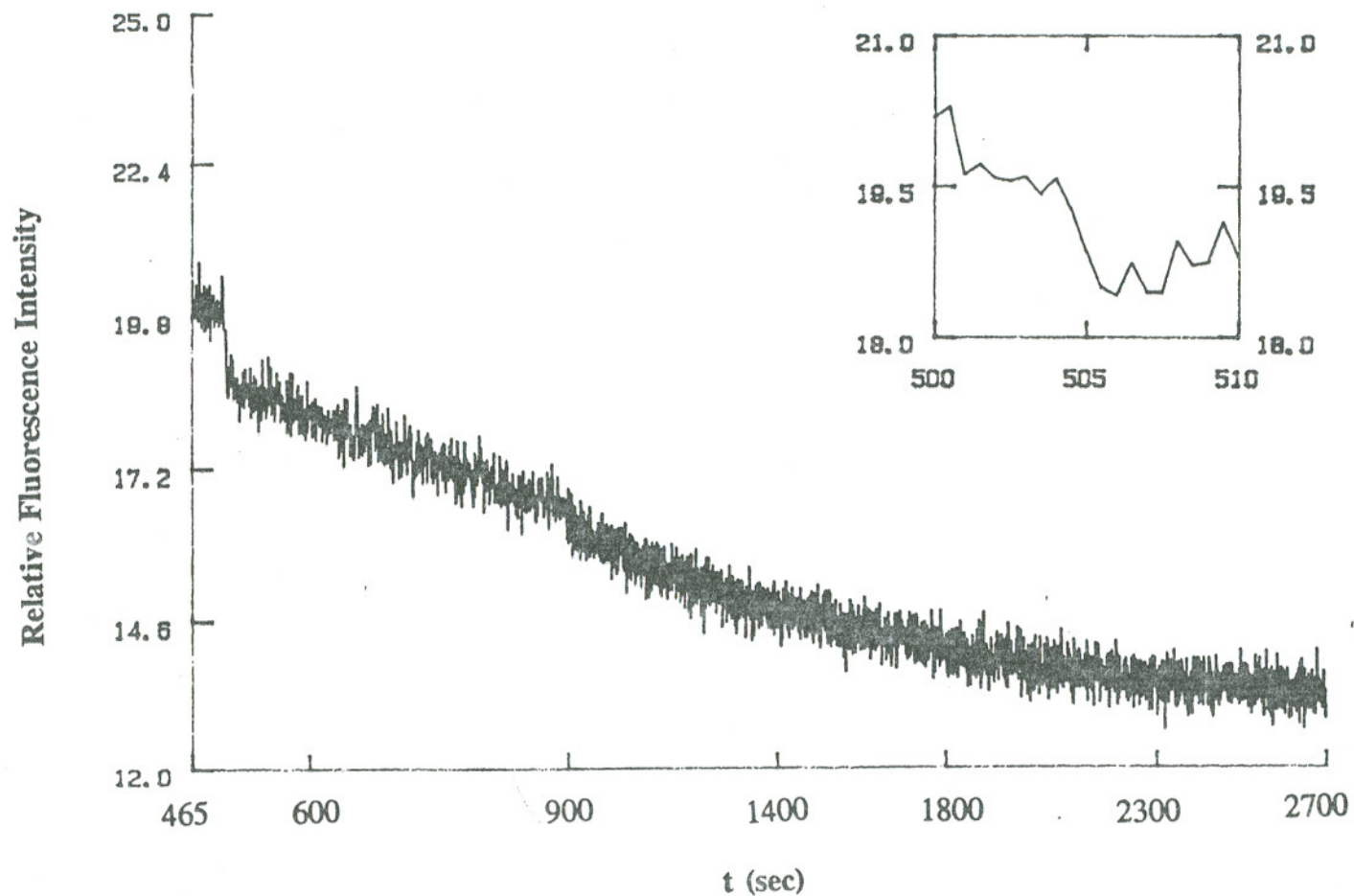
Figure 3-20. Changes in relative fluorescence intensities at λ_{ex} = 455 nm and λ_{em} = 510 nm with time upon stopped-flow mixing equal volumes of 20 mM Tris-HCl, pH 2.02 and DHP vesicles with entrapped pyranine in 20 mM Tris-HCl, pH 8.32. The inset shows an enlargement of the initial changes following mixing.

of protons into vesicles. This uncompensated charge influx would lead to the formation of transmembrane electric potential (inside positive) which eventually would slow further proton influx to a counterion-limited proton-counterion exchange.

c. Leakage of Pyranine

Pyranine is a polyanionic molecule containing three sulfonate groups. Once entrapped inside anionic DHP vesicles, it should not easily leak out because the interfacial electrostatic repulsive force is large. Any leakage of pyranine occurring during the pH jump might be checked for using the pyranine fluorescence quencher, thiamine[29].

An 8 mM DHP vesicle suspension with entrapped pyranine was prepared in 20 mM Tris-HCl buffer. Immediately before applying the pH jump, 2 mM thiamine was added to the DHP vesicles. The excitation spectra of entrapped pyranine in the presence and absence of thiamine are shown in Figure 3-21. Then the pH jump was initiated by mixing equal volumes of DHP vesicles and Tris-HCl solution that contained no thiamine. Following completion of the pH jump experiments, 2 mM thiamine was added to the mixture. The excitation spectra are shown in Figure 3-22. No quenching was observed, indicating that pyranine efflux from the vesicles did not occur during the pH jump experiments.

D. Estimation of the H^+/OH^- Permeability Coefficient

Nichols and Deamer first reported high H^+/OH^- permeability across egg phosphatidylcholine liposomes[6]. They prepared internally highly buffered and externally lightly buffered liposomes and monitored the small external pH change (about 0.1 pH unit) with a pH meter upon adding a small amount of acid or base. The net flux of proton and hydroxyl ions across a membrane (J_{net}) is:

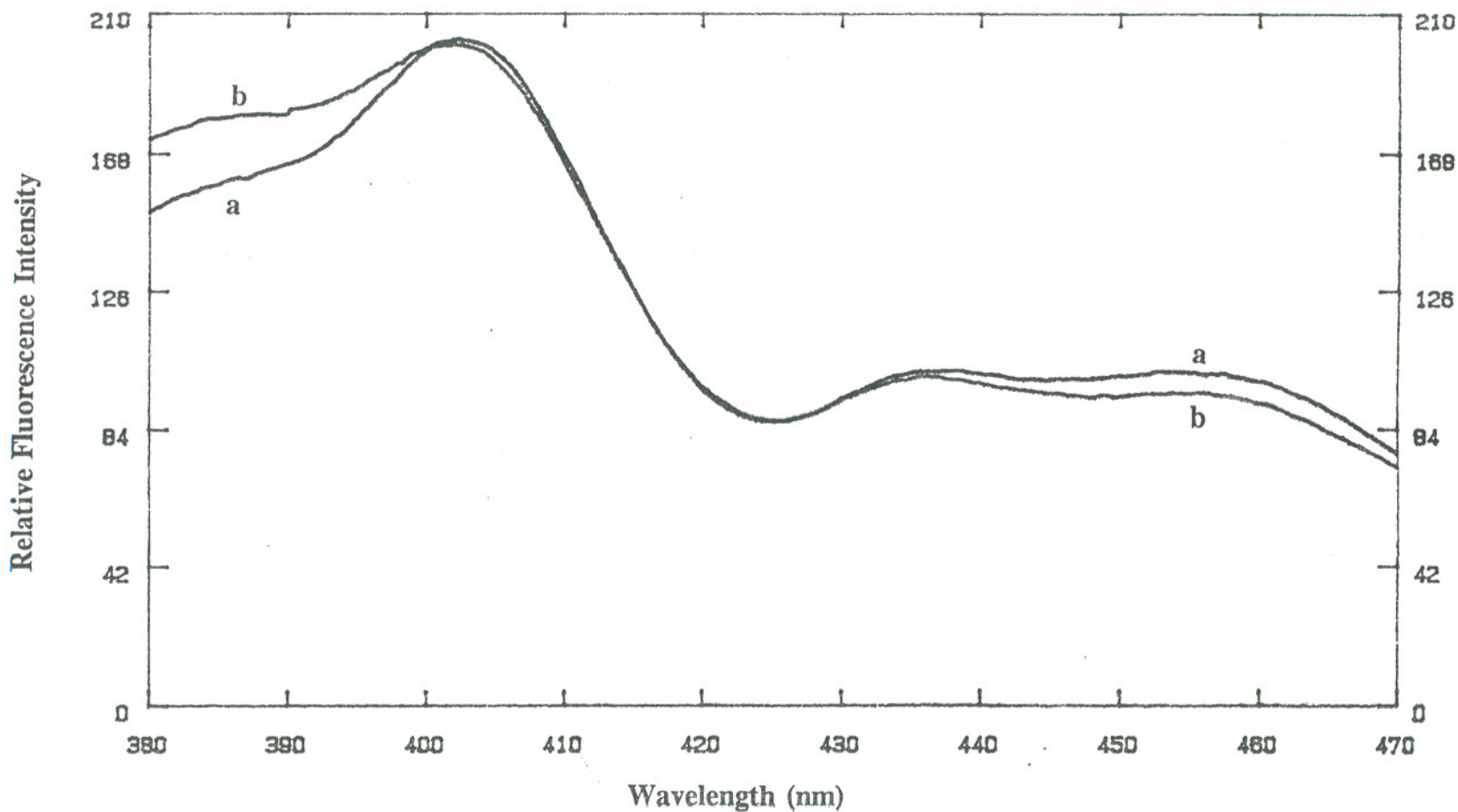$$J_{net} = P_H ([H^+]_o - [H^+]_i) + P_{OH} ([OH^-]_i - [OH^-]_o) \qquad (16)$$

Figure 3-21. Excitation spectra (λ_{em} = 510 nm) of an 8 mM DHP vesicle suspension with entrapped pyranine (about 0.01 μM) in 20 mM Tris-HCl buffer, pH 7.88 (trace a), and with 2 mM thiamine added before initiation of the pH jump (trace b).

a

b
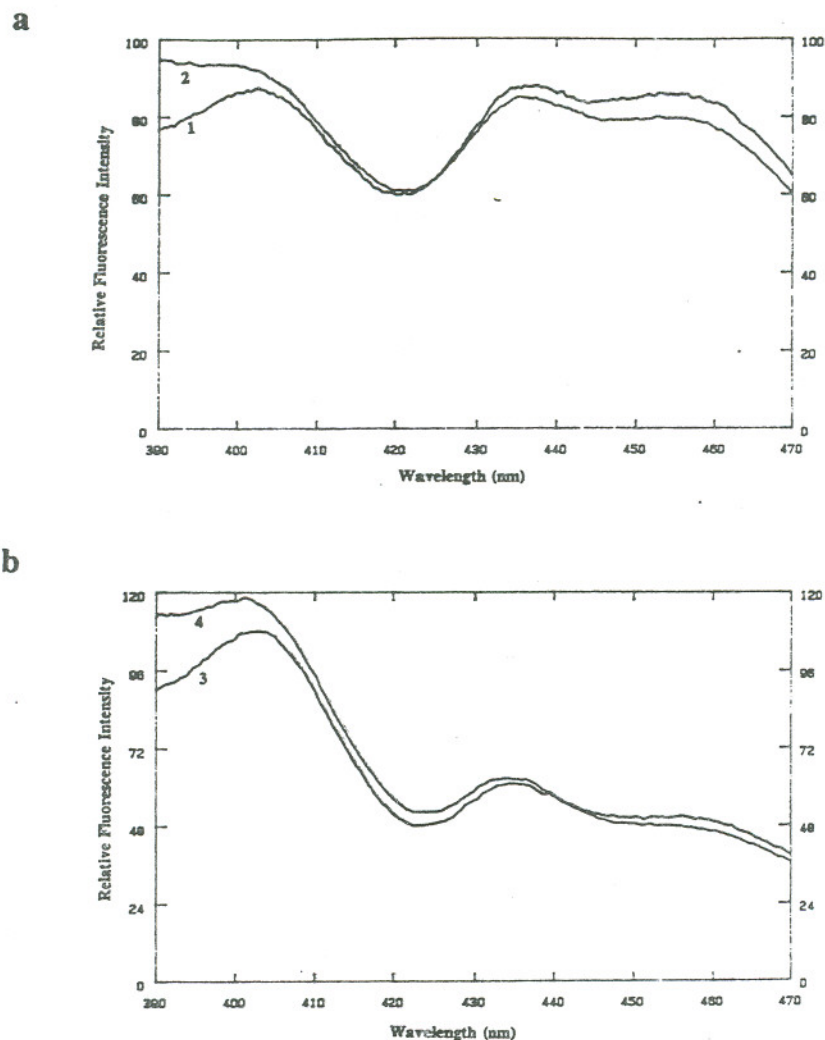
Figure 3-22. (a) Excitation spectra (λ_{em} = 510 nm) of the final reaction solution from the pH jump experiment (trace 1), and with 2 mM thiamine added to the suspension (trace 2). 0.5 ml of 20 mM Tris-HCl solution, pH 9.56, was added to 0.5 ml of 8 mM DHP vesicle suspension with entrapped pyranine (about 0.01 μM) in 20 mM Tris-HCl buffer, pH 7.88. After the system reached equilibrium, 2 mM thiamine was added to the final solution. (b) Excitation spectra (λ_{em} = 510 nm) of the final reaction solution from the pH jump experiment (trace 3), and with 2 mM thiamine added to the suspension (trace 4). 0.5 ml of 20 mM Tris-HCl solution, pH 3.12 was added to 0.5 ml of 8 mM DHP vesicle suspension with entrapped pyranine (about 0.01 μM) in 20 mM Tris-HCl buffer, pH 7.88. After the system reached equilibrium, 2 mM thiamine was added to the final solution.

where P_H and P_{OH} are the permeability coefficients for protons and hydroxyls, respectively; $[H^+]_o$ and $[H^+]_i$ are the internal and external proton concentrations of the liposomes, respectively; $[OH^-]_o$ and $[OH^-]_i$ are the internal and external hydroxyl concentrations of the liposomes, respectively. This flux equation is based upon the assumptions that (i) the flux is not limited by the development of a diffusion potential, (ii) the proton and hydroxyl permeabilities are independent of the direction of flux, and (iii) the proton and hydroxyl ions move independently.

For a small acid or base pulse around pH 7.0, the difference in proton concentrations across the membrane is approximately equal and of opposite sign to the difference in hydroxyl concentrations:

$$[H^+]_o - [H^+]_i = [OH^-]_i - [OH^-]_o \tag{17}$$

They defined the net permeability coefficient (P_{net}) of H^+/OH^- as:

$$P_{net} = P_H + P_{OH} \tag{18}$$

Then substituting Equations (17) and (18) to Equation (16), they obtained:

$$J_{net} = P_{net} ([H^+]_o - [H^+]_i) \tag{19}$$

The net H^+/OH^- flux can also be calculated from the derivative of the external pH with respect to time (dpH_o / dt) multiplied by the appropriate factors:

$$J_{net} = (dpH_o / dt) (\beta_o V_o / A) \tag{20}$$

where A is the total surface area of the vesicles ($A = 4\pi(R^2 + r^2)$); β_o is the buffer capacity of the external solution; and V_o is the external volume. Therefore, P_{net} could be estimated from the time course of external pH change upon a pH jump according to the equation:

$$dpH_o / dt = P_{net} A([H]_o - [H]_i) / \beta_o V_o \tag{21}$$

The internal pH was assumed to be equal to that of the external pH at equilibrium, and was calculated from the following equation:

$$pH_i = R(pH_o - pH_o^i) + pH_i^i \tag{22}$$

where pH_i and pH_o are the internal and external pH of the liposomes, respectively; pH_o^i and pH_i^i are the initial external and internal pH of liposomes, respectively; and R is the ratio of the change in internal pH to the change in external pH. Substituting

Equation (22) into Equation (21), they obtained:

$$dpH_o / dt = P_{net} A (10^{-pH_o} - 10^{-R(pH_o - pH_o^i) + pH_i^i}) / \beta_o V_o \qquad (23)$$

They solved the equation by trial-and-error estimation of P_{net} and integrating numerically until a value was found that accurately predicted the actual experimental pH recording at a given time. P_{net} was estimated to be around 10^{-4} cm/sec; it was insensitive to variations in lipid composition and surface charge.

Because we measured directly the time course of the internal pH change, the analogous equations given below are valid:

$$dpH_i / dt = P_{net} A ([H^+]_i - [H^+]_o) / \beta_i V_i$$

$$dpH_i / dt = P_{net} A (10^{-pH_i} - 10^{-R'(pH_i - pH_i^i) + pH_o^i}) / \beta_i V_i \qquad (24)$$

where β_i and V_i are internal buffer capacity and volume, respectively. R' is the ratio of the change in external pH to the change in internal pH. P_{net} can be expressed as follows:

$$P_{net} = \beta_i (d\, pH_i / d\, t) V_i / A ([H^+]_i - [H^+]_o) \qquad (25)$$

Cafiso and Hubbell studied electrogenic H^+/OH^- transport in egg phosphatidylcholine and diphytanoylphosphatidylcholine sonicated vesicles using phosphonium (I) and N-tempoyl-N-hexylamine (II) spin labels[45]:
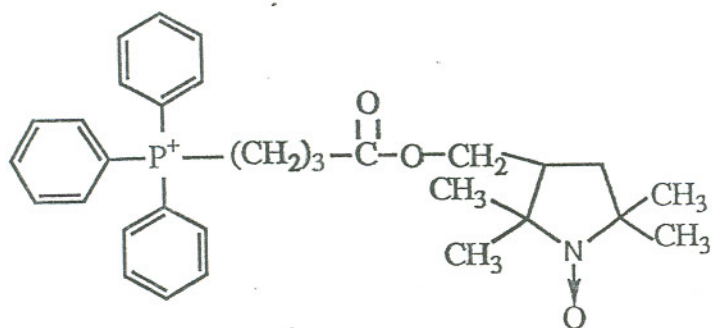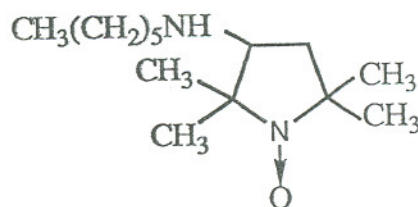
(I)   (II)

Both transmembrane potentials (I) and pH gradients (II) were computed from the high field resonance amplitudes of these spin-labels. Gradients of pH were established across these vesicle bilayers by either diluting the vesicle suspension into the appropriate buffer or by adding base to the existing vesicle-buffer suspension. An independent value for P_{net} could be obtained from the initial time rate of change of internal pH in vesicles according to the equations:

$$P_{net} = \beta_i(\partial \, pH_i \, / \, \partial \, t)_{\Delta\Psi=0} V_i \, / \, A([H^+]_i - [H^+]_o)$$

$$P_{net} = \beta_i(\partial \, pH_i \, / \, \partial \, t)_{\Delta\Psi=0} r^2 \, / \, 3R([H^+]_i - [H^+]_o) \tag{26}$$

where β_i is the internal buffer capacity, V_i is the vesicle internal volume, A is the vesicle geometric-mean surface area, given by $A = 4\pi Rr$. They obtained a permeability coefficient of H^+/OH^- around 10^{-7} cm/sec.

The equations for P_{net} developed each by Nichols and Cafiso are essentially the same except for the surface area A, which was expressed as $4\pi(R^2 + r^2)$ and $4\pi Rr$, respectively. The ratio of the former to latter area is 2 using R = 130 Å and r = 90 Å. Another difference was that Nichols dealt with an extremely small transmembrane pH gradient (about 0.1 pH unit), thus ensuring that the rate of decay of the gradient was not limited by build-up of a transmembrane potential, while Cafiso dealt with a large pH gradient (about 1.0 pH unit). In this case, P_{net} was calculated from initial rate of pH change.

For our pH jump experiments, we could estimate P_{net} according to equation (26) from the slow rate of change of pH_i versus time. In this calculation, we assume that the fast phase is due to changes involving the external pyranine, so that the condition $\Delta\Psi = 0$ is met. Results are given in Table 3-7, for which P_{net} was around 10^{-4} to 10^{-5} cm/sec.

Table 3-7.   Estimation of the H^+/OH^- Permeability Coefficient Across DHP Vesicle Bilayers[a]

pH_i	pH_o	ΔpH	β_i (M pH^{-1})	$10^5 \cdot (\partial pH_i/\partial t)_{\Delta\Psi=0}$ (pH sec^{-1})	$10^5 \cdot P_{net}$ (cm/sec)
7.18	8.25	1.07	0.68	7.33	17.1
7.05	8.20	1.15	0.61	4.72	7.21
7.05	6.02	-0.13	0.61	87.6	12.7
7.13	8.28	1.15	0.66	5.57	11.2
7.97[b]	9.00	1.03	0.53	12.0	135
8.40[b]	7.11	-1.29	0.27	15.4	11.8
7.68[b]	6.49	-1.19	0.70	9.64	4.66
6.99[b]	7.59	0.60	0.57	9.44	14.8
7.17[b]	7.82	0.65	0.67	2.13	5.56

a)   DHP vesicles with entrapped pyranine were prepared in 20 mM Tris-HCl buffer as described in Experimental Methods. The pH jump experiment was done by mixing 0.5 ml of DHP vesicles and 0.5 ml of the same buffer at a different pH. pH_i was the initial internal pH of the DHP vesicle suspension before a pH jump. pH_o was the final external pH of the DHP vesicles after a pH jump. ΔpH was the difference of pH_o and pH_i. All pH values were obtained from pyranine fluorescence excitation profiles. β_i was the calculated internal buffer capacity (Figure 3-16). $(\partial pH_i/\partial t)_{\Delta\Psi=0}$ was the initial slope of slow change process in a pH_{in} versus time curve in a pH jump experiment.

P_{net} was calculated from the equation:

$$P_{net} = \beta_i r^2 (\partial pH_i/\partial t)_{\Delta\Psi=0} / 3R([H^+]_{i.} - [H^+]_o).$$

b) DHP vesicles with entrapped pyranine were prepared in water and neutralized with NaOH or tetrabutylammonium hydroxide as described in Experimental Methods. The pH jump experiment was done by adding small amount of NaOH or HCl to 1 ml of DHP vesicle suspension. Other symbols were the same as in footnote a.

V. Incorporation of Bacteriorhodopsin Into DHP Vesicle Bilayers

Various ways exist for incorporating bR into lipid vesicle bilayers[26]. Two general approaches have been developed, based upon whether or not detergents are used. In this work detergents were not used, but cosonication or incubation of the protein and lipids was attempted. In earlier studies, bR has been successfully incorporated into phospholipids using these techniques, but application to dihexadecylphosphate membranes has not been previously attempted.

In order to obtain an asymmetric protein orientation in lipid bilayers, low protein to lipid ratios should be used so that most vesicles contain one or fewer protein molecule[46]. For DHP vesicles, assuming 4×10^3 DHP molecules per vesicle, a 1:1 ratio of bR to DHP vesicle is 1:84 (w/w) or 1:4000 (mole/mole).

A. Cosonication Method

Purple membrane appears as oval or round sheets with average diameter of 0.5 μm. Sonicating purple membrane breaks up the native membrane sheets into smaller fragments about 0.1 μm in diameter. Continued sonication can lead to destruction of the chromophore[47].

8 mM DHP powders were first sonicated in 20 mM Tris-HCl buffer for two 10-minute pulses separated by a 5-minute interval. The suspension was then passed through a 0.2 μm pore size cellulose nitrate membrane filter to remove titanium particles. Then about 7 μM bR solution was added to above sonicated DHP vesicles suspension. The mixture was cosonicated in an ice bath 8 times for 3-minute periods with 5-minute intervals. The color of the purple membrane decreased as the sonication time increased. The suspension was then passed through a 0.2 μm filter. The absorption spectra of the mixture before and after sonication are shown in Figure 3-23. Three effects are observed upon sonication. First, light scattering in the
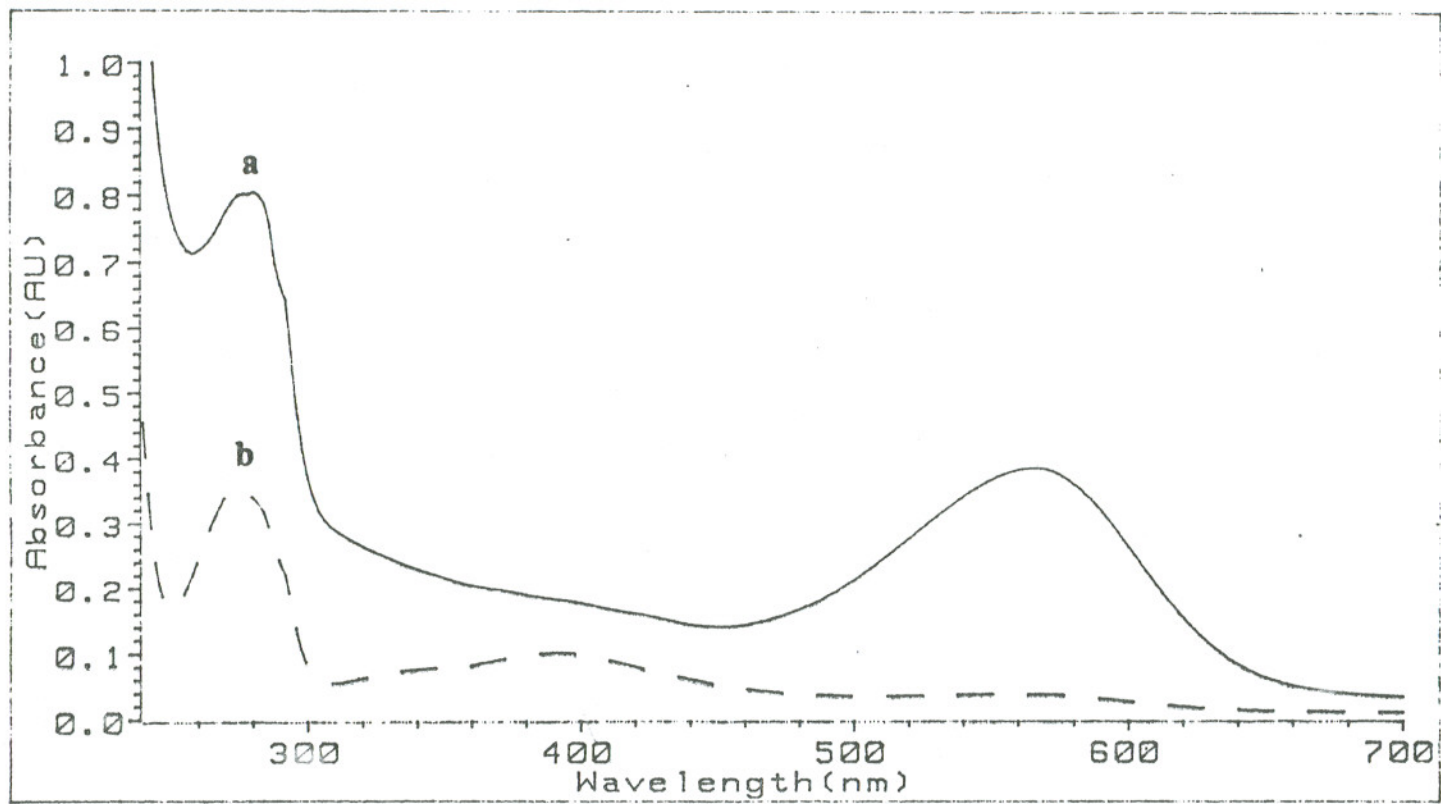
Figure 3-23. Absorption spectra of a mixture of 7 μM bR and preformed 8 mM DHP vesicles in 20 mM Tris-HCl buffer before (trace a) and after (trace b) cosonication 8 times 3-minute periods.

ultraviolet region was reduced; second, the absorption intensity at 570 nm decreased, and third, a new absorption maximum at 390 nm appeared, which might be the result of dissociation of retinal from the protein. If the mixture of DHP vesicles and purple membrane was cosonicated for 10 minutes under argon gas, the chromophore was not destroyed. The absorption spectra before and after sonication are shown in Figure 3-24. Only the first two effects were observed.

The cosonicated mixture was centrifuged at 20°C in a Ty 65 rotor at 36,000 rpm for 90 minutes. The supernatant was clear and colorless, although a purple pellet was found at the bottom of the centrifuge tube. The supernatant was isolated for UV/Vis measurement. The absorption spectrum had no bR peak at 570 nm, but exhibited scattering from the DHP vesicles. Apparently the pure vesicles, the vesicles incorporated with protein and the unincorporated protein cannot be cleanly separated on the basis of their sedimentation rates. Therefore, the distribution of bR in the lipid vesicles was characterized by centrifugation on a sucrose density gradient, which relied upon differences in buoyant density between the protein and lipids[1]. A linear gradient containing 12 ml of 5-35% (w/w) sucrose in 20 mM Tris-HCl (pH 7.8) buffer was layered on top of a 1-ml 45% sucrose cushion. The cosonicated vesicle sample was then added and centrifuged at 17500 rpm for 17 hours at 20°C in a Beckman SW 27.1 swinging bucket rotor. An opalescent band appeared in the middle of the gradient (Figure 3-25); however, its absorption spectrum (Figure 3-26) gave no indication of the presence of bR. I conclude that bR was not incorporated into DHP vesicle bilayers by these procedures.

B. Incubation Method

8 mM preformed DHP SUVs were mixed with 5 μM purple membrane. The mixture was incubated at 60°C for 3 to 15 hours. The absorption spectra of the mixture before and after incubation are shown in Figure 3-27. The scattering was larger after incubation, which might be caused by fusion of the vesicles. The
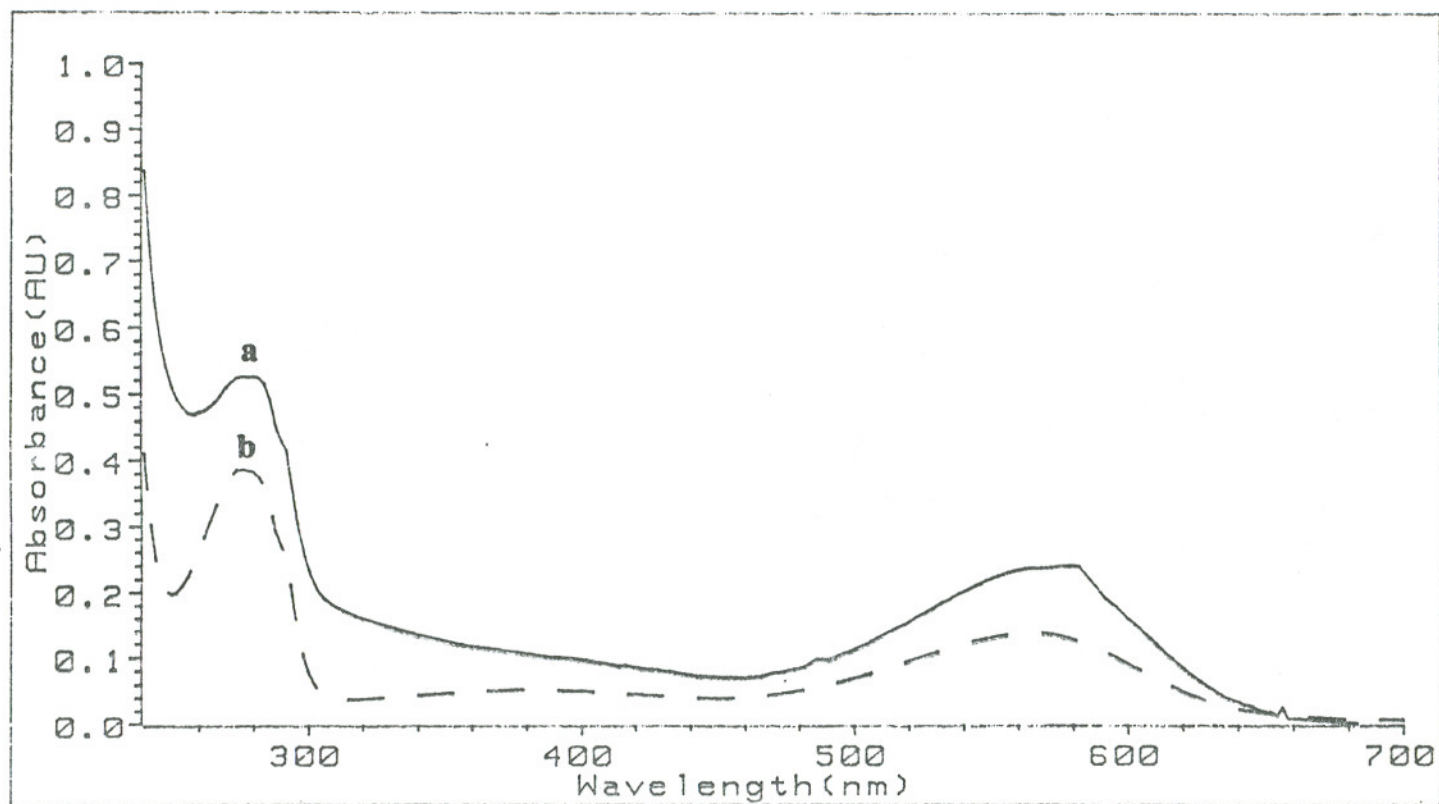
Figure 3-24. Absorption spectra of a mixture of 5 µM bR and 8 mM DHP vesicles in 20 mM Tris-HCl buffer before (trace a) and after (trace b) cosonication for 10 minutes under argon gas.
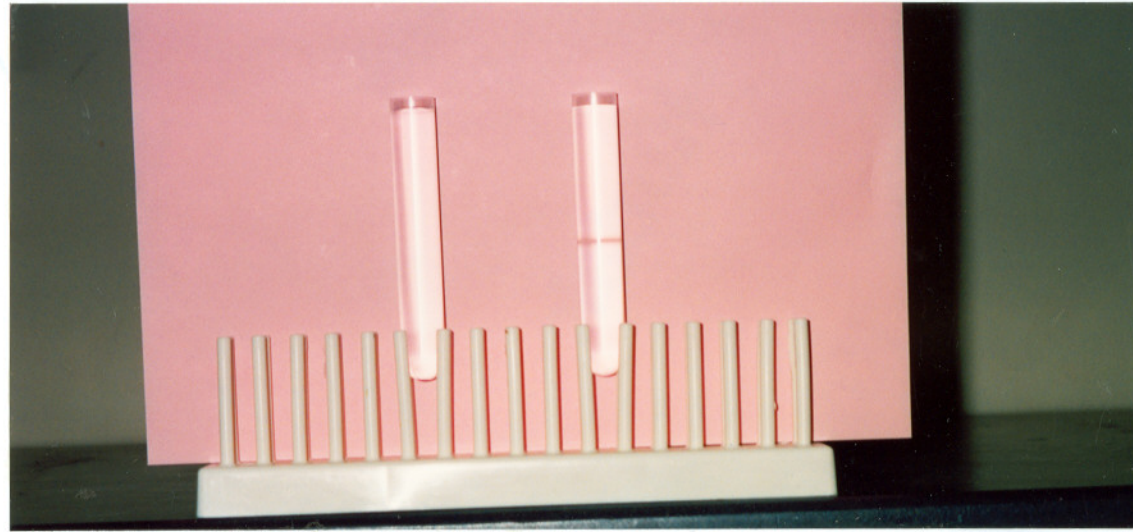
Figure 3-25. (a) The cosonicated mixture of 8 mM DHP vesicles and 3 μM bR on 5-35% sucrose gradient layered on 1-ml 45% sucrose cushion in 20 mM Tris-HCl, pH 7.80, centrifuged at 17500 rpm for 17 hours at 20°C in a Beckmann SW 27.1 swinging bucket rotor. (b) 2 μM bR on the same sucrose density gradient.
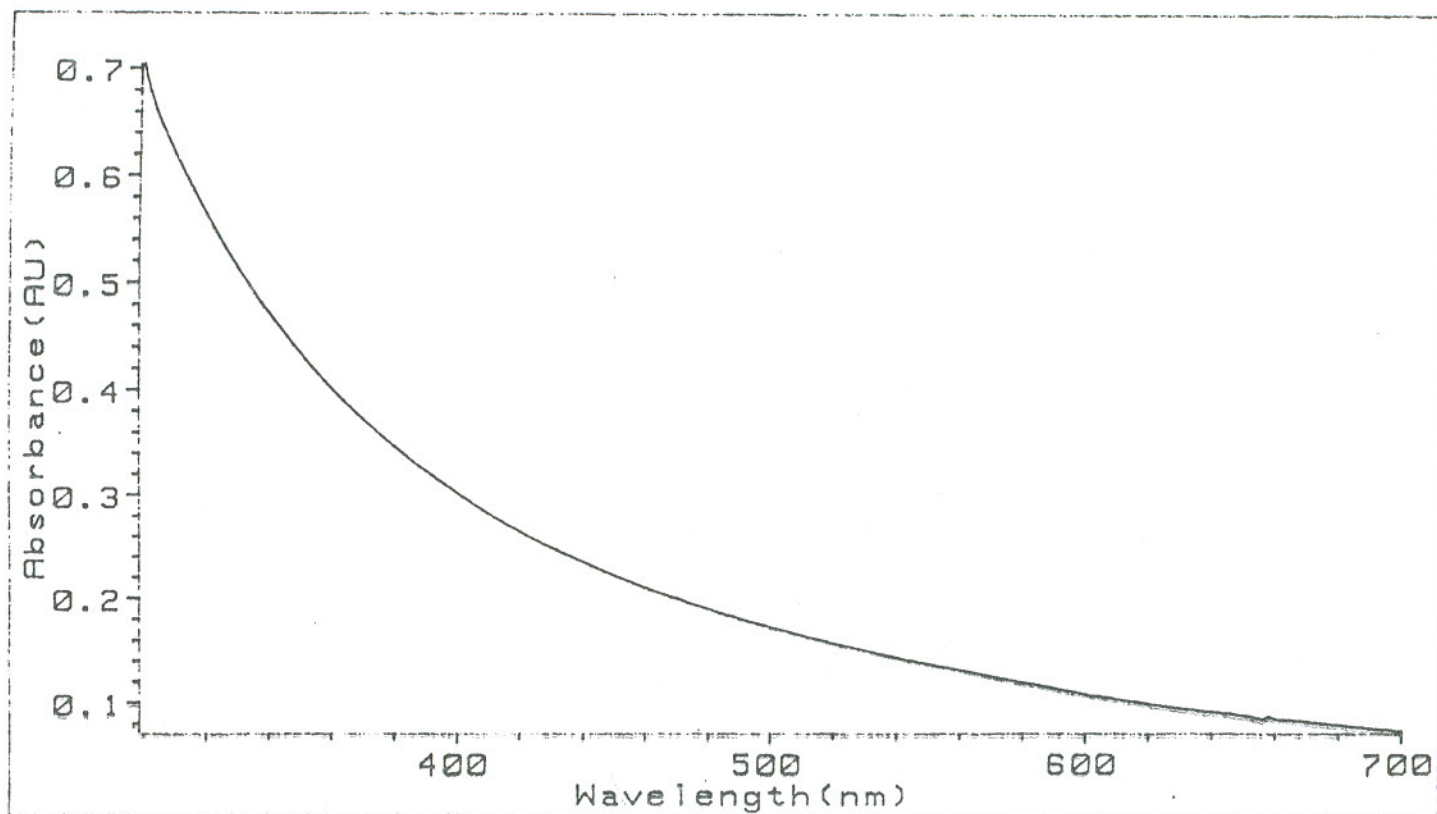
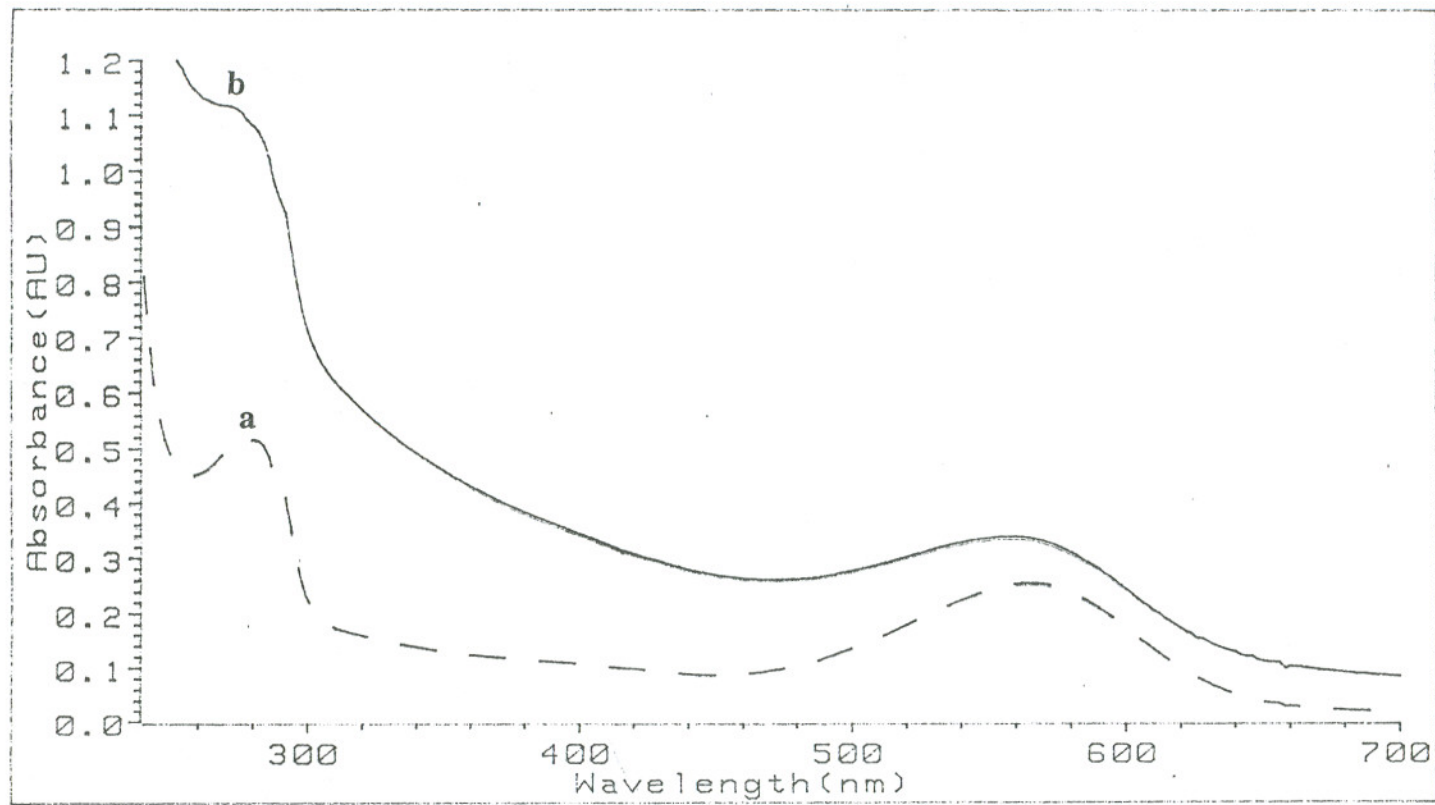Figure 3-26. Absorption spectrum of the band in Figure 3-25 (a).

Figure 3-27. Absorption spectra of a mixture of 8 mM DHP SUVs and 5 μM bR before (trace a) and after (trace b) incubation at 60°C for 3 hours.

incubated mixture was centrifuged at 20°C in a Ty 65 rotor at 36,000 rpm for 90 minutes. The absorption of supernatant was measured and smaller scattering of DHP vesicles was observed after incubation (Figure 3-28).

The incubated mixture was separated on a sucrose density gradient as before. A purple band was isolated from the middle of the gradient; its absorption spectrum is shown in Figure 3-29. This species might be an aggregate of purple membrane and DHP vesicles, but it was not characterized any further.
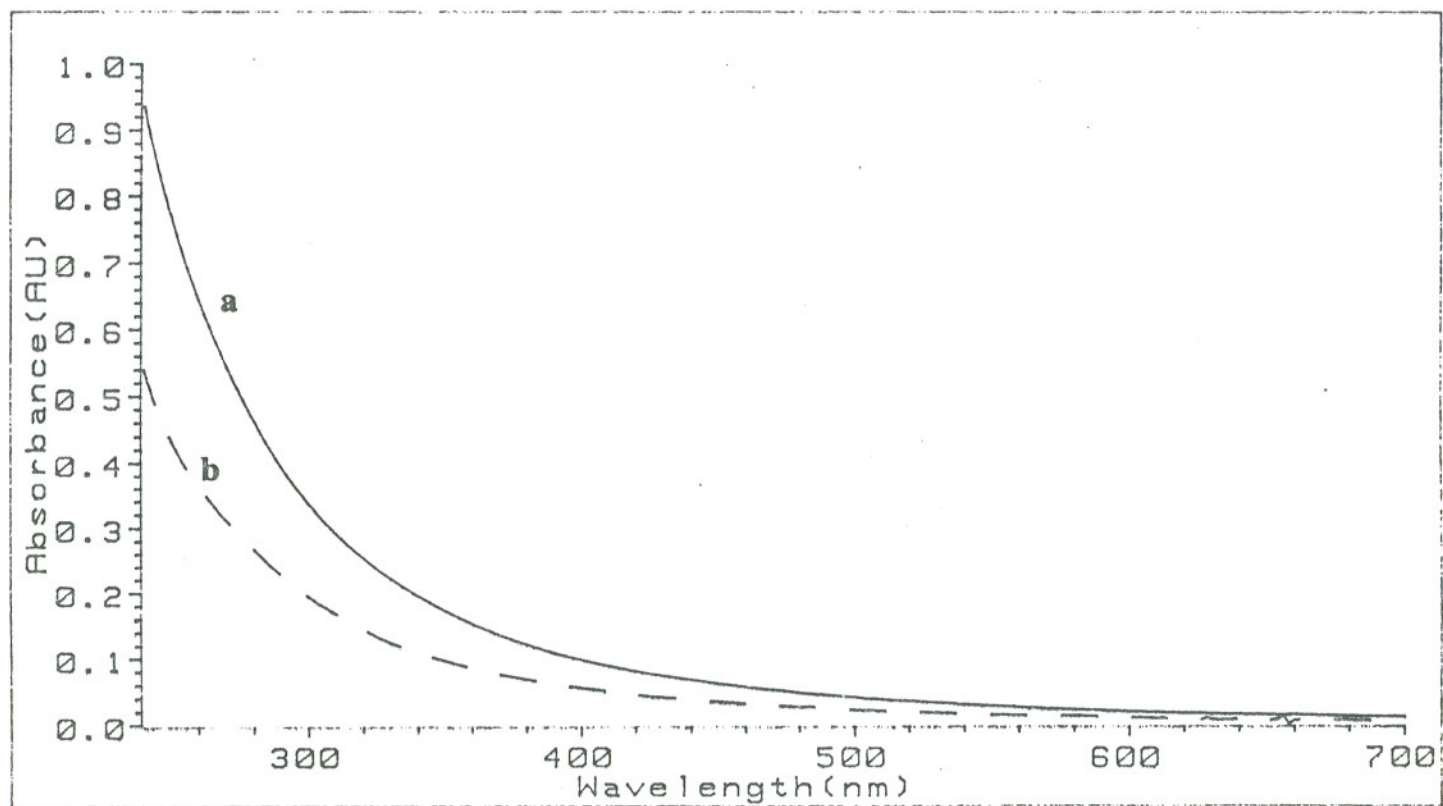
Figure 3-28. Absorption spectra of the DHP SUVs (trace a) and the supernatant of an incubated mixture of 8 mM DHP SUVs and 5 μM bR (60°C, 3 hours) after centrifugation at 36,000 rpm for 90 minutes at 20°C (trace b).
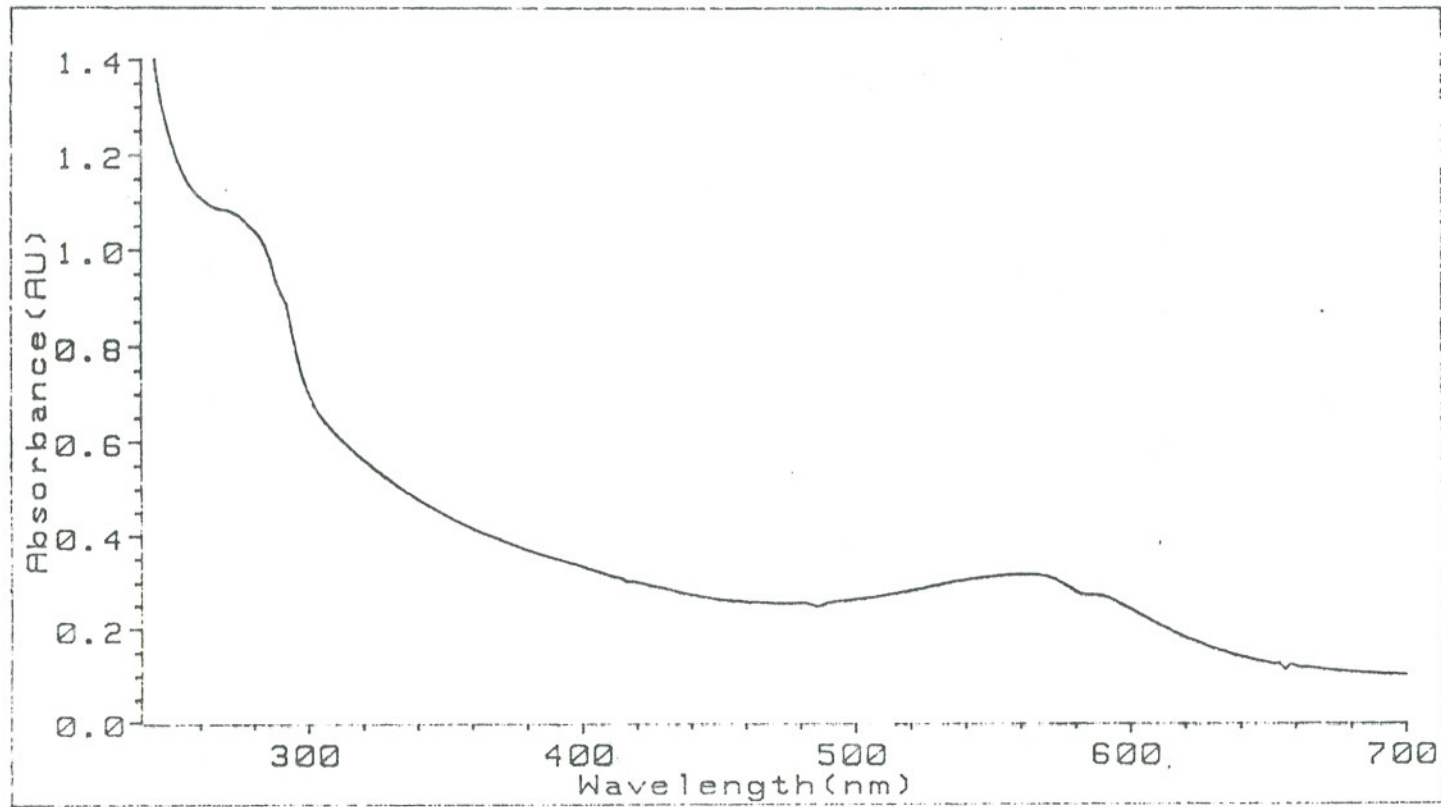
Figure 3-29. Absorption spectrum of the purple band of an incubated mixture of 8 mM DHP vesicles and 4 μM bR (65°C, 4.5 hours) isolated from a 5-35% sucrose gradient.

CHAPTER 4

CONCLUSIONS

The results of the pH jump experiments are controversial. The fast initial change of the internal pH of DHP vesicles after an external pH jump is not fully understood yet. Several possible explanations have been explored.

Dilution effects and leakage of pyranine during the pH jump experiments have been excluded. Evidence of "electroporation" phenomena was also sought using atomic absorption spectroscopy to monitor K^+ ion diffusion, but was inconclusive. Additional experiments using more sensitive radioactive probes such as $^{22}Na^+$, $^{86}Rb^+$, or ^{14}C- labeled glucose, sucrose to probe for pore formation are desirable. There are several lines of evidence favoring some pyranine on the external medium of the DHP vesicles. First, the dialysis experiments indicate that pyranine accumulates in the chamber containing the vesicles, consistent with some binding. This has two consequences, one being that it is difficult to completely remove the unentrapped pyranine from the external medium of DHP vesicles by gel filtration chromatography, the other being that the entrapped pyranine is bound to the internal surfaces of vesicles to an unknown extent, thus reporting the false internal pH values. Second, the gel filtration column fractionation experiment suggests that the external pyranine cannot be removed from the DHP vesicles completely. Third, the fast initial phase in the stopped-flow mixing experiment implies that there is some external pyranine because the protonation/deprotonation rate is too large to be associated with transmembrane movement. Finally, the rate-enhancing effect of the lipophilic tetraphenylphosphonium cation on the slow pH change process proves that the transmembrane movement of H^+/OH^- occurs only in the slow phase, although no entrapment of tetraphenylphosphonium could be demonstrated. Only one experimental result, i.e., the lack of pyranine fluorescence quenching by added

90

thiamine, is consistent with complete removal of external pyranine. Assuming that the fast initial pH change following pH perturbation of the external medium is caused by the presence of external pyranine, we estimate the permeability coefficient of H^+/OH^- across the DHP vesicle bilayers for the slow phase of the pH jump experiments to be around 10^{-5} - 10^{-4} cm/s, which in fair agreement with the high values reported for other vesicle bilayers.

Promising results were obtained for incorporation of bacteriorhodopsin into DHP vesicle bilayers, i.e., incubation of mixtures of preformed DHP vesicles and bR above the phase transition temperature of the vesicle can lead to association of these two species. Further experiments to characterize this interaction, and the orientation of bR incorporated in the vesicle bilayers are necessary, however. Other incorporation methods including the use of detergents are also desirable.

REFERENCES

1.   Gennis, R. B. In *Biomembranes: Molecular Structure and Function* Cantor, C. R., Eds., Springer-Verlag New York *Inc.*, 1989, pp 235-256.

2.   Hauser, H.; Phillips, M. C.; Stubbs, M. *Nature (London) 239* (1972) 342-344.

3.   Johnson,S. M.; Bangham, A. D. *Biochim. Biophys. Acta 193* (1969) 82-91.

4.   Pike, M. M.; Simon, S.S.; Balschi, J. A.; Springer, C. S. Jr. *Proc. Natl. Acad. Sci. USA 79* (1982) 810-814.

5.   Mimms, L. T.; Zampighi, G.; Nozaki, Y.; Tanford, C.; Reynolds, J. A. *Biochem. 20* (1981) 833-840.

6.   Nichols, J. W.; Deamer, D. W. *Proc. Natl. Acad. Sci. USA 77* (1980) 2038-2042.

7.   (a) Nagle, J. F. *J. Bioenerg. Biomembr. 19* (1987) 413-426.
      (b) Gutknecht, J. *J. Bioenerg. Biomembr. 19* (1987) 427-442.
      (c) Perkins, W. R.; Cafiso, D. S. *J. Bioenerg. Biomembr. 19* (1987) 443-455.
      (d) Deamer, D.W. *J. Bioenerg. Biomembr. 19* (1987) 457-479.
      (e) Verkman, A. S. *J. Bioenerg. Biomembr. 19* (1987) 481-493.

8.   Mclaughlin, S. G. A.; Dilger, J. P. *Physiol. Rev. 60* (1980) 825-863.

9.   Nagle, J. F.; Morowitz, H. I. *Proc. Natl. Acad. Sci. USA 75* (1978) 298-302.

10.   El-Mashak, E. M.; Tsong, T. Y. *Biochem. 24* (1985) 2884-2888.

11.   Tsong, T. Y. *Biophys. J. 60* (1991) 297-306.

12.   Tsong, T. Y. *Bioelectrochem. Bioenerg. 24* (1990) 271-295.

13.   Kinosita, K. Jr.; Tsong, T. Y. *Nature 268* (1977) 438-441.

14.   Serpersu, E. H.; Kinosita, K. Jr.; Tsong, T. Y. *Biochim. Biophys. Acta 812* (1985) 779-785.

15.   Teisse, J.; Tsong, T. Y. *Biochem. 20* (1981) 1548-1554.

16. Glaser, R. W.; Leikin, S. L.; Chernomordik, L. V.; Pastushenko, V. F.; Sokirko, A. I. *Biochim. Biophys. Acta 940* (1988) 275-287.

17. Weaver, J. C. In *Interfacial Phenomena in Biological System* Bender, M., ed., Marcel Dekker, *Inc.*, 1991, pp 253-277.

18. Fendler, J. H. *Membrane Mimetic Chemistry* Wiley-Interscience: New York, 1982.

19. Hurst, J. K. In *Kinetics and Catalysis in Microheterogeneous Systems* Gratzel, M.; Kalyanasundaram, K., Eds., Marcel Dekker: New York, 1991, pp 183-226.

20. Patterson, B. C.; Hurst, J. K. *J. Chem. Soc., Chem. Commun. 17* (1990) 1137-1138.

21. Patterson, B. C. *Ph.D. Dissertation,* Oregon Graduate Institute of Science and Technology, 1990.

22. Oesterhelt, D.; Stoeckenius, W. *Nature New Biology 233* (1971) 149-152.

23. Blaurock, A. E.; Stoeckenius, W. *Nature New Biology 233* (1971) 152-155.

24. Oesterhelt, D.; Stoeckenius, W. *Proc. Natl. Acad. Sci. USA 70* (1973) 2853-302.

25. (a) Khorana, H. G. *J. Biol. Chem. 263* (1988) 7439-7442.
    (b) Henderson, R.; Baldwin, J. M.; Ceska, T. A.; Zemlin, F.; Beckmann, E.; Downing, K. H. *J. Mol. Biol. 213* (1990) 899-929.

26. Van Dijck, P. W. M.; Van Dam, K. *Methods Enzymol. 88* (1982) 17-25.

27. Humphry-Baker, R.; Thompson, D. H.; Lei, Y.; Hope, M. J.; Hurst, J. K. *Langmuir 7* (1991) 2592-2601.

28. Kano, K.; Fendler, J. M. *Biochim. Biophys. Acta 509* (1978) 289-299.

29. Koller, E.; Kriechbaum, M.; Wolfbeis, O. S. *Spectr.3 Num. 11* (1988) 37-39

30. *Guide to Ion Exchange*, Bio-Rad Laboritories, 140-9997.

31. Flewelling, R. F.; Hubbell, W. L. *Biophys. J. 49* (1986) 531-540.

32. Ames, B. N. *Methods Enzymol. 8* (1966) 115-118.

33. *Instructions Model 703 Atomoc Absorption Spectrophotometer*; Perkin-Elmer Corporation 993-9454, 1978.

34. Oesterhelt, D.; Stoeckenius, W. *Methods Enzymol. 31* (1974) 667-678.

35. *Instruction manual for Hoefer gradient makers SG 5, 15, 30, 50, 100*; Hoefer scientific instruments 10905/7-85.

36. Krupinski, J.; Hammes, G. G. *Biochem. 24* (1985) 6963-6972.

37. *Fluorescence spectrophotometer model MPF-66 operating Directions*; The Perkin-Elmer Corporation 646-000.

38. Clement, N. R.; Gould, J. M. *Biochem. 20* (1981) 1534-1538.

39. Cantor, C. R.; Schimmel, P. R. *Biophysical Chemistry* W. H. Freeman and Company: San Francisco, 1980, pp 1335-1339.

40. (a) Pekkarinen, L.; Linschitz, H. *J. Am. Chem. Soc. 82* (1960) 2407-2411.
    (b) Houlding, V. H.; Kalyanasundaram, K.; Grätzel, M.; Milgrom, L. R. *J. Phys. Chem. 87* (1983) 3175-3179.

41. Englefield, M. J. *Mathematical Methods for Engineering and Science Students* Edward Arnold (Publishers) Ltd., 1987, pp 161-178.

42. (a) Tricot, Y.-M.; Furlong, D. N.; Sasse, W. H. F.; Daivis, P. *J. Colloid Interface Sci. 97* (1984) 380-391.
    (b) Carmona-Ribeiro, A. M. *J. Colloid Interface Sci. 139* (1990) 343-350.

43. Lakowicz, J. R. *Principles of Fluorescence Spectroscopy* Plenum Press, New York, 1983.

44. (a) Sowers, A. E.; Lieber, M. R. *FEBS Lett. 205* (1986) 179-184.
    (b) Rosemberg, Y.; Korenstein, R. *Biophys. J. 58* (1990) 823-832.

45. (a) Cafiso, D. S.; Hubbell, W. L. *Biophys. J. 44* (1983) 49-57.
    (b) Cafiso, D. S.; Hubbell, W. L. *Biochem. 17* (1978) 187-195.
    (c) Cafiso, D. S.; Hubbell, W. L. *Biochem. 17* (1978) 3871-3877.
    (d) Cafiso, D. S. *Ann. Rev. Biophys. Bioenerg. 10* (1981) 217-244.

46.   Vance, D. G.; Vance, J. E. *Biochemistry of Lipids and Membranes* The Benjamin/Cummings Publishing Company, *Inc.* 1985.

47.   Racker, E. *Biochem. Biophys. Res. Commun.* 55 (1973) 224-230.

BIOGRAPHICAL SKETCH

The auther was born in October, 1964, in Tianjin, China. In 1983, she graduated from Nankai High School, Tianjin. She received her B.S. degree in Chemistry in 1987, and her M.S. degree in Physical Chemistry in 1990 from Nankai University. Immediately thereafter, she began her studies at the Oregon Graduate Institute with Dr. James K. Hurst.